



Review

Sensing of Digestive Enzymes—Diagnosis and Monitoring of Pancreatitis

Jiaju Yin ^{1,†}, Tianrui Cui ^{1,†} , Yi Yang ^{1,*} and Tian-Ling Ren ^{1,2,*}

¹ School of Integrated Circuit and Beijing National Research Center for Information Science and Technology (BNRist), Tsinghua University, Beijing 100084, China; yjj22@mails.tsinghua.edu.cn (J.Y.); ctr19@mails.tsinghua.edu.cn (T.C.)

² Center for Flexible Electronics Technology, Tsinghua University, Beijing 100084, China

* Correspondence: yiyang@tsinghua.edu.cn (Y.Y.); rentl@tsinghua.edu.cn (T.-L.R.)

† These authors contributed equally to this work.

Abstract: This paper is a comprehensive review of the techniques for the detection of pancreatic enzymes, which are common biochemical indicators of pancreatitis, including amylase, trypsin, chymotrypsin, elastase, and lipase. Pancreatitis is a disease with self-digestion due to the abnormal activation of digestive enzymes in the pancreas. Hospitalization is often required due to the lack of convenient therapeutic agents. The main recent results are reported in this review, especially the techniques that enable portability and Point-of-Care testing (POCT). This is because timely diagnosis at the early stage and avoiding recurrence after recovery are the keys to treatment. It is also important to reduce the rate of misdiagnosis and to avoid overtreatment. Various detection methods are discussed, with particular attention given to the implementation of chemical sensing and probe design. The new sensing technology for digestive enzymes makes it possible to perform early screening for pancreatitis in remote areas or in one's own home.

Keywords: pancreatitis; sensors; α -amylase; trypsin; lipase



Citation: Yin, J.; Cui, T.; Yang, Y.; Ren, T.-L. Sensing of Digestive Enzymes—Diagnosis and Monitoring of Pancreatitis. *Chemosensors* **2023**, *11*, 469. <https://doi.org/10.3390/chemosensors11090469>

Academic Editor: Danila Moscone

Received: 31 May 2023

Revised: 2 August 2023

Accepted: 17 August 2023

Published: 22 August 2023



Copyright: © 2023 by the authors. Licensee MDPI, Basel, Switzerland. This article is an open access article distributed under the terms and conditions of the Creative Commons Attribution (CC BY) license (<https://creativecommons.org/licenses/by/4.0/>).

1. Introduction

1.1. Pancreatitis

The pancreas is an essential part of the human digestive system. The pancreas secretes pancreatic juice, which contains necessary digestive enzymes such as pancreatic amylase, pancreatic protease, and pancreatic lipase, which digest proteins, fats, and sugars [1–3]. The pancreas also has many necessary roles: the bicarbonate contained in the pancreatic fluid can enter the duodenum to neutralize stomach acid; the islets of the pancreas, as an endocrine organ, secrete insulin and glucagon to regulate blood sugar in the body; and pancreatic polypeptides control gastrointestinal motility, pancreatic fluid secretion, and gallbladder contraction [4,5].

Pancreatic enzymes secreted by the pancreas are inactive as pancreatic zymogen before being excreted with pancreatic juice. After entering the duodenum, it is transformed into active digestive enzymes through bile and intestinal kinase [1]. Bile reflux into the pancreatic duct due to gallstones and kinase released by bacterial infection may lead to the abnormal activation of pancreatic zymogen in the pancreas [4]. The converted trypsin can lead to self-digestion in the pancreatic tissue and cause pancreatitis [6,7]. This may lead to impaired pancreatic function, necrosis, multi-organ failure, and death.

Acute pancreatitis (AP) is a disease that often requires hospitalization [8,9]. The incidence of AP is 34 per 100,000 persons per year in high-income countries [10]. It was found in 25.4–98.7 per 100,000 U.S. adults with health insurance during 2001–2013 [11]. Of all AP patients, 20% develop moderate and severe pancreatic or peripancreatic tissue necrosis or organ failure, with a mortality rate of 20–40% [12–16]. AP is the fifth leading cause of in-hospital death and the second leading cause of length of stay in the

United States [17]. The mortality rate of pancreatitis has decreased in recent years with the development of diagnostic and treatment techniques. However, the total number of deaths caused by the rising incidence has not decreased and remains a major threat to people's health [18].

Gallstones are the most common cause of AP, and the remaining common risk factors for pancreatitis include alcohol consumption, smoking, hypertriglyceridemia, drug reactions, and genetics (Figure 1) [4,12,17–21]. It may lead to severe abdominal pain, diabetes, malnutrition, bloating and diarrhea, endocrine dysfunction, and cardiovascular events [12].

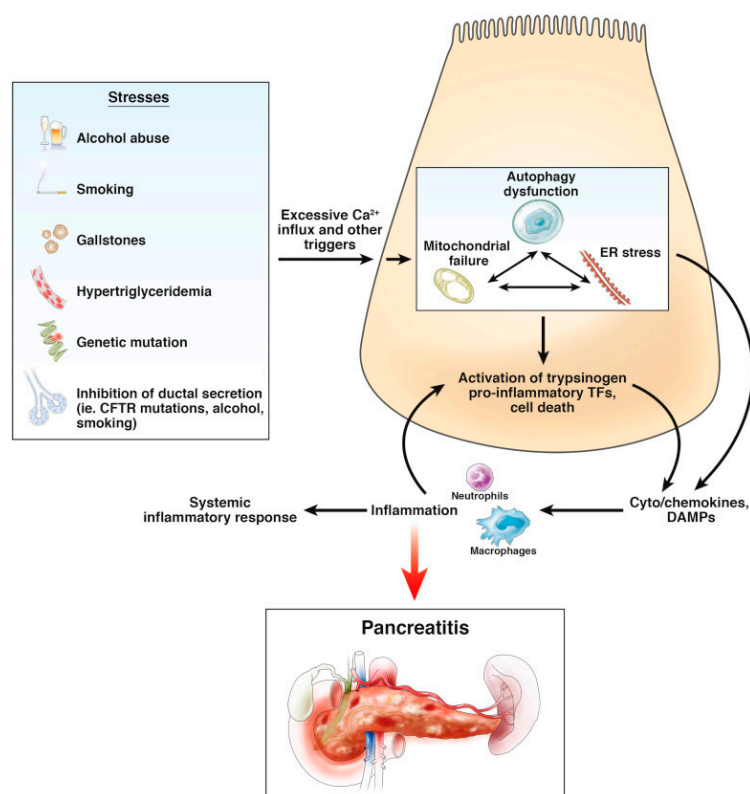


Figure 1. Summary of environmental stressors and genetic factors known to increase the risk for pancreatitis. Reproduced with permission from [19], copyright 2019 by the AGA Institute.

During COVID-19, many statistics also found an association with AP [22–25]. In one statistic from China, pancreatic injury was present in 17% of COVID-19 patients [22]. SARS-CoV-2 induced by COVID-19 may cause AP [25]. In a Turkish statistic, 29.8% of patients admitted to the hospital had high lipase activity. This group had an ICU admission rate of 36.1% and a mortality rate of 24.6%, while the total ICU admission rate was 9.9% and the mortality rate was 6.4% [26].

The diagnosis of some patients in high-risk groups who experience one or more episodes of pancreatitis may turn into chronic pancreatitis (CP) (Figure 2). This results in 3–35% of patients with AP progressing to CP [8,9,27,28]. CP is a chronic inflammatory disease causing irreversible changes in the tissue and function of the pancreas. In addition to AP, CP has different triggers. The mortality rate of common CP approaches 50% within 20–25 years after the onset of the disease [29,30].

Pancreatitis is also a high-risk factor for pancreatic cancer. Pancreatitis is a high-mortality disease and is expected to be the second leading cause of cancer death in the United States by 2030 [31].

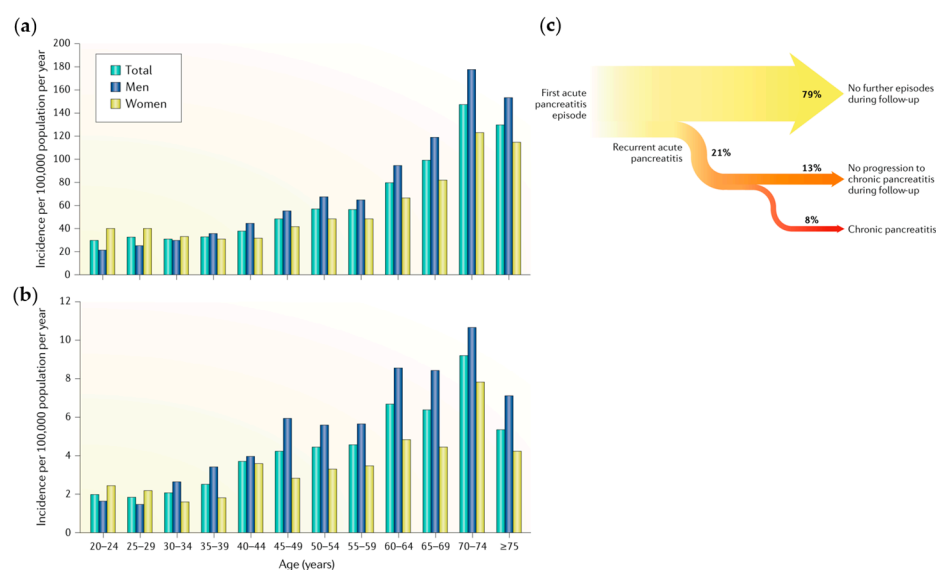


Figure 2. Statistical results related to pancreatitis: (a) incidence of acute pancreatitis stratified by age and sex; (b) incidence of chronic pancreatitis stratified by age and sex; (c) acute pancreatitis develops into chronic pancreatitis and pancreatic cancer. Reproduced with permission from [8], copyright 2018 Springer Nature.

1.2. Diagnosis and Treatment of Pancreatitis

Diagnostic imaging such as computed tomography (CT) and nuclear magnetic resonance (MRI) can determine the status of the pancreas and thus diagnose and evaluate pancreatitis [9,12,17,18,32]. Imaging methods using artificial intelligence to evaluate the pancreas of CP patients versus the normal human pancreas have also been reported [33]. However, imaging methods have high equipment requirements and need to be performed in a large hospital. Body fluid testing is a diagnostic modality that has the potential to be more convenient. Pancreatic lipase and pancreatic amylase in blood and urine exceeding three times the standard values are also common diagnostic criteria [34].

In addition, the elevation of cytokines, C-reactive protein, and IgG are correlated with pancreatitis [12,17,29,35]. In recent reports, microRNAs [36], short-chain fatty acids produced by intestinal microbial metabolism [37], and the body's circadian regulatory system [38] have all been shown to be involved in the onset and progression of pancreatitis. However, these studies are still a long way from helping to diagnose pancreatitis.

We still lack accurate staging and disease surveillance techniques for pancreatitis [9]. This manifests itself in two ways. One is the high rate of misdiagnosis, which leads to delayed treatment. In one statistic, misdiagnosis was caused by the absence or slight elevation of early blood and urine amylase in some patients. In one study, the misdiagnosis rate at the early admission stage was 17.58% and the misdiagnosis time was 2.2–4.1 days [39]. This is because pancreatitis causes a great impact on the overall metabolism of the body, which makes the diagnosis difficult. Second, there is the occurrence of overmedication. Of the 1660 high-risk individuals tested in one study, 257 underwent pancreatic surgery, but there were only 59 high-risk lesions [40,41]. This demonstrates the difficulty of relying on imaging alone for correct diagnosis and the importance of biochemical testing to avoid overtreatment.

Prompt diagnosis is essential for the treatment of pancreatitis. Early detection and intervention can effectively reduce morbidity and mortality [18,42]. Patients who reach the stage of pancreatic necrosis have a complication rate of 82% and a mortality rate of 23%. In contrast, before this stage, the complication rate is only 6% and the mortality rate is 0% [32]. The timely diagnosis of pancreatitis is difficult in underdeveloped areas or scenarios where medical resources are insufficient. Diagnosis based on abdominal pain, which has minimal equipment requirements, may not determine the etiology due to poor localization [43].

The development of AP is unpredictable, and health monitoring should be performed for at least 48 h after complications [12]. Patients with AP can resume eating and drinking when they subjectively feel hungry, but this may also cause a recurrence of pancreatitis [17]. During treatment with methods such as pancreatic enzyme replacement, tailored and personalized medical treatment is recommended to cope with the high mortality rate and to avoid surgical treatment whenever possible [12,29]. Pancreatic function should also continue to be monitored after the end of treatment. Pancreatic function generally returns to normal after three months of remission of AP, and the resumption of episodes leading to CP should be avoided [9,17].

1.3. Point-of-Care Testing

In current clinical diagnostics, the definitive diagnosis of pancreatitis relies on three criteria: (1) abdominal pain consistent with the features of pancreatitis, (2) serum lipase or amylase levels three times higher than the upper limit of the standardized values, and (3) signs of pancreatitis on imaging [34]. In a study of the International Classification of Diseases, Tenth Revision (ICD-10) diagnostic codes for acute pancreatitis in the U.S. healthcare system, the overall PPV was 61% [37]. This result is hardly ideal.

Pancreatitis often requires hospitalization due to the lack of convenient therapeutic agents [9,19]. Starting treatment at the mild stage is an effective means of reducing mortality. Therefore, it is important to perform quick and easy early screening to avoid delaying treatment when symptoms such as abdominal pain occur. Currently, in all populations, PPV is higher in hospitalized patients than in emergency and outpatient settings [37]. The result flanks the need for more detailed testing for the diagnosis of pancreatitis.

In addition to the prompt treatment of severe cases, a more accurate classification of pancreatitis can help to better treat patients with mild to moderate cases. Randomized clinical trials on patients with mild to moderate AP have shown that starting a low-fat solid oral diet within 24 h of admission to the hospital does not increase instances of negative outcomes and may also provide positive benefits for patients with AP [44]. Therefore, it may be beneficial to monitor the status of patients with pancreatitis more frequently to resume this diet promptly when symptoms subside.

These needs have led to Point-of-Care testing (POCT), an important trend in the development of medical technology today (Figure 3) [45–48]. We need technologies that enable detection and diagnosis in real time and with ease. In order to cope with in-hospital misdiagnosis and mortality, research on POCT to implement more timely and appropriate treatment is relevant. This is also needed to facilitate people in areas with insufficient medical resources to avoid the harm caused by untimely diagnosis or even misdiagnosis of pancreatitis. People in areas with sufficient medical resources can also easily self-test when minor abdominal pain or discomfort occurs.

In a recent review summarizing the effectiveness of multiple biochemical tests, urine trypsinogen-2 levels can be highly accurate in diagnosing AP [49]. Advanced imaging methods such as endoscopic ultrasound and artificial intelligence (AI) image analysis can contribute to a better diagnosis [50,51]. But these tests, which can be performed only in large hospitals, are not sufficient to solve the previously mentioned problem of the unsatisfactory overall diagnosis and treatment of pancreatitis. There is still a need to look into POCT technology.

For the diagnosis of pancreatitis, the most meaningful approach remains the sensing of digestive enzymes. This is because pain determination is relatively subjective, and the miniaturization of and ease of access to imaging equipment are often difficult. Among the criteria for the clinical diagnosis of pancreatitis, pancreatic enzyme sensing is the easiest way to achieve these goals.

In order to achieve the goal of POCT, the blood amylase and lipase tests that are now used in hospitals need to be transformed into sensing that can be implemented on miniaturized and portable devices. The ratio of different digestive enzymes in pancreatic

enzymes is not constant [3,52]. Therefore, the simultaneous testing of multiple digestive enzymes can help better diagnose pancreatitis.

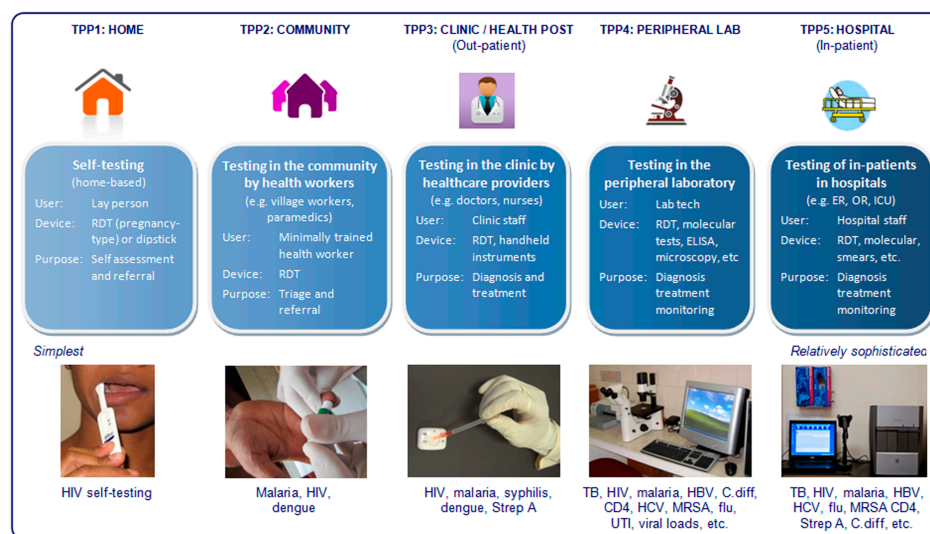


Figure 3. Diversity of target product profiles, users, and settings within the spectrum of Point-of-Care testing. Reproduced from [48] under the terms of the CC-BY Creative Commons Attribution License, copyright 2012 Public Library Science.

After being secreted into the digestive tract, digestive enzymes also partially enter into the bloodstream or through the glomerulus into urine [1,6,53,54]. In addition to blood samples, the realization of mid-marker sensing in non-invasive samples such as urine and saliva can also greatly improve ease of use.

1.4. Summary

This article summarizes the techniques for detecting pancreatic enzymes, a common biochemical indicator of pancreatitis. These enzymes include amylase, protease, and lipase. The main recent results are reported. Since digestive enzymes work mostly by catalyzing the hydrolysis of chemical bonds in macronutrients, there is some commonality in their detection methods. Compared to the diversity of proteins and lipids, the monomers of starch are relatively unitary.

In Section 2, laboratory methods for detecting amylase and optical, mechanical, electrical, and several other types of sensing ideas are described, with particular reference to the principles of each method. Section 3 describes sensing three proteases: trypsin, chymotrypsin, and elastase. The categorization of the studies is consistent with that of amylase, and the principles already presented in Section 2 will not be repeated, but rather the design of special probes, chemistries, and other principles specific to the proteases will be emphasized. Section 4 describes the sensing of lipases, with a similar structure to the previous two sections.

The principles, probe design, and methods of amplifying the signal are described for each method. Finally, advances made for POCT are presented, including miniaturized and portable devices or sensing that can be implemented with common devices such as cell phones. Each section will summarize a table of POCT advances.

2. Detection of Amylase

2.1. Pancreatic Amylase

Approximately 40–50% of calorie intake in the diet comes from carbohydrates [55,56]. Since the human intestinal epithelium can only absorb small molecules of glucose, the ingested large molecules need to be broken down by the action of enzymes [1].

Pancreatic amylase is a hydrolase secreted by the pancreas that hydrolyzes the α -1,4-glycosidic bond [1,57]. It is a type of α -amylase. It has no effect on α -1,6-glycosidic bonds on branches. In ingested food, it can act on α -1,4-glucan, such as soluble starch, straight-chain starch, and glycogen. The decomposition products are mainly maltose, with a small amount of maltotriose as well as glucose produced. The activity of α -amylase requires calcium ions and a pH suitable for its work [1,57].

Amylase is the only glycosidase secreted from human pancreatic juice [1,58,59]. The human salivary glands also secrete alpha-amylase. Also, α -amylase can pass through the glomerulus and be detected in urine. Therefore blood, saliva, and urine are body fluids that can be tested for α -amylase [1]. However, for this reason, amylase is less specific than markers such as lipase for the diagnosis of pancreatitis [57]. Amylase was detected in 72% of hand swabs in another study, demonstrating that sweat may also be available for amylase sensing [60].

This section summarizes research on α -amylase sensing. It begins with a description of the analytical methods commonly used in the laboratory, followed by a summary of existing reports categorized according to optical, mechanical, electrical, and other methods. For each method, the principles, the design of chemical sensing, and advances in the portability of devices will be summarized separately.

2.2. Laboratory Chemical Analysis

Measurement of α -amylase in the laboratory can be conducted by a variety of more general methods, including chromatography and spectroscopy. A basic approach is to mix the sample to be measured with a substrate containing starch and, after a period of catalytic reaction, use mass spectrometry and chromatography to detect the starch content and thus analyze the concentration of amylase in the sample [61]. This method takes advantage of the intrinsic property of α -amylase in that it can hydrolyze starch, which is also the basic principle of many sensors. Barber et al. reported that substrates and digestion products in enzyme activity assays could be quantified directly by high-performance anion-exchange chromatography with pulsed amperometric detection (HPAE-PAD) [62].

Methods such as UV-visible spectrophotometry are also widely used for detecting α -amylase, such as detecting α -amylase content and activity in drugs or food [63]. Since starch, glucose, etc., do not have a distinct color in the visible range, color-developing substances are often introduced for better measurement of amylase activity by chromatography. In addition to directly detecting sugars, preparing substances with distinct colors by chemical reactions is also an idea for detection. Weng et al. reported that the reaction of maltose, a product of the amylase hydrolysis of starch, with 3,5-dinitro salicylic acid (DNS) produced the brown product 3-amino-5-nitrosalicylic acid (3A5NA), and also reported a method of detecting the reflected light spectrum. Based on the spectral results, especially comparing the absorbance of reflected light at 520 nm, it was possible to analyze the maltose concentration and thus obtain the amylase concentration and activity [64]. However, this method has not been used for the detection of amylase secretion by the pancreas.

These methods often require large laboratory instruments. But this idea of using the properties of digestive enzymes to break down the substrate for sensing and using the rest of the substrate to amplify the signal is very important. In order to achieve portable detection or to adapt to Point-of-Care application scenarios, this paper summarizes more studies that have the potential for miniaturization.

2.3. Optical Methods

2.3.1. Amylose-Iodine Colorimetry

The formation of blue complexes with iodine is an important property of starch, and they disappear as it is hydrolyzed. This is a simple and effective method for amylase sensing. The colorimetric method is a simplification of the chromatographic method. For colors with obvious absorption peaks, the measurement results can be obtained conveniently by comparing the absorbance at the wavelength of the absorption peak. Colorimetric methods

often require compounds designed with distinct colors, and the end result can be captured directly by the human eye or a cell phone camera, thus enabling portable measurements.

The combination of starch and iodine results in a Prussian blue solution. This reaction has good stability and can be preserved by being applied to paper. Dutta et al. reported that when a sample containing amylase is applied to paper, it hydrolyzes the starch, causing the blue color to fade [65]. The amylase content can then be analyzed by shining a light source on the paper and detecting the intensity of the transmitted or reflected light (e.g., using a photoresistor). Ascorbic acid will keep the reaction of starch with iodine because it is easily oxidized when iodine is present again. Therefore, human blood samples must be pretreated with sufficient KIO_3 solution to neutralize ascorbic acid. This method's minimum detection limit and linearity may not be optimal, but there is good potential for portability.

The advantage of this method is that paper-based sensors are less expensive to manufacture, but the distribution of α -amylase during the infiltration of liquid specimens into the paper needs to be considered. Hyung et al. conducted a study on this and found that α -amylase aggregates at the head of the paper [66]. Applying starch only to the head of the paper, they found that there was also no α -amylase distribution at the end where there was no starch, indicating that the amylase had been depleted previously. This study illustrates that paper-based sensors, if using a passive diffusion method, should consider different α -amylase distributions at different sites.

The paper-based platform technique of Adhikary et al. had a detection limit of 70 mg/mL for a 5 min reaction. Visible switch structures were formed by preparing ionic gels formed by chitosan-triphosphate nuclei encapsulated with starch-iodine shell-structured bioaffinity particles. The coated test strips had a 30 min detection line of 1.25 mg/mL [67]. This technique has good stability and can be used in areas such as forensic investigations and also has great potential for rapid pancreatitis screening in non-large-hospital scenarios.

2.3.2. Special Substrate Colorimetry

Colorimetric methods have been investigated in two ways: more pronounced absorbance changes and more portable measuring devices.

By designing substrates or products of different colors, colorimetry can be performed at different wavelengths, and there are already many amylase-sensing implementations based on this principle. Fuentes et al. used a kinetic spectrophotometric assay to determine alpha-amylase. The method uses 4,6-ethylidene(G7)-p-nitrophenol(G1)-alpha-D-maltoheptaoside (ethylideneG7PNP) as a substrate of the enzyme. The intermediate product of the substrate hydrolysis reacts with alpha-glucosidase, giving p-nitrophenol as the final product of the reaction. The rate of p-nitrophenol formation is directly proportional to the alpha-amylase activity of the sample and can be determined by measuring the absorbance at 405 nm [68]. Visvanathan et al. developed a red quinone based on the reaction of maltose with glucose oxidase (GOD). After calibrating the wavelength at which the absorbance peak was located, the absorbance of the solution after the reaction of amylase with maltose was measured, and then the concentration of the reaction product glucose was measured. They used this method to analyze α -amylase inhibitors [69].

Such a line of thought can be carried further. The signal can be further amplified if, instead of forming a colored compound by forming a colored compound with the reaction product, the reaction product is allowed to further catalyze the production of a colored compound from something else in the substrate. The resulting tetramethylbenzidine (TMB) oxidation method has many applications in the colorimetric sensing of digestive enzymes and is summarized in Section 3.2. Starch can act as a stabilizer for nanoparticle clusters of copper and gold. These nanoclusters exhibit a strong peroxidase-like activity and are able to catalyze the oxidation of 3,3',5,5'-tetramethylbenzidine in the presence of hydrogen peroxide (H_2O_2), resulting in a blue solution. The α -amylase detection mechanism is based on the digestion of starch by α -amylase, which leads to the aggregation of nanoclusters (NCs), resulting in an increase in nanoparticle size and, thus, a decrease in Cu/Au NCs

peroxidase-like activity. It was shown that the gradual addition of α -amylase resulted in a linear decreasing trend of peroxidase activity. The method enables the colorimetric detection of α -amylase with a detection limit of 0.04 U/mL, which has good selectivity for α -amylase in serum [70]. Chen et al., on the other hand, used γ -cyclodextrin (γ -CD) as an amylase probe in combination with a specially designed MOF-929-NH₂ with strong peroxidase properties [71]. The detection limit was reduced by more than 300-fold compared to the starch–gold nanoparticle combination.

In addition to designing chemical principles, improving sensors is also an important research direction. Specialized colorimetric equipment tends to have a large size and weight, limiting its application. A colorimetric detection device that can be miniaturized was also designed by Hsiao et al. A handheld instrument with a chemical colorimetric strip was used to detect reducing sugars from starch hydrolysis in the substrate using a DNS assay (Figure 4) [72]. A good correlation was achieved compared to a commercial ultraviolet-visible spectroscope. All these studies have greatly expanded the application scenario of colorimetric methods. Thongprajukaew et al. also achieved good detection using the camera of an iPhone (Figure 4d), which greatly enhanced the portable use of the colorimetric method. They used a standard DNS staining method to label maltose. The amylase changes the concentration of maltose upon the addition of the sample, which in turn changes the overall absorbance of the liquid. There was no significant difference in the results using the iPhone camera compared to the spectrophotometer, with a Pearson correlation coefficient close to 1 ($r = 0.999$, $n = 36$, $p < 0.0001$) [73]. Based on the same color-development method, Dangkulwanich et al. also implemented UV-vis spectroscopy using a smartphone [74]. Students used this method to realize the measurement of amylase activity.

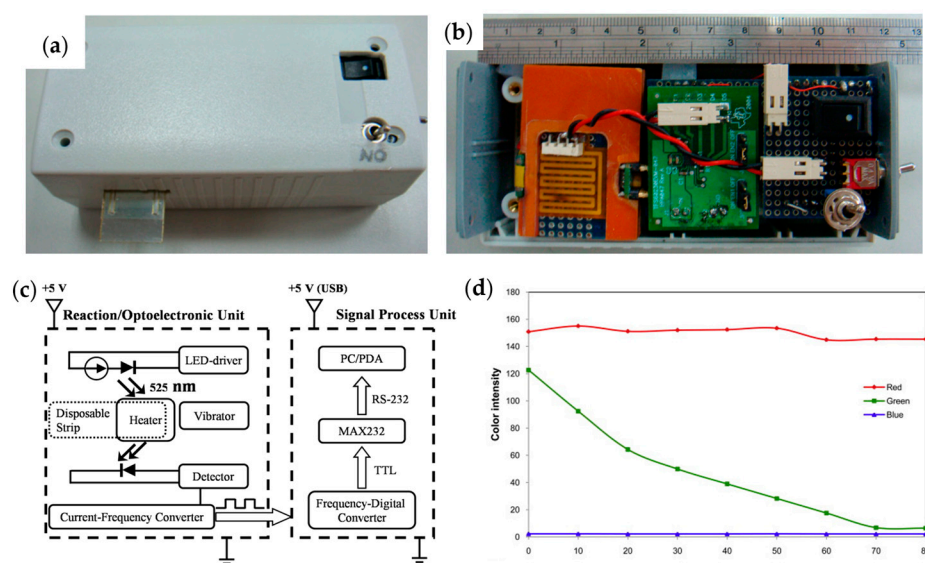


Figure 4. Appearance (a), internal structure (b), and circuit diagram (c) of the handheld colorimeter. Reproduced from [72] under the terms of the CC-BY Creative Commons Attribution License, copyright 2019 MDPI. (d) Relationship between maltose concentration and RGB intensity detected by iPhone. Reproduced with permission from [73], copyright 2014 by Elsevier Ltd.

The popularity of smartphones has facilitated the measurement aspect of colorimetric methods. But the need to have colored compounds leads to the necessity of sample pre-processing. The colorimetric method's detection limit is inferior to the fluorescence method.

2.3.3. Fluorescence Methods

The colorimetric method requires an external light source to illuminate and detect the projected or reflected light. In contrast, if the marker is fluorescently labeled, it can be

self-luminous, and thus the structure of the light source in the system can be subtracted (Figure 5) [75]. By designing probes with fluorescent properties in the substrate, the effect caused by the enzyme on the optical properties of the substrate can be further enriched, and the miniaturization potential of the device can be further increased.

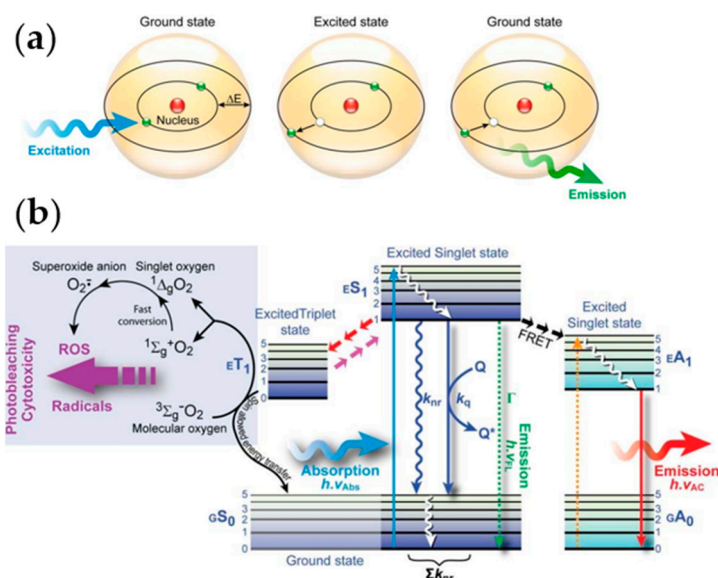


Figure 5. (a) Schematic diagram of the luminescence principle of fluorescence. (b) Schematic diagram of the energy bands of fluorescence and related phenomena. Reproduced from [75] under the terms of the CC-BY Creative Commons Attribution License, copyright 2012 MDPI.

The core of the fluorescence method is that it allows the presence of amylase to modulate the occurrence or absence of fluorescence. Based on this, there are two main ideas. One is to design probes that can be quenched by the starch in the substrate so that fluorescence cannot be emitted in the absence of amylase, and fluorescence is activated after the amylase hydrolyzes the starch. The second is to design fluorescent probes that can be quenched by starch hydrolysis products, where the fluorescence is emitted in the absence of amylase and quenched after the starch is hydrolyzed.

An example of the first approach is realized by Wang et al. They achieved fluorescence detection by AIE luminescence, achieving 0.007902 U/mL for α -amylase detection. They designed TTAM with high fluorescence quantum yield and assembled it with β -cyclodextrins (β -CD) as a supramolecular system. TTAM spins freely within the β -CD cavity, leading to fluorescence quenching. α -Amylase breaks down the complex and reorganizes TTAM into aggregates, reverting to the yellow fluorescence generated by the AIE property [76]. In addition to starch, specially designed probes that can be recognized by amylase have also been reported. Shi et al. designed a rapid, highly sensitive fluorescent assay to directly determine α -amylase in human body fluids. They used an aggregated luminescence method with a probe composed of two methoxy-substituted tetraphenyl ethylene (TPE) core chains and a maltose unit. The probe is soluble in water molecules and does not fluoresce. α -Amylase catalyzes the cleavage of the α -1,4 glycosidic bond in the probe, and the maltose unit is released. The chromophore 4-(2,2-bis(4-methoxyphenyl)-1-phenylethenyl) phenol aggregates, which in turn fluoresces by aggregation-induced emission (AIE) [77].

Fluorescent polymers that can be quenched by α -amylase were designed by Li et al. [78]. Perylene is a classic organic chromophore with strong π - π stacking. The α -cyclodextrin (α -CD) molecules can form four hydrogen bonds because there is a glucose unit in the position of the distortion. The α -CD plays a key role in the specific response of the α -amylase. The combination of these substances activates the fluorescent structure. The fluorescence is extinguished after the polymer is broken down by amylase (Figure 6). Attia et al. reported a study using fluorometric detection. The α -amylase enzyme was measured

to react with the starch in the substrate to produce maltose. Maltose significantly affected the fluorescence quenching of CdS nanoparticles (NPs). The α -amylase activity in saliva samples was effectively assessed [79]. They presented an improved method in 2016 using the reaction product of α -amylase with the substrate to quench the fluorescence luminescence of the binuclear complex. With a correlation coefficient of 0.999 and a detection limit of 7.4×10^{-10} mol/L, it was effective in detecting amylase activity in the urine and serum of patients with pancreatitis. α -Amylase biomarkers showed a significant improvement in early diagnostic sensitivity (96.88%) and specificity (94.41%) [80].

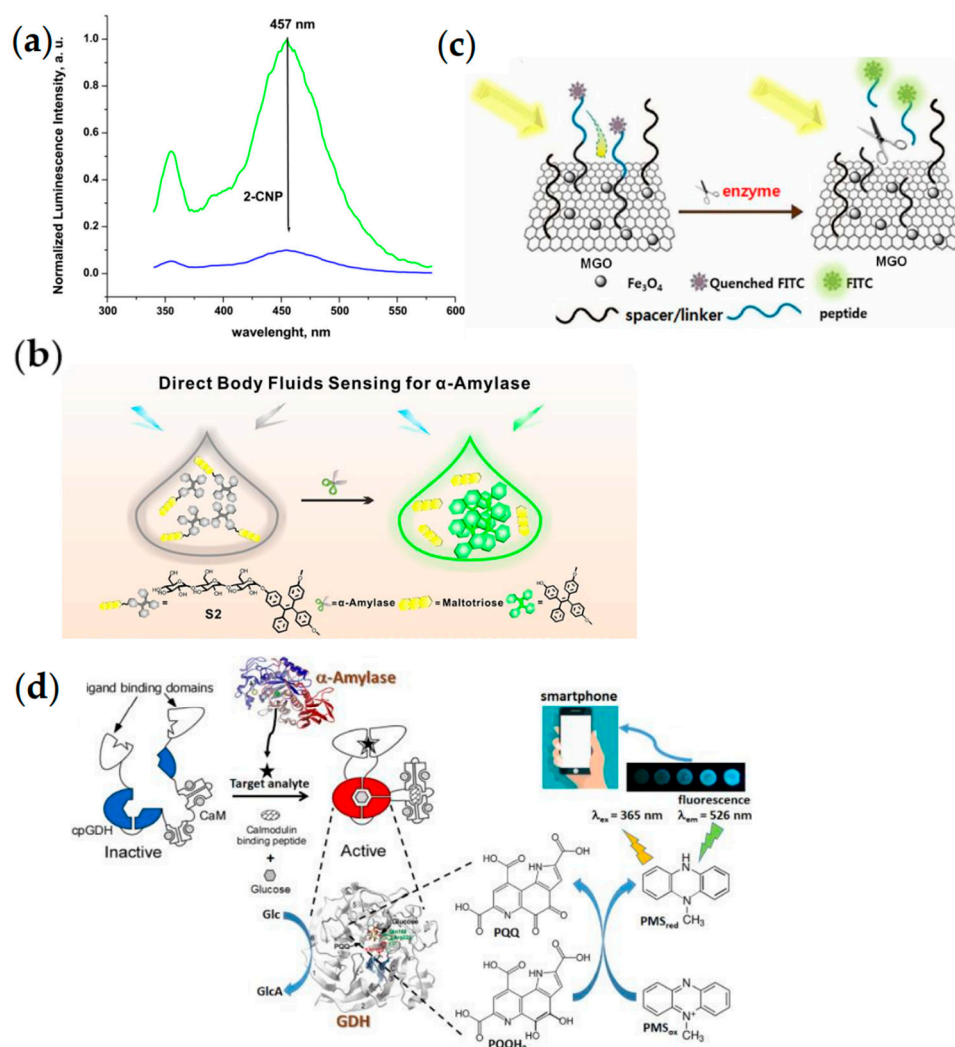


Figure 6. Different ideas for fluorescence detection methods. (a) The introduction of α -amylase causes the fluorescence to be quenched and the brightness to decrease. Reproduced with permission from [80], copyright 2016 by Elsevier Ltd. In (b–d), fluorescence is activated after the introduction of α -amylase. The principles of quenching fluorescence include limiting the travel of structures where fluorescence can occur and immobilizing a substance on the fluorescent substance that can quench fluorescence. (b) The substrate restricts the aggregation of the fluorescent substance. Reproduced with permission from [77], copyright 2018 by American Chemical Society. (c) The substrate immobilizes the fluorescent material near the MGO material, which can quench the fluorescence. Reproduced from [81] under the terms of the CC-BY Creative Commons Attribution License, copyright 2020 MDPI. (d) Reacts to produce fluorescent chemicals. Reproduced with permission from [82], copyright 2022 by Elsevier Ltd.

Similar to colorimetric methods, the measurement of fluorescence often requires the use of specialized optical equipment. To achieve portability, a study reported sensing

using a smartphone camera. Wells et al. implemented a fluorometric measurement of α -amylase with a detection limit of 2 pM using a Samsung GALAXY S20+ cell phone. α -Amylase activates an α -amylase-activated PQQ-dependent glucose dehydrogenase (Amy-GDH) on the surface of the sensor. The glucose oxidation reaction with a poly-maleimide reduction is catalyzed using the Amy-GDH enzyme. After shaking in the HEPES buffer and irradiation using a UV lamp, fluorogenic phenomena occur and are captured by the smartphone camera [82].

As can be reflected in the above introduction, the fluorescence detection method of digestive enzymes often uses nutrients as the material connecting the fluorescent substance to the quenched substance (Figure 6) [81]. Fluorescence is released in the presence of digestive enzymes. This has many applications in the sensing of the remaining digestive enzymes.

Fluorescence methods have a wealth of signal amplification methods that allow for high sensitivity. However, as the reaction becomes more complex, the processing of the sample tends to increase.

2.3.4. Liquid Crystal Phase Transition Methods

Pham Thi Kim et al. designed a novel liquid crystal-based sensor to achieve the detection of α -amylase at 100 ng/mL in an aqueous solution and 500 ng/mL in urine samples. [83]. These devices are characterized by long-term stability, taglessness, and ease of use. Specifically, in the microvasculature LC droplets are oriented parallel to each other at the interface with water, forming two bright lines. α -Amylase decomposes β -cyclodextrin and releases its encapsulated sodium dodecyl sulfate (SDS). SDS is a surfactant molecule. SDS induces LC droplets to align at the vertical interface when in contact with the surfactant solution, forming a tetra valve-shaped optical image. The liquid crystal phase change method allows the action of amylase to be visualized (Figure 7).

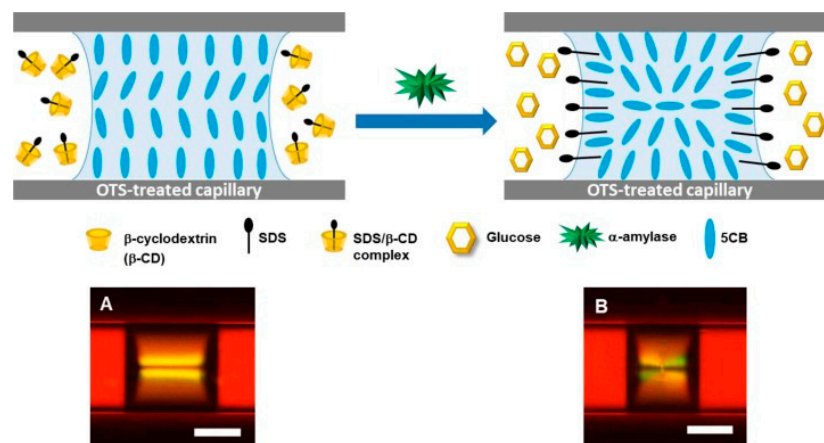


Figure 7. The hydrolysis of the substrate by amylase affects the arrangement of the liquid crystal molecules, showing different patterns. (A) Two bright lines indicate the planar orientation of the LC at the LC-aqueous interface after adding a synthetic β -CD/SDS solution, (B) four petal-shaped texture indicates a switch to the homeotropic orientation after the addition of a α -amylase hydrolyzed solution of β -CD/SDS. Scale bar = 200 μ m. Reproduced with permission from [83], copyright 2020 by Elsevier Ltd.

2.3.5. Surface Plasmon Resonance

Finally, there is a special optical detection method, surface plasmon resonance (SPR) (Figure 8) [84–87]. It utilizes electromagnetic waves coupled to oscillations of carriers within a conductor, which in turn transforms the chemical signal into a change in the intensity of reflected light.

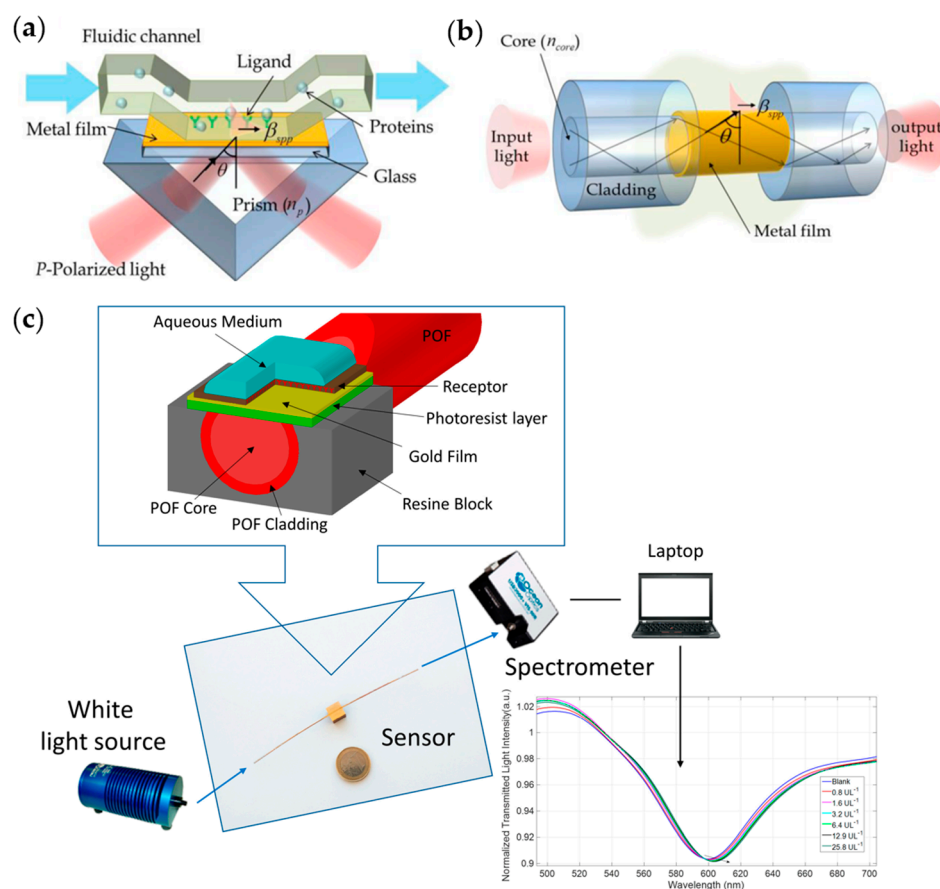


Figure 8. Basic schemes for SPR sensors with (a) Kretschmann-configuration-based coupling and (b) waveguide-based coupling. Reproduced from [87] under the terms of the CC-BY Creative Commons Attribution License, copyright 2011 MDPI. (c) Fiber-based SPR for alpha-amylase detection. Reproduced from [88] under the terms of the CC-BY Creative Commons Attribution License, copyright 2021 MDPI.

Its basis is that when a nanometallic layer receives electromagnetic wave irradiation, its carriers undergo an overall oscillation due to electric field forces. The resonance occurs when the frequency of the incident light coincides with the intrinsic frequency of the carrier oscillation, and in turn, a distinct absorption peak can be observed in the reflected light. The dielectric constant and refractive index of the environment in which the metal is located affect the carrier oscillation frequency, affecting the intensity of the absorption peak and the frequency at which the peak is located. By immobilizing a substrate on the metal surface, the change in intensity of reflected light can be manifested when the marker binds or reacts with the substrate. Compared to colorimetric methods that measure the absorbance of the compound itself, the SPR method applies optical measurements to the detection of antigen–antibody binding reactions and has the potential to provide a more sensitive and selective assay [88]. The combination of fiber optics and other technologies also promotes the low-cost and convenient application of SPR technology [89,90].

Studies utilizing the SPR method to detect amylase have been reported. On the surface of a 60 nm gold layer, anti-amylase antibodies were immobilized by Qasquardini et al., and they formed self-assembled monolayers by α -octyl sulfate and immobilized the antibodies by forming covalent bonds with the surface via acetamide-carbodiimide coupling (Figure 8d) [88]. The plastic-optical-fiber-based SPR sensor used has a very low manufacturing cost, allowing fast and accurate detection [89]. This sensor detects amylase levels in fluid samples drained from drains after pancreatitis surgery with a limit of detection (LOD) of 0.5 U/L, which was log-linear in the 0.8–25.8 U/L range. As a simple, rapid, and inexpensive method, it has 92% accuracy compared to the gold standard.

2.3.6. Chemiluminescence Methods

In addition to colorimetric and fluorescence methods, Zhang et al. reported a chemiluminescence (CL)-based method for α -amylase detection. Similar to the work of Dehghani et al. [70], they also exploited the fact that starch can stabilize Cu/Au nanoclusters. The α -amylase hydrolysis of starch leads to nanoparticle clusters that exhibit reduced peroxidase-like activity. The reaction rate of catalytic H_2O_2 generation of reactive oxygen species is reduced, resulting in a weakened CL signal. The minimum LOD was 0.006 U/mL, and the detection range was 0.05 to 8 U/mL [91].

2.4. Mechanical Methods

Mechanical methods are also a common class of detection techniques. When the type and concentration of a substance change it changes the viscosity of the solution or the mass of the probe. This type of change in mechanical properties alters the mechanical response of a solution to an external force, for example, the intrinsic frequency of mechanical vibrations, flow velocity, etc., which in turn can be sensed mechanically.

2.4.1. Resonance Methods

A class of resonant sensors was realized based on mechanical vibrations or the resonance of acoustic waves. The quartz crystal microbalance (QCM) takes advantage of the piezoelectricity of the material to realize the coupling of mechanical vibrations of the surface with electrical signals. The change in surface mass will affect the system's resonant frequency [92–96]. In shear test mode, it is also possible to characterize the viscosity of the liquid in contact with the sensor [97–99]. Related studies are reported in Section 3.3.

Ventura et al. realized a study to implement a pancreatic amylase assay using a QCM. This is also a sensor device with good durability and ease of use, suitable as a portable HAS detection device. The principle is based on a thin gold layer, which was functionalized using the photochemical immobilization technique (PIT). In this way, vertically oriented antibodies are immobilized, exposing their binding sites, which affects the system's resonant frequency after the marker is bound. Their improvement is the formation of a sandwich structure by binding the antibody to amylase, which allows further signal amplification and achieves an LOD of 10 U/L. The sensor can be applied to the detection of amylase concentrations in body fluids such as serum and urine at levels higher than 20 U/L [100].

2.4.2. Viscosity Methods

Zhao et al. reported an α -amylase assay based on changes in solution viscosity, achieving an LOD of 0.017 U/mL [101]. In branched starch solutions, the proportion of hydrolyzed branched starch affects the overall viscosity of the solution, which in turn changes the diffusion length of the aqueous solution on the pH test paper (Figure 9). This method uses paper that is commonly and inexpensively available and does not require pretreatment of the pH test paper, such as substrate fixation, making it an ideal portable assay.

2.5. Electrical Methods

Optical methods have a large volume of light sources and photoelectric sensors. Electrical information of the sample solution, such as conductivity, current, etc., can be measured directly to achieve portability or even wearable sensors. Electrical sensors can have a high level of integration and digitize the electrical signal directly.

2.5.1. Resistance Measurement

A flexible patch sensor was prepared by Bhattacharjee et al. Vortex currents were generated within the droplet by applying a thermal gradient containing starch and an $FeSO_4$ substrate in the liquid. As the amylase hydrolyzes the starch, it changes the concentration of ions within the droplet, which changes the conductivity of the droplet. The change in

resistance can be detected between the electrodes of the patch sensor. The sensitivity of the sensor is almost three times higher than that of the optical sensor [102].

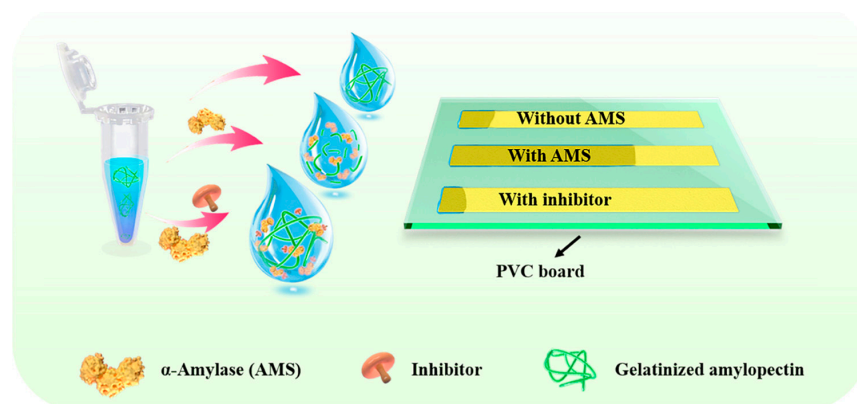


Figure 9. Principles of sensing by the viscous method. Hydrolysis by trypsin increases the fluidity of the liquid, which can flow longer distances on pH test paper. Reproduced with permission from [101], copyright 2022 by American Chemical Society.

Mandal amplified the resistance changes by NPs. The sensor was composed of a glass substrate coated with an electrically conducting polyaniline-emeraldine-salt film covered with starch-coated AuNPs. The amylase causes an increase in the resistance of the device after consuming the starch layer. The detection range of this method is from 25 to 110 U/L. The chloride ions and AuNPs catalyze the reaction of amylase with starch [103].

2.5.2. Giant Magnetoresistive Sensors

In addition to changes in electrical conductivity, changes in magnetic conductivity can also be used to measure chemical substances [104,105]. The giant magnetoresistive (GMR) sensor is a promising biosensor [106–108]. However, this approach often requires magnetic particles to label marker molecules and has high sensitivity for green-synthesized Fe_3O_4 nanoparticle tags because of their ferromagnetic properties. A 0.098 mV/mg/mL detection was also achieved by Mabarroh et al. using Fe_3O_4 tags labeled with α -amylase [109].

2.5.3. Electrochemical Methods

Electrochemical methods are also one form of translating chemical reaction occurrence directly into electrical signals.

First, electrochemical sensing can detect antigen–antibody binding reactions with appropriate signal amplification methods. This is more difficult with optical methods, especially colorimetric methods. The advantage of this method over detecting changes in the hydrolysis reaction is that the effect of temperature, collection time, and other factors on amylase activity can be excluded. But the technique of antibody immobilization and preservation is critical. The amplification of electrochemical reaction signals was studied by Martins et al. They detected the reaction between α -amylase and α -amylase antibodies immobilized on an electrode (Figure 10a). The addition of zinc oxide and copper oxide was found to amplify the electrochemical signal collected by the graphite electrode by 40% with a minimum LOD of 0.00196 U/mL [110]. The large surface area, high conductivity, and biocompatibility of graphene were used by Teixeira et al. to design high-performance electrochemical sensors. They used polyaniline for electropolymerization on the graphene surface and immobilized antibodies on polymer films for the detection of the presence of α -amylase. Cyclic voltammetry (CV) and electrochemical impedance spectroscopy (EIS) measurements were used for electrochemical analysis. The response was linear for α -amylase concentrations in the 1~1000 international units/L (IU/L) range with an LOD of 0.025 IU/L [111].

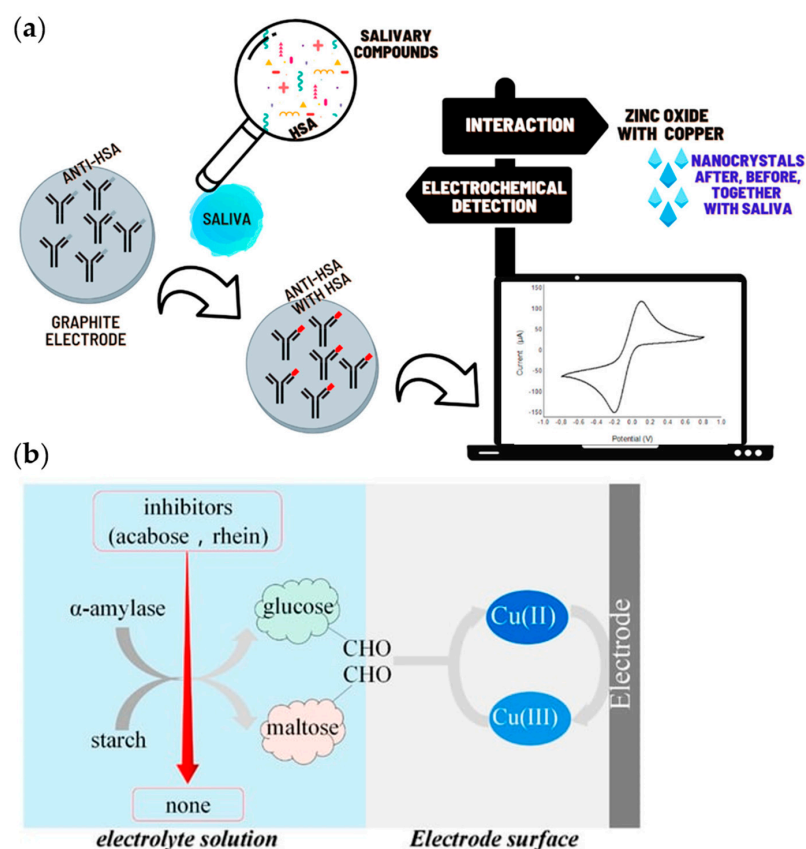


Figure 10. (a) Electrochemical method for sensing anti- α -amylase antibodies bound to α -amylase. Reproduced from [110] under the terms of the CC-BY Creative Commons Attribution License, copyright 2021 MDPI. (b) Schematic diagram of ion electrochemical detection using the reductive nature of amylase hydrolysis products. Reproduced from [112] under the terms of the CC-BY Creative Commons Attribution License, copyright 2022 MDPI.

Then, the idea of detecting the concentration of substrate and hydrolysis products, and thus analyzing the concentration of amylase, still applies. Garcia et al. detected salivary α -amylase (sAA) in human saliva samples using screen-printed carbon electrodes (SPCE). Basically, the first reaction is the hydrolysis of starch by sAA to produce maltose. Then, the generated reducing sugar promotes the conversion of $[\text{Fe}(\text{CN})_6]^{3-}$ into $[\text{Fe}(\text{CN})_6]^{4-}$ in a second reaction. The method has a minimum LOD of 1.1 U/mL and accuracy between 90% and 97% [113]. The glucose assay was designed by Min et al. using copper oxide and boron-doped graphene oxide as electrodes. The copper oxide was oxidized to Cu(III) at an oxidation peak of +0.4 V (Figure 10b). Cu(III) ions act as electron transfer carriers upon the addition of glucose, rapidly transferring electrons from glucose to the electrode. The LOD for glucose was 0.7 μM , and its cost-effective, simple, and reliable properties are also expected to be used for α -amylase activity detection [112]. Mahosenaho et al., on the other hand, used a combination of more enzymes. They used three enzymes, GOD, alpha-glucosidase (GD), and mutarotase, immobilized on a Prussian-blue-modified screen-printed electrode. The screen-printed electrode had a working electrode of graphite, a counter electrode, and a silver reference electrode. The response of the sensor was improved six-fold by the addition of the combined enzymes [114].

Finally, similar to optical sensing, some researchers have made efforts to miniaturize electrical sensing devices. Electrochemical test strips for testing amylase concentration were designed by Sun et al. [115]. A carefully designed microfluidic channel allows a saliva sample that has reflected the starch in the sample for some time to flow through two channels. Both channels contained $[\text{Fe}(\text{CN})_6]^{3-}$, but one was in the alkaline condition and the other was neutral. In the presence of amylase, the hydrolyzed maltose reduces

$[\text{Fe}(\text{CN})_6]^{3-}$ to $[\text{Fe}(\text{CN})_6]^{4-}$ and causes a potential difference between the two channels. The convenience of the electrical measurement method was demonstrated by the study of a smartphone-powered potential reader that reads potential information directly and sends it directly to the cell phone through the USB port, as reported by Zhang et al. The substrate reagents included starch, $\text{K}_3[\text{Fe}(\text{CN})_6]$, and NaOH . The measured potential was linearly correlated with the logarithm of the α -amylase concentration with a correlation coefficient of 0.995. The minimum LOD was 0.12 U/mL, with a good fit in the 30 U–1 kU/mL range. The cost of a single device is less than USD 0.2, the substrate is stable at room temperature, and it only needs to be plugged into a cell phone to work, providing good ease of use and portability [116].

The great advantage of the electrical method is that electrical signals can be processed by computers or intelligent devices with relative ease. Equipment for electrical measurements is also often superior in size to optical systems that require the construction of light paths.

2.6. Other Methods

2.6.1. Blood Glucose Meter Methods

Many studies for detecting α -amylase are based on the use of α -amylase and coenzymes to break down polysaccharides into glucose and thus measure glucose concentration. The portable glucose meter is an existing and well-established method for glucose concentration detection. Wang et al. used maltopentaose as the substrate, and α -amylase in the sample would break it down into maltotriose and maltose. α -Glucosidase added as a coenzyme would further break it down into glucose, which was detected by the glucose meter. The LOD obtained by this method is 20 U/L [117]. Due to the low equipment requirement of this method, it is suitable for the Point-of-Care field, especially in rural areas where laboratory conditions are lacking.

2.6.2. Antigen Test Strip Methods

The Rsidtm saliva test, reported by Casey et al., is a lateral flow immunochromatographic strip test (Figure 11a). Two human salivary amylase monoclonal antibodies are used, which upon binding to amylase form a red line on the strip, allowing direct reading of the results by the human eye. The LOD for amylase in salivary body fluids can be as low as 50 ng/mL [118].

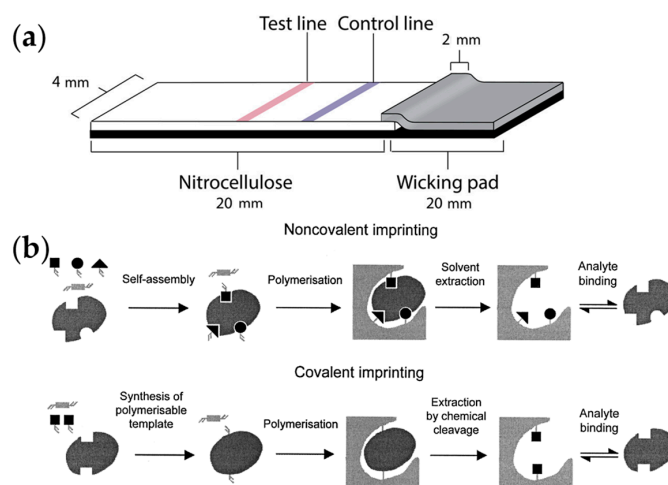


Figure 11. Some special methods. (a) Antigen test strips that were widely used during the COVID-19 outbreak. Reproduced from [119] under the terms of the CC-BY Creative Commons Attribution License, copyright 2020 American Chemical Society. (b) Molecularly imprinted polymers for sensing molecules. Reproduced with permission from [120], copyright 2000 by American Chemical Society.

2.6.3. Isothermal Titration Calorimetry

Isothermal titration calorimetry (ITC) is a commonly used technique for the study of molecular interactions and is of increasing importance in enzyme kinetic studies due to its general applicability and sensitivity [121–123]. Compared to methods such as spectrophotometry and chromatography, it allows direct measurement of reaction rates [123–125]. However, it requires relatively specialized equipment. If there are future advances in portability, it will have great potential for POCT applications.

2.6.4. Molecularly Imprinted Polymer Methods

Molecularly imprinted polymers (MIP) are also a sensing technology that is easily miniaturized and portable (Figure 11b) [126]. The sensing principle is based on the immobilization of α -amylase in a gold layer surface treated with a cysteamine self-assembled monolayer and electropolymerization using a pyrrole monomer. After the α -amylase is removed, a molecular imprint is left in the polymer. This is followed by electrical analysis using techniques such as square wave voltammetry [127]. The advantage of this method is that it does not require high molecular organics such as antibodies and has better stability and lower cost.

Also, a fluorescence assay using molecular imprinting technology (MIP) was reported by Yan et al. The accuracy and precision of measuring α -amylase activity were higher than that of the conventional UV-visible method, demonstrating the MIP method's potential for measurement accuracy [128].

2.7. Summary

The sensing methods of amylase mainly include the hydrolytic substrate method, antibody method, and molecular blotting method. The hydrolytic substrate method includes probes such as starch-iodine, TMB-H₂O₂, and starch-gold nanoparticles. There are also methods for the direct reading of electromagnetism information from solutions. The specific results are shown in Table 1. Many methods can be distinguished by the naked eye or a cell phone camera, and some methods can be achieved by test strips or portable sensors, all of which facilitate the timely diagnosis and long-term follow-up of pancreatitis.

Table 1. Amylase sensing technology.

Type	Probes/Substrates	LOD	Sensing Range	POCT Progress	Ref.
Amylose Sensing	Transmittance sensing of amylose-iodine blue compounds	\	10–110 U/L	Paper-based	[65]
	Chitosan-triphosphate nuclei encapsulated with amylose-iodine shell structure	1.25 mg/mL	\	Human-eye readable	[67]
	Starch-stabilized CuNPs; TMB color development	0.04 U/mL	0.1–10 U/mL	Human-eye readable	[70]
	Starch-stabilized CuNPs and AuNPs	0.006 U/mL	0.05–8 U/mL	Human-eye readable	[91]
	Starch fixes AuNPs and increases resistance after being decomposed	\	25–100 U/L	Achieved POCT device	[103]
	Viscosity changes after starch hydrolysis	0.017 U/mL	0–10 U/mL	Paper-based	[101]
Hydrolysis products Sensing	3,5-dinitrosalicylic acid sensing reducing sugars	\	0.1–1 U/mL	Handheld	[72]
	Reduction in a substrate by a reducing sugar produces a potential difference	\	125–2000 U/mL	Portable Test Strips	[115]

Table 1. Cont.

Type	Probes/Substrates	LOD	Sensing Range	POCT Progress	Ref.
	Dinitro salicylic acid staining method to label maltose	$3.5 \pm 0.3 \mu\text{mol/mL}$	0–70 $\mu\text{mol/mL}$	Using smartphone	[64,73]
	Reduced phenazine methosulfate upon glucose oxidation by Amy-GDH	2 pM	2–150 pM	Using smartphone	[82]
	Hydrolysis improves electrical conductivity	\	15–110 U/L	Miniature patch electrode	[102]
	Reduction in trivalent iron ions by reducing sugar	1.1 U/mL	1.1–10.7 U/mL	Miniaturized equipment	[113]
	Reduction in trivalent iron ions by reducing sugar	0.12 U/mL	30 U–1 kU/mL	Using smartphone	[116]
	Blood glucose meter	20 U/L	\	Blood glucose meter	[117]
Antigen-Antibodies	Fiber optic SPR	0.5 U/L	0.8–25.8 U/L	Cheap and small fiber optic structure	[88]
	Test strips	50 ng/mL	\	Easy-to-use, portable	[118]

3. Detection of Protease

Protein is an important and diverse nutrient. In contrast to starch, which is made from the polymerization of glucose, which is a monomer, proteins are made from the polymerization of 20 different amino acids. This means that protein molecules can have a much higher degree of complexity. Proteases are produced in the body by more than just the pancreas. Cells, especially lysosomes, contain tissue proteases, the detection of which has been reported to reflect viral infections [129]. This article focuses on the proteases secreted by the pancreas for the digestion of food. Depending on the chemical bonds that are hydrolyzed, different types of proteases digest proteins in the body. The most abundant of these is trypsin, followed by chymotrypsin and elastase.

Protease sensing has a high degree of similarity to amylase, and there are three main types of specific recognition: antigen–antibody binding, substrate hydrolysis, and special methods. The methods of acquiring signals can also be categorized as optical, mechanical, and electrical. Sensing principles similar to those of amylase will not be repeated in this section. However, special chemical mechanisms designed for proteases will be shown.

3.1. Trypsin

Trypsin is a type of protease. It is a serine protein hydrolase secreted by the pancreas and has a selective hydrolytic effect on arginine and lysine peptide chains. It is the most specific protease. Peptides containing trypsin recognition sites can be used as reaction substrates. Alternatively, anti-trypsin antibodies can also have good specific recognition of trypsin. By displacing different substrates, many techniques used for sensing amylase can be used for trypsin sensing. However, due to the different chemical properties of substrates, trypsin, and hydrolysis products, the design of probes and signal amplification methods differ.

Among the sensing studies of various types of digestive enzymes, trypsin is one of the most abundant. The spectroscopic method consists of high versatility and can be used to detect proteases such as amylase. Kuar et al. designed a substrate consisting of a negatively charged tetraphenyl sulfonyl derivative (Su-TPE) and a positively charged polyelectrolyte fish sperm protein (PrS), which was detected using different spectroscopic techniques employing ground-state absorption spectroscopy, steady-state emission spectroscopy, and time-resolved emission spectroscopy after the hydrolysis of PrS by trypsin. The LOD was 0.22 nM [130].

Trypsin accounts for approximately 19% of the total protein in pancreatic juice and is the most abundant of all pancreatic digestive enzymes [1]. Trypsinogen is the most important of all digestive enzymes because it regulates the rest of the digestive enzymes. Its detection is important for the diagnosis of pancreatitis. The next few subsections summarize the research on trypsin sensing.

3.2. Optical Methods

3.2.1. Colorimetry

Proteins have no common and stable-colored compounds similar to starch. A common idea for detecting proteases using colorimetric methods is to use the hydrolysis of proteins by proteases to affect the oxidizability of oxides in solution. The increased oxidizability will result in the oxidation of TMB to blue ox-TMB, enabling sensing. The specific substrates, methods to achieve oxidizability, and techniques to further amplify the signal are abundantly reported.

Cai et al. designed a colorimetric method based on CuNPs for protease detection. The colorimetric principle is the oxidation of TMB to ox-TMB, which in turn appears blue. The oxidation of TMB relies on the peroxidase (POD) property of CuNPs, which catalyzes the production of reactive oxygen species from H_2O_2 . By means of two cysteine peptide templates, the CuNPs were aggregated to form a shuttle-like structure, which inhibited their POD activity. In the presence of trypsin, the peptide chains were hydrolyzed, and the CuNPs were dispersed into the solution, exhibiting strong POD activity and thus sensing. This is somewhat similar to the previous study that used starch to polymerize nanoparticles and thus inhibit the catalytic activity of the nanoparticle structure. An LOD of 0.82 nM and a linear detection range of 3–1000 nM was eventually achieved [131]. Zhang et al. in 2015 found that Cyt c barely catalyzed this process, but trypsin-hydrolyzed Cyt c exhibited POD-ness. [132]. Wu et al. immobilized an Fe-NC single-atom catalyst (SAC) in a gelatin hydrogel. Trypsin hydrolyzed the gelatin and released the Fe-NC SAC, which catalyzed H_2O_2 to generate reactive oxygen species, which in turn oxidized TMB [133]. Wang et al. utilized the simulated peroxidase properties of AuNCs and stabilized them with bovine albumin (BSA). The trypsin decomposition of BSA affected the peroxidase action, inhibited the oxidation of TMB, and was detected by a colorimetric assay [134]. Luo et al. used the oxidative nature of ox-TMB to etch gold nanopyramids (AuNBPs), affecting their aspect ratios and thus achieving color changes. AuNPs were encapsulated using BSA, which has POD properties. Trypsin hydrolyzed BSA, exposing more catalytically active sites, which in turn led to a change in the color of the solution [135].

Lin's study used Pro-stabilized platinum nanoparticles (PtNPs), a unitary structure with oxidase-like activity [136]. Contrary to the study by Cai et al. [131], the peptide chain here served to avoid PtNP aggregation. After the breakdown of Pro by trypsin, the PtNPs become less active because of aggregation, and the color of the solution changes as a result. In another study reported later, Lin et al. designed structures with the more oxidase-like activity of PtNPs and used substrates with more pronounced color change, which lowered the LOD to 0.6 ng/mL with a linear range of 1–70 ng/mL. Citrate-capped terminated platinum nanoparticles (Cit-PtNPs) had stronger oxidase-like activity, using 3-methyl-2-benzothiazolinone hydrazone hydrochloride (MBTH) as a substrate to generate MBTH (-NH-) radicals. Also, in the substrate n-ethyl-n-(2-hydroxy-3-sulfopropyl)-m-toluidine sodium salt (TOOS), amateur Cit-PtNPs reacted. The catalytic mechanism of Cit-PtNP-like oxidase activity is a simultaneous two-electron reduction process and a four-electron reduction process during catalysis. The colorless compounds form blue-violet quinoid dye by disproportionation reactions [137].

Alternatively, nonspecific single-stranded DNA (ssDNA) can also interact with proteases, and its different interactions with different proteins can enable specific sensing. Chen et al. reported studies in which gold nanoparticles immobilized on the surface of ssDNA were desorbed when trypsin interacted with ssDNA and aggregated in a salt environment, producing colorimetric signal changes. Combining three different ssDNAs could

achieve the effective differentiated detection of nine different proteins [138]. Liu et al. used a similar principle by replacing AuNPs with silver nanoparticles (AgNPs), which were released from the ssDNA surface in the presence of trypsin. Adding TMB and H_2O_2 to the substrate, the AgNPs catalyze their reaction, changing the color and absorbance of the TMB solution [139].

3.2.2. Fluorescence Methods

As introduced in Section 2.3, fluorimetry is a common method of sensing digestive enzymes. The common idea is that the fluorescence is in a quenched state in the presence of protein and peptide substrates (Figure 12). When trypsin is introduced, the fluorescence is activated and thus sensed. It has been demonstrated that fluorescence quenching can be achieved by the electrostatic adsorption of trypsin with a fluorescent substance such as $MoSe_2$. Arora et al. revealed the mechanism of fluorescence inhibition by trypsin through the formation of complexes using Vant Hoff plots, fluorescence spectroscopy, and testing at different pH values. However, since the trypsin concentration in body fluid samples tends to be low, most studies still use specially designed substrates that can be hydrolyzed by trypsin for fluorescence sensing [140]. Specific ideas include the use of protein adsorption to directly affect fluorescence [141] or peptide chain linkage to quench the fluorescence of the substance [142] (Figure 12).

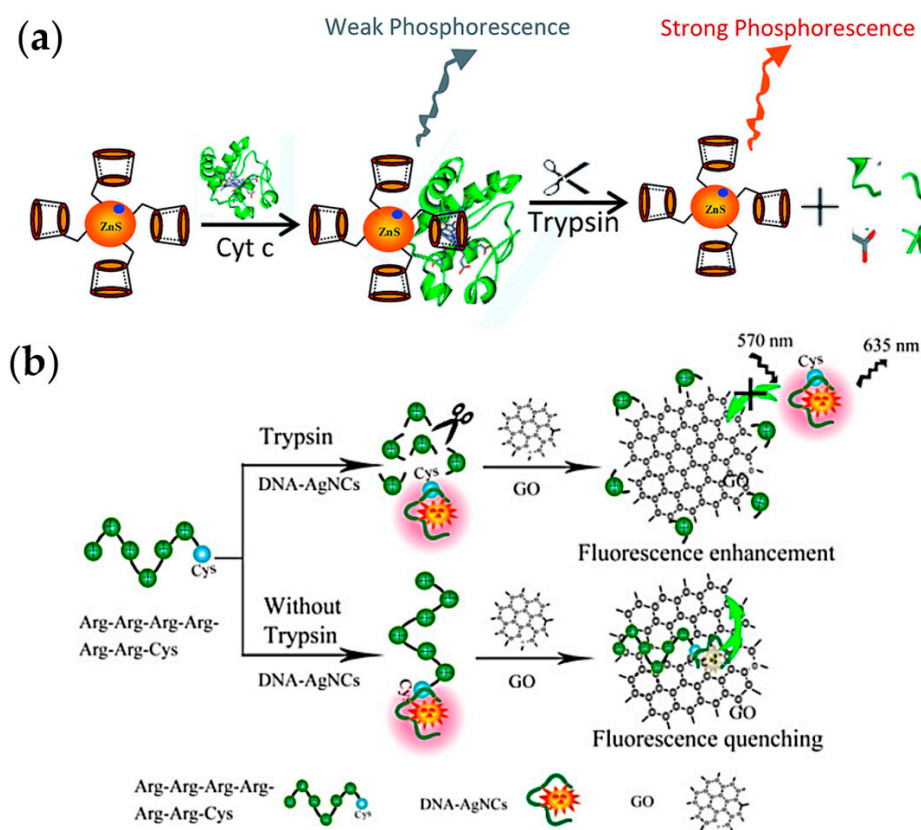


Figure 12. Fluorescent assay for trypsin. (a) Release of Cyt c from Mn-ZnS QDs. Reproduced from [141] under the terms of the CC-BY Creative Commons Attribution License, copyright 2017 by the Royal Society of Chemistry. (b) Release of AgNCs from graphene oxide. Reproduced from [142] under the terms of the CC-BY Creative Commons Attribution License, copyright 2016 MDPI.

First, the aggregation and release of metal nanostructures is the approach used in a large number of reports. The direct quenching of the fluorescence of AgInS quantum dots (AIS QDs) by trypsin was reported by Wang et al. The presumed reason was that when AIS QDs were irradiated, the photogenerated electrons were trapped by the positively charged

trypsin, resulting in the failure of the complexation of the photogenerated electron–hole pairs [143]. Milicevic et al. configured four fluorophores and three cleavage sites on the peptide chain to achieve a 0.5 ng/mL LOD for trypsin [144]. In 2011, using fluorescent metal nanoclusters, trypsin detection was performed by Hu et al. Gold nanoparticle clusters were prepared using BSA as a stabilizer and reducing agent. Trypsin decomposed the BSA, which destroyed the cluster structure and led to a decrease in fluorescence intensity [145]. Qu et al. used new fluorescent particles and peptide chains for polymerization by glutathione-capped gold nanoclusters (GSH-AuNCs) bound to positively charged arginine-rich peptides (Arg9). The aggregation-induced emission enhancement (AEE) of positively charged Arg9-GSH-AuNCs was induced by electrostatic attraction using polyuridylic acid (polyU) as a polyanion [146]. Xue et al. then used cationic fish sperm proteins adsorbed onto the surface of GSH-AuNCs to inhibit the self-assembly of the apparatus. The introduction of trypsin enhances fluorescence [147]. Zhao et al. also achieved trypsin detection using AuNCs. They used 11-mercaptotetradecanoic acid-covered AuNCs with carboxyl groups bound to Cu^{2+} , and the fluorescence was quenched. Trypsin catalyzed the BSA cleavage of amino acid/peptide fragments with stronger binding to Cu^{2+} , thus releasing the AuNCs to restore fluorescence [148]. Zheng et al. introduced 3-mercaptopropionic acid stabilized CdTe quantum dots (CdTe QD), whose electron attraction for trypsin promoted the breakdown of BSA covered on AuNCs [149]. Zhou et al. reported the work of quenching the fluorescence of silicon quantum dots (SiQDs) using triangular silver nanoprisms (TSNPRs) due to the internal filtering effect (IFE). Pro can strongly adsorb TSNPRs and release them from SiQDs. And the presence of trypsin breaks down Pro, leading to the quenching of fluorescence [150].

Secondly, carbon is also often used to make conductor materials that modulate the fluorescence effect. The detection of trypsin was also achieved by Hou et al. using carbon nanoparticles (CNPs) as a fluorescence quencher. The peptide chains were labeled using 5-carboxyfluorescein (FAM) containing Arg6 as a fluorescent substance. CNPs were oxidized by nitric acid with negatively charged functional groups and quenched fluorescence by an electrostatic interaction with the peptide chains via mutual adsorption. The protease decomposition of peptide chains releases FAM from CNPs and activates the fluorescence effect (Figure 13a) [151]. Using the coumarin derivative, Poon et al. quenched the fluorescence effect of graphene quantum dots using fluorescence resonance energy transfer (FRET). BSA linked the two and released the graphene quantum dots after trypsin hydrolyzed them, reactivating the fluorescence [152]. Wu et al. applied this method to the FRET effect between upconversion nanoparticles (UCNP) and AuNPs [153]. Xu et al. reported that the trypsin hydrolysis of a specially designed negatively charged peptide chain released a positively charged short peptide chain that induced the aggregation of AuNPs and that using FRET quenched the fluorescence of amino-functionalized carbon dots (CDs) [154]. A fluorometric-based protease detection technique using carbon quantum dots (CQDs) as a fluorescent material was also developed by Chen et al. Negatively charged CQDs are induced to aggregate by fisetin (Pro). Carbon quantum dots are well suited to the construction of biosensors because they can be easily modified and do not require complex surface functionalization to achieve the CQD/Pro aggregation caused by electrostatic interactions. The aggregation system causes fluorescence quenching, and the entry of Try hydrolyzes Pro and disperses CQDs, which in turn activates the fluorescence production (Figure 13b) [155]. A fluorescent probe involving tetraphenyl porphyrin tetrasulfonic acid (TPPS) with BSA as the substrate achieved an ultra-low-detection limit of 0.013 ng/mL for trypsin [156].

Chen et al. achieved a minimum LOD of 8.8 pg/L using molecularly imprinted fluorescence. Near-infrared carbon dots (NIR CDs) were used and combined with molecular blotting for the first time to measure trace amounts of trypsin. Trypsin was assembled onto the CDs@ZIF-8 surface via *in silico* interactions between APTES and TEOS and formed a molecular blot upon removal. The template proteins quench fluorescence upon rebound into the blotting cavity [157].

Subsequently, the design of peptide chains for the specific recognition of hydrolysis by proteases is also an important area of improvement for tryptic sensing. Giel et al. designed tryptic sensing that does not require special materials such as nanoparticles but instead relies on fluorescent polymer probes [158]. The β -aryl sulfonyl-containing probe was bound to BSA by forming covalent bonds with nucleophilic amino acids to form a fluorescent sensing system. When the probe is hydrolyzed by trypsin, it does not fluoresce in an aqueous solution. The complex and multifaceted structure of proteins brings convenience to the design of probes. Sun et al. quenched the anionic fluorochrome Eosin Y using fish sperm protein, achieving a trypsin LOD of 0.21 ng/mL and a linear detection range of 0.4–56 ng/mL [159]. The detection of trypsin in untreated urine samples was also achieved by Park et al. by utilizing fisetin [160]. They also analyzed the enhancement of exciton migration induced by fisetin as the reason why fluorescence was quenched with high sensitivity. Li et al. quenched poly(dopamine) nanoparticles (PDNs) with Pro binding. In dopamine nanoparticle (PDNP) fluorescence, the binding was also achieved by the negative electrical properties of PDNPs. By the same mechanism, the recovery of fluorescence was used to detect trypsin [161]. Gu et al. used thiosemicarbazone T as a fluorescent probe. This was performed by selecting DNA with a strong binder for cytochrome c (Cyt c) and also containing a g-quadruplex fraction with a high affinity for thiosulfonamide T, combined with the Cyt c hydrolysis of the Cyt c protein by trypsin, which exposes the g-quadruplex portion of the DNA, allowing thioredoxin T binding and enhanced fluorescence intensity [162]. Duan et al. used the peroxidase activity of the product after the hydrolysis of Cyt c by protease to form hydroxyl radicals, which in turn oxidizes o-phenylenediamine to 2,3-diaminophenothiazine. The latter quenched the fluorescence of tungsten disulfide quantum dots (WS₂ QDs) by fluorescence resonance transfer (FRET) [163]. Ou et al., on the other hand, quenched the fluorescence response of copper nanoparticles (CuNPs) directly using Cyt c hydrolysis products. The free cysteine residues released from the hydrolysis of Cyt c by trypsin form metal–ligand bonds with copper atoms through sulfur atoms to form complexes that quench the fluorescence [164]. Yin et al. used the positive charge of Cyt c to sense the aggregation of negatively charged nitrogen-doped carbon quantum dots (N-CQDs) and quenched the fluorescence of the latter [165].

Finally, this paper still summarizes the portable technology for tryptic colorimetric sensing. Hu et al. made this technique portable by 3D printing, which can be used based on a smartphone for POCT. An MIL-101 carrier was used to increase the number of imprinted sites using its porosity. Two types of CdTe, green and red, were introduced into the imprint to achieve fluorescence sensing. Cell phone cameras were used for measurements [166] (Figure 13d,e). Manmana et al. prepared hydrogels using polyethylene glycol diacrylate and fluorescein derivatives as the fluorescent detection probes. After hydrolysis of the gel by trypsin, certain areas of fluorescence fading can be seen, which can be observed by the naked eye. And the length of the faded region can be used to sense the trypsin concentration [167]. Zhao et al. combined two different fluorescent substances and achieved significant color changes by ratio modulation. The fluorescence of catechol B at 574 nm was inhibited using a fish sperm protein as a substrate. TPE was also immobilized to emit fluorescence at 472 nm. The ratio of the two fluorescences changed after trypsin decomposed the fish sperm protein, producing a color change visible to the naked eye [168].

3.2.3. Liquid Crystal Phase Transition Methods

Studies using LCs for trypsin detection have also been reported (Figure 14). A self-assembled monolayer of phosphatidylethanolamine-sn-glycero-3-phosphate-rac-(1-glycerol) sodium salt (DOPG) was prepared at the water/LC interface by Hu et al. The transfer of positively charged poly-L-lysine (PLL) here leads to an interaction with the negatively charged DOPG, resulting in the disorganization of the DOPG molecules, which in turn leads to the change in liquid crystal arrangement and the conversion of LCs from dark to bright. After the trypsin breaks down the PLL molecules, the DOPG and LCs resume their regular arrangement and turn dark [169]. Cetyltrimethylammonium bromide (CTAB) was

incorporated into the gelatin hydrogel by Ping et al. and released during the hydrolysis of gelatin by trypsin. Cetyltrimethylammonium bromide formed a monolayer molecular film on the surface of LCs, which in turn achieved the orderly arrangement of LCs and turned from good to dark under crossed polarizers. The LOD was 34 ng/mL [170].

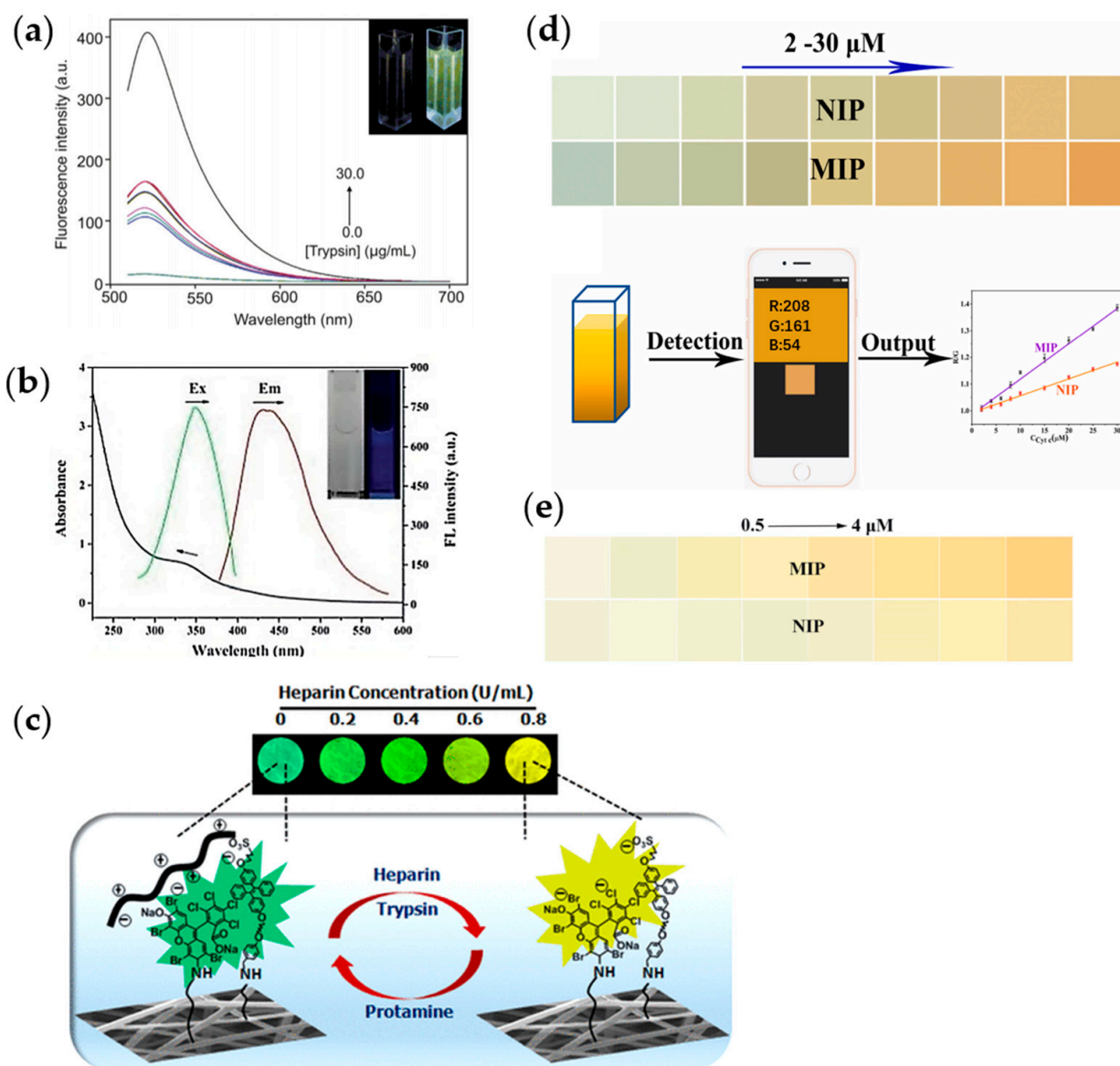


Figure 13. Schematic diagram of fluorometric sensing of trypsin. (a) The addition of trypsin causes an increase in fluorescence intensity. Reproduced from [151] under the terms of the CC-BY Creative Commons Attribution License, copyright 2020 by Elsevier B.V. (b) Change in fluorescence frequency. Reproduced from [155] under the terms of the CC-BY Creative Commons Attribution License, copyright 2020 by the Royal Society of Chemistry. (c) Fluorescence color change. Reproduced with permission from [168], copyright 2017 by American Chemical Society. (d) Fluorescence colors of different concentrations of substrates were captured by cell phone. (e) Effect of the introduction of trypsin on the two fluorescence colors. Reproduced with permission from [166], copyright 2023 by Elsevier B.V.

3.2.4. Localized Surface Plasmon Resonance

Localized surface plasmon resonance (LSPR) is an SPR-like plasma resonance phenomenon that occurs on conductor particles whose sizes are smaller than the wavelength of incident light [171,172]. Since the nanoparticle size is smaller than the wavelength of the

incident light, the carrier may undergo overall oscillation under the electric field during the period. Similar to the SPR effect on nanometallic layers, the change in the surrounding refractive index after the occurrence of a chemical reaction can be detected, and thus sensing can be achieved. LSPR can also be used for Trypsin detection (Figure 15).

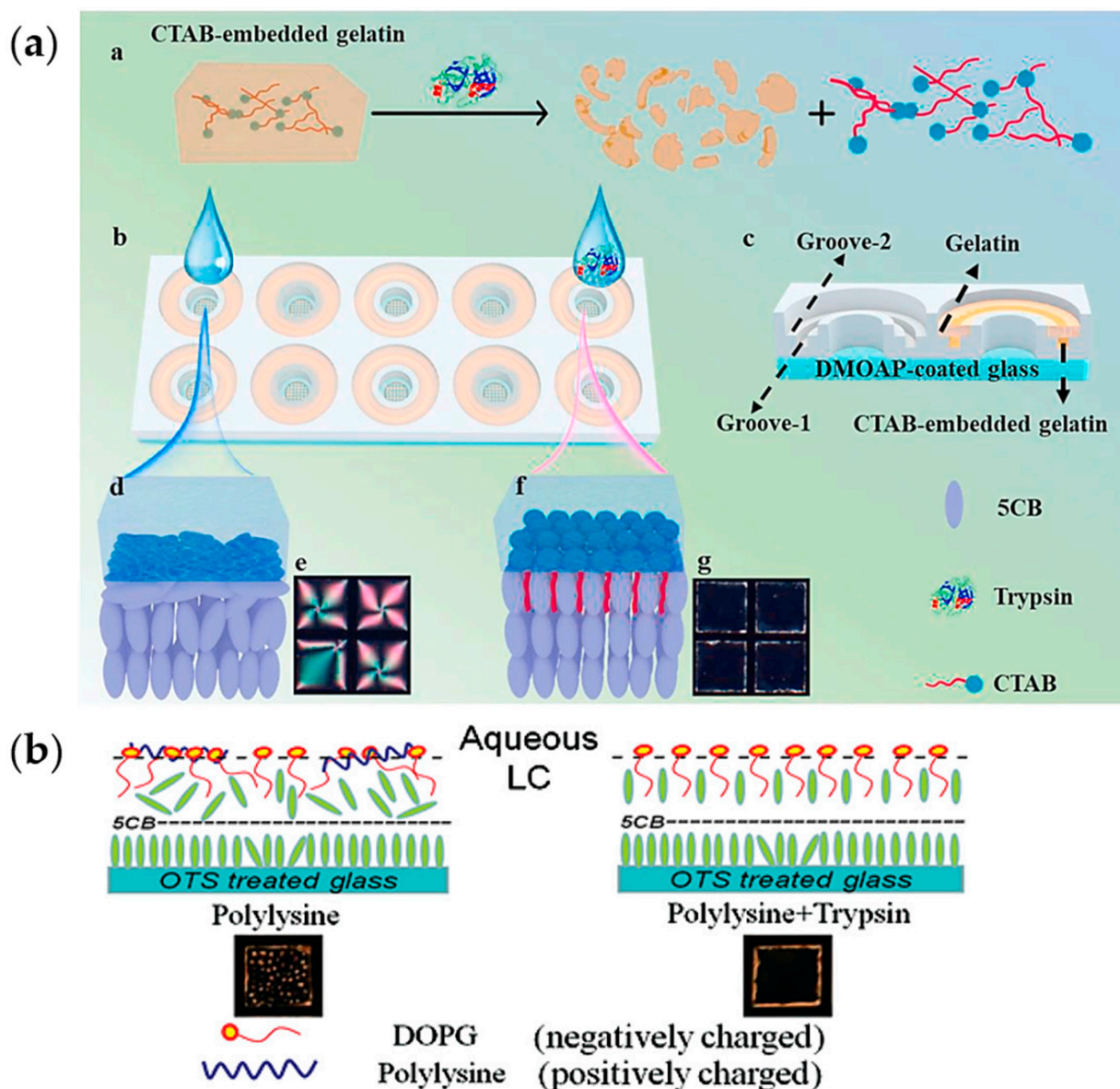


Figure 14. The hydrolysis of the substrate by trypsin affects the arrangement of the liquid crystal molecules, showing different patterns. **(a.a)** Illustration of the gelatin hydrogel decomposition and surfactant release induced by trypsin. **(a.b)** The whole and **(a.c)** cross-sectional view of the LC sensing device. The groove-1 is filled with the mixture of the gelatin hydrogel and CTAB. The groove-2 is coated with an additional thin layer of the gelatin hydrogel. In the absence of trypsin, the orientation of LC molecules is in a **(a.d)** planar state at the aqueous/LC interface, resulting in a **(a.e)** bright optical image; In the presence of trypsin, the orientation of LC molecules is in a **(a.f)** homeotropic state at the aqueous/LC interface, resulting in a **(a.g)** dark optical image. **(a)** Reproduced with permission from [170], copyright 2021 by Elsevier B.V. **(b)** Reproduced with permission from [169], copyright 2012 by American Chemical Society.

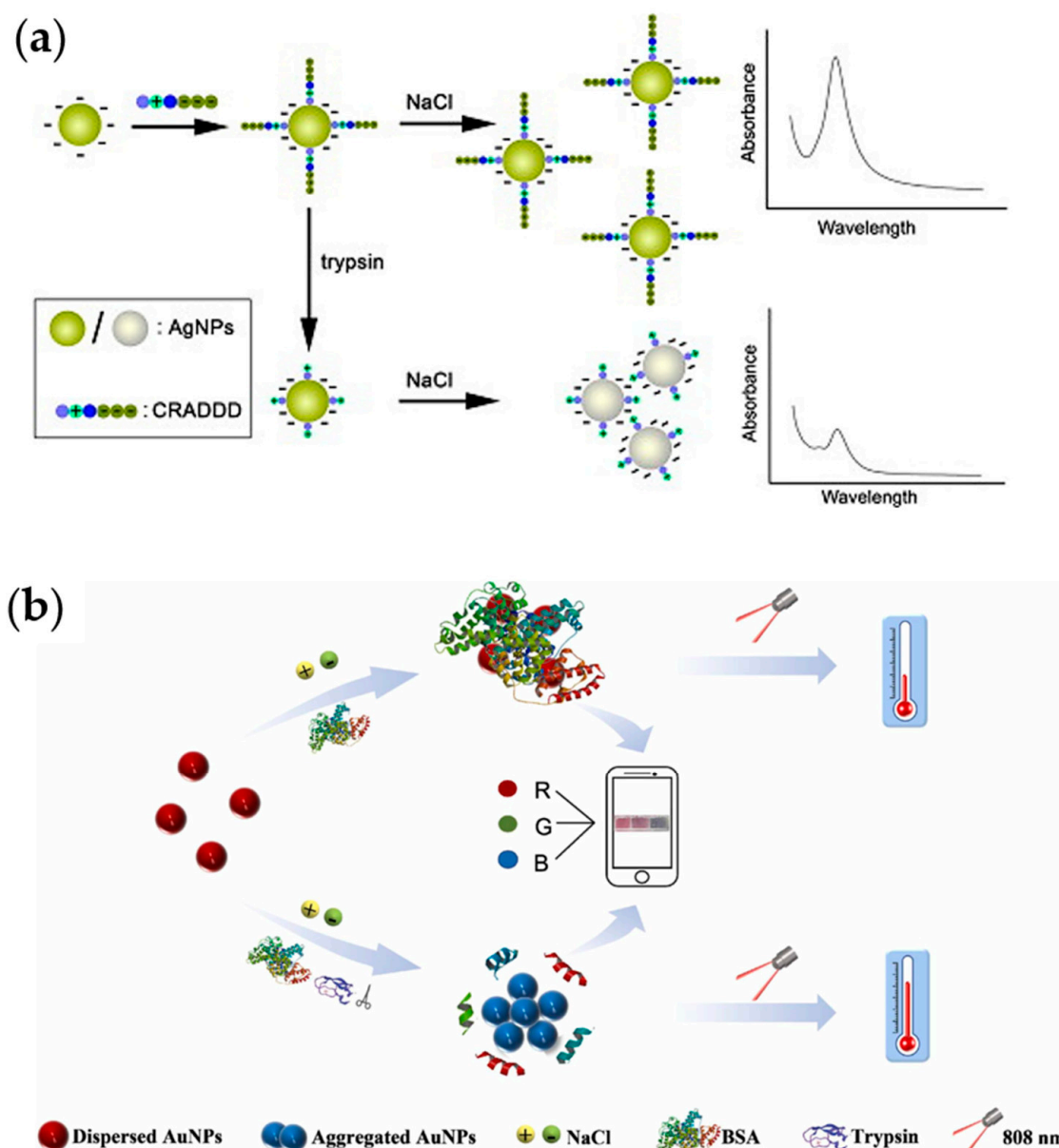


Figure 15. (a) Principle of trypsin assay using LSPR. Hydrolysis of the substrate alters the aggregation of the nanoparticles and affects the occurrence of their LSPR effect. Reproduced with permission from [173], copyright 2013 by Elsevier B.V. (b) Color sensing of changes in the LSPR effect of nanoparticles using a cell phone. Reproduced with permission from [174], copyright 2022 by Elsevier B.V.

The implementation of LSPR sensors using a smartphone camera was reported by Dutta et al. They prepared gold nanoparticles (AuNPs) as conductors for the occurrence of the LSPR effect. The cysteine residues on the surface of trypsin will form covalent bonds with the gold surface and achieve coupling between trypsin and gold nanoparticles. This will change the LSPR effect spectrum of the gold nanoparticles. The light is emitted by a light source in a specially designed optical accessory, passed through a solution, and then passed through a columnar lens to achieve spectroscopy, and the results are collected with a cell phone camera [175]. This handheld sensing can be applied to field applications in different scenarios.

Miao et al. stabilized AgNPs with short peptides, which undergo clustering after the short peptides are broken down by trypsin. Changes in the LSPR effect cause a change in their color, achieving an LOD of 2 ng/mL and a linear detection range of 2.5–200 ng/mL (Figure 15a) [173]. Guo et al. also designed a trypsin assay based on the LSPR effect

of AuNPs. BSA inhibited the clustering of AuNPs. After the entry of trypsin, which hydrolyzed BSA, AuNPs aggregated due to electrostatic effects, and their absorption spectra of the LSPR effect changed from red to blue RGB values. This method does not require the use of a specially designed optical device but can be achieved directly by a smartphone to distinguish colors and can achieve dual-mode sensing through the simultaneous photothermal effect (Figure 15b) [174]. It is favorable for POCT.

3.2.5. Electrochemiluminescence Method

Liu et al. investigated the application of the electrochemiluminescence (ECL) phenomenon of the luminol-H₂O₂ system in trypsin detection. Luminol was excited and its ECL effect was quenched by black phosphorus nanosheets (BPNs) via resonance energy transfer (ECL-RET). After Pro was bound to the BPNs via electrostatic interactions, blocking the ECL-RET, the luminescence was restored. A decrease in luminescence intensity was observed after the hydrolysis of Pro by trypsin, which was linear with trypsin concentration. The LOD was 63.3 ng/mL. Detection can be achieved in the range of 100 ng–5 µg/mL [176].

3.3. Mechanical Methods

Dong et al. reported a study on the detection of trypsin using a peptide-functionalized quartz crystal microbalance (QCM) gold electrode. The gold nanoparticles with a certain length of peptide chain sequestered on them caused a change in resonance intensity, i.e., the QCM measured their mass. When trypsin is present, it hydrolyzes the peptide chain, and the QCM can measure the decrease in the mass of the peptide chain, which in turn enables the detection of trypsin [177]. Dizon et al. also used the QCM method and achieved an LOD of 0.2 nM for trypsin in milk [178]. Piovarci et al. used acoustic wave-based biosensors operated in the thickness-shear mode (TSM) to measure the hydrolysis of β-casein by trypsin (Figure 16). β-Casein was bound to a piezoelectric quartz crystal sensor, and its hydrolysis reduced the overall mass and increased the resonance frequency [179].

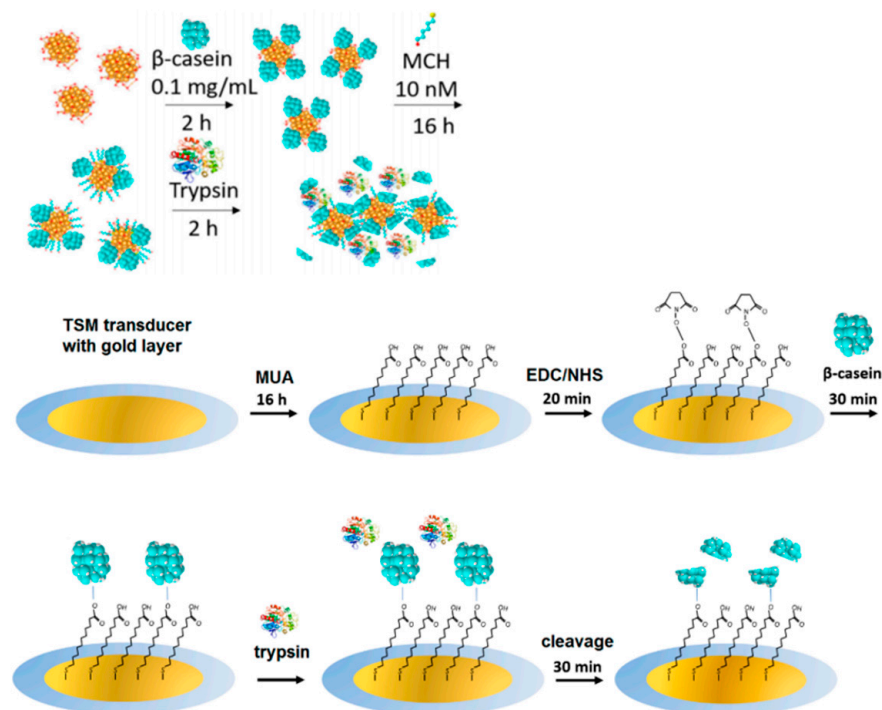


Figure 16. Schematic diagram of the principle of the shear method for sensing trypsin. After trypsin hydrolyzes the substrate, the change in mass and viscosity leads to a change in mechanical resonance frequency. Reproduced from [179] under the terms of the CC-BY Creative Commons Attribution License, copyright 2021 MDPI.

Lee et al. implemented the detection of trypsin using a grating resonance absorber (RA). Polymethacrylic acid (PMAA) was fabricated as a brush-like plasma grating. Its tail was fixed with gelatin, which changes the resonance absorption peak of the grating upon decomposition by trypsin. The detection of trypsin was achieved by measuring the shift of the absorption peak of RA [180].

3.4. Electrical Methods

3.4.1. Circuit Parameter Testing

A capacitive trypsin sensor with a minimum LOD of 0.3 pM was prepared by Erturk et al. The electrode surface of the capacitor was treated with 3-aminopropyl-triethoxysilane (APTES) ethanol to introduce amino groups. The trypsin was immobilized under the modification of glutaraldehyde. The MIP was formed by polymerizing tyramine using cyclic voltammetry [181].

Palomar et al. prepared silicon nanopores on which casein was immobilized after the preparation of functionalized gold on the surface. The hydrolysis of casein by trypsin enlarged the nanopore size and amplified the ionic current through the pore. The minimum LOD was 0.005 ng/mL [182].

Zaccheo et al. designed sensors with trypsin to etch the protein layer, which in turn enabled circuit conduction. An aluminum protein protective layer was prepared above the photodiode, blocking the light incidence. By adding NaOH to the sample to be tested, the NaOH can react with the aluminum layer only if the trypsin destroys the protein layer, causing light to shine on the photodiode and lighting up the LED in the circuit [183].

Zhou et al. designed a biological α -hemolysin protein nanopore. Only peptide substrates, which are broken down by trypsin, can pass through the pore. Neither the trypsin itself nor the lysine-containing peptides in the substrate can pass through. The concentration of trypsin, therefore, affects the magnitude of the current passing through the pore under an external electric field. The LOD of trypsin is 1.4 ng/mL [184].

3.4.2. Electrochemical Method

The antigen–antibody binding for electrochemical sensing is also used in trypsin sensing (Figure 17b). Yi et al. used multi-walled carbon nanotube (MWCNT)-modified electrodes to measure serum trypsin concentration using differential pulse voltammetry and achieved an ultra-low LOD of 0.002 ng/mL. Multi-walled carbon nanotubes with gold nanoparticles, which have a high specific surface area and strong conductivity, can immobilize a large amount of substrate. Using an anti-trypsin antibody as a substrate, the electrochemical signal is detected when trypsin binds to it. There was good linearity in the range of 0.1–100 ng/mL [185]. Rahmati et al. used amorphous Ni(OH)₂ nano-cassettes, multidimensional hollow structures providing a large surface area, using covalently immobilized NH₂-functionalized aptamers. A 0.3 fg/mL LOD and a log-linear range of 1 fg–500 ng/mL were achieved [186]. Hu et al. achieved a label-free assay by detecting the binding of trypsin to specific antibodies using an electrochemical method. A 0.58 ng/mL LOD and a linear range of 1–200 ng/mL were achieved. Signal generation is based on a polysulfhydrylsulfanine–nanogold nanocomposite (PTh-NG) structure. Differential pulse voltammetry allows the accurate determination of trypsin binding to antibodies. The good electrical conductivity of gold nanoparticles facilitates electron transfer and increases the amount of the immobilized substrate through their large specific surface area [187].

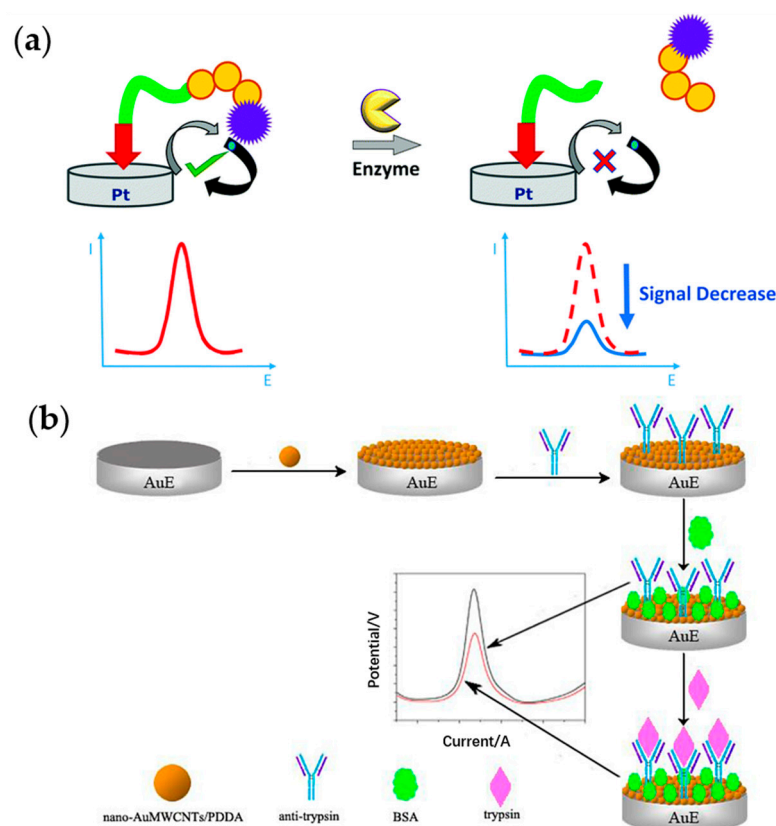


Figure 17. Principles of electrochemical methods for the detection of trypsin. (a) Hydrolysis of the immobilized substrate using trypsin. Reproduced from [188] under the terms of the CC-BY Creative Commons Attribution License, copyright 2022 by the Royal Society of Chemistry. (b) Anti-trypsin antibody specifically binds to trypsin. The black curve in the graph shows the results in the absence of trypsin. With the addition of trypsin, the signal is shown as a red curve. Reproduced from [185] under the terms of the CC-BY Creative Commons Attribution License, copyright 2014 MDPI.

In 2010, Adjemian et al. performed electrochemical measurements using cyclic voltammetry. The electrodes used a gold disc working electrode, a counter electrode made of platinum, and an additional KCL-saturated glycerol electrode as a reference electrode. On the surface of the gold electrode, peptide chains of 4–7 amino acids in length were immobilized, and the ends were chosen to be labeled with low-potential alkyl ferrocene (Fc), which is insensitive to the surrounding medium, making the peptide chains more susceptible to cleavage by proteases. When the peptide chain is cleaved by a protease, Fc is released, and there will no longer be a current signal conducted to the electrode via its oxidation in cyclic voltammetry. By measuring the current at the electrode, it is possible to quantify the number of peptide chains that still have Fc labeled and thus detect proteases. A fast response can be achieved for proteases in the range of 1–1000 nM [189]. A similar method was used by Barsan et al., but the labeling of the top of the peptide chain was changed to the organic ABZ, and the electroactivity of ABZ was utilized. The peptide chain was immobilized using a self-assembled para-aminothiophenol (PATP) monolayer on a gold electrode [190]. Hu et al. also used Fc labeling, but in contrast to Adjemian’s method, they aggregated the Fc label to the electrode surface in the presence of trypsin. The minimum LOD was 0.064 ng/mL. They immobilized the no-jam peptide to the electrode surface by immobilizing the n-terminus to the electrode surface and hydrolyzed it by trypsin to form a free carboxyl group at the c-terminus. The carboxyl–carboxyl bond will bind the atom transfer radical polymerization (ATRP). Under electrochemical control, the ATRP surface will trigger graft polymerization (SI-GOP) with ferrocenyl methyl methacrylate (FcMMA) in the substrate as a monomer and be detected by the electrode [191].

Ucar et al. used miniaturized Pt electrodes that have the potential to be used in implantable sensing (Figure 17a) [188].

Poma et al. immobilized gelatin on an electrode with the electrochemical redox mediator (4-((4-aminophenyl)imino)-2,6-dimethoxycyclohexa-2,5-dien-1-one) embedded in it. The redox mediator was released into the solution after the trypsin decomposition of gelatin and was measured by AC voltammetry [192]. Shin et al. used trypsin to cleave the peptide bond of a p-aminophenol (AP)-coupled oligopeptide, releasing the electrochemically active AP. Cyt c acted as an oxidoreductase and, together with H₂O₂ and AP, formed an electrochemical-enzyme redox cycle. An LOD of 50 ng/mL was achieved [193].

Choi et al. combined the MIP technique with electrochemical measurements. They used an o-phenylenediamine monomer and a trypsin protein for polymerization on a gold-covered quartz crystal electrode to form a 3D-MIP membrane with better detection performance than a 2D-MIP membrane [194]. Zhao et al. used the amphiphilic electropolymerizable macromonomer poly(AM-co-HEA-co-NVc) (PAHN), and a self-assembled 3D-MIP was implemented [195].

3.5. Chymotrypsin and Elastase

In addition to trypsin, the pancreas secretes chymotrypsin and elastase. Similar to pancreatic protease, they both break down peptides. Chymotrypsin accounts for about 9% of the total pancreatic fluid protein and is the second most abundant serine protease [196]. Trypsin, chymotrypsin, and elastase are endopeptidases of the serine protease family, which are highly homologous in their X-ray crystal structures. The difference is that they have different specificity pockets that allow only specific peptide bonds to be hydrolyzed [1]. Elastase cleaves the carboxyl terminus of glycine and alanine, while chymotrypsin cleaves the carboxyl terminus of aromatic amino acids such as tryptophan, phenylalanine, and tyrosine [1].

Keim et al. counted the correlation between elastase and rennet in human fecal samples and CP. An enzyme-linked immunosorbent assay (ELISA) was used. The sensitivities of elastase and chymotrypsin were 77.8% and 57.8%, respectively, and the specificities were 76.0% and 52.7%. Although better than previous elastase assays, this result is not sufficient as a standard for clinical testing [197]. However, due to their similarity to trypsin, the sensing methods are also highly versatile. This section can also be seen as a complement to the previous part.

3.6. Detection of Chymotrypsin

Liu et al. exploited the optical quenching of fluorescence by graphene oxide (GO) and AuNPs to achieve the monitoring of chymotrypsin. They immobilized the functional peptide (EKEPPPPC) by Au-S bonding. GO was modified with sulfhydryl groups to obtain GO-SH, which formed covalent bonds with AuNPs and better immobilized the particles. After peptide breakdown by chymotrypsin, AuNPs were more tightly bound to GO, and absorbance was improved. This method achieved a low LOD of 0.25 pg/mL [198].

Gao et al. devised an assay for the detection of chymotrypsin using a GO-AuNP system to quench fluorescence. They took advantage of the abundant surface functional groups of GO, the large specific surface area of AuNPs, and good electrical conductivity to immobilize peptides as substrates. The AuNPs were treated with NaBr to ensure that the peptide chains could be stably attached to the surface by sulfhydryl groups. Pyrene, which has a large extinction coefficient, long lifetime, good stability in an aqueous solution, and easy chemical modification, was used as a fluorescent dye to label the peptides. The fluorescence of pyrene is quenched in the vicinity of AuNPs and GO. After chymotrypsin cleavage of the peptide chain, pyrene fluoresces away from AuNPs and GO [199]. Fluorescence quenching by this system was further investigated by Liu et al. They used CuNCs, added EDC and NHS to provide carboxyl groups, and bound the peptide chains with covalent bonds, and the other end was immobilized to the GO-AuNP system (Figure 18). It was found that adding

PCN to the GO-AuNP system for linking AuNPs could further improve the sensitivity. The lowest LOD of 3.91 pg/mL was finally achieved [200].

In addition, chymotrypsin probes with bioaffinity were developed. The detection can be realized in living cells. And thanks to the use of red [201] or near-infrared [202] light, it can penetrate the tissue to be measured. These studies make it possible to monitor pancreatic chymotrypsin in real time.

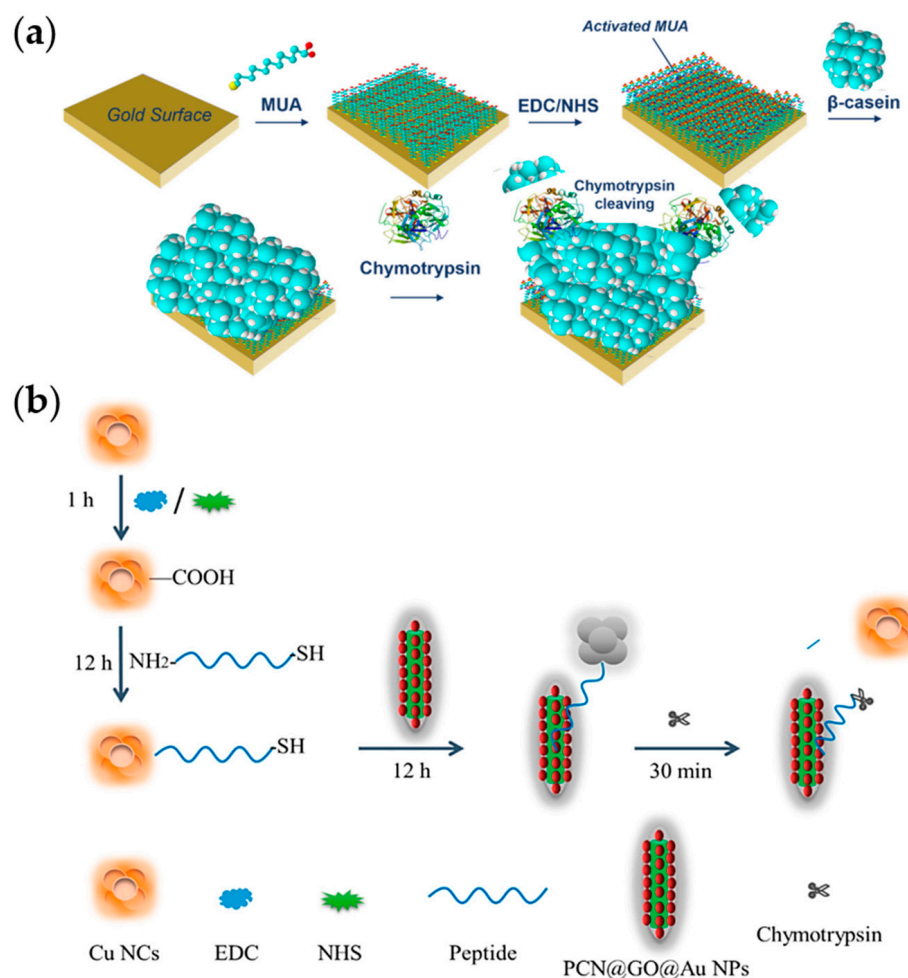


Figure 18. (a) Chymotrypsin sensing using QCM. Reproduced from [203] under the terms of the CC-BY Creative Commons Attribution License, copyright 2021 MDPI. (b) Chymotrypsin-degrading peptides release CuNCs from the graphene oxide surface and activate fluorescence for sensing. Reproduced from [200] under the terms of the CC-BY Creative Commons Attribution License, copyright 2023 MDPI.

The QCM method for pancreatic chymotrypsin detection was implemented by Piovarci et al. The sensor with β -casein immobilized on the surface of a quartz crystal was made (Figure 18a). The differentiation of different enzymes can be achieved by multi-harmonic QCM intramural supply analysis and machine learning [203].

Viscometry was used for the detection of chymotrypsin by Ping et al. A gelatin hydrogel was fixed on the pH test paper, which immobilized the water molecules from flowing. The protease hydrolyzed the gelatin and released the water molecules, which in turn flowed on the pH test paper [204].

3.7. Detection of Elastase

Kakizaki et al. developed a method to determine pancreatic injury using a pancreatic-specific antigen as a marker. A sensitive sandwich enzyme immunoassay for human

elastase III fluorometric determination was developed using a rabbit anti-human elastase III antibody. The LOD was 0.3 pg per tube [205]. The significance of elastase in the detection of pancreatitis is also reflected by the increase in serum pancreatic elastase 1 in AP and chronic recurrent pancreatitis [206]. The fecal pancreatic elastase 1 (FPE1) assay can also be used to monitor the exocrine function of the pancreas [207–209]. Huta et al. measured the elastin content in stool using a kit with ELISA for the analysis of its use in pancreatic exocrine insufficiency (PEI) [207].

Another common elastase in the human body is human neutrophil elastase (HNE). A number of studies have reported on its detection techniques and association with physiological phenomena such as inflammation [210–216]. Yang et al. implemented paper-based elastase sensing suitable for POST. The distribution of the substrate and elastase was guided by creating hydrophobic and hydrophilic zones [217]. Huang et al. [218] and Li et al. [219] designed fluorescent probes with bioaffinity, respectively, which are expected to enable real-time elastase sensing in vivo. Assays based in part on the common characteristics of elastase may have the potential for pancreatic elastase sensing. More pancreatic elastase sensing techniques are yet to be investigated.

3.8. Summary

In contrast to trypsin, the substrate targeted by protease needs to be specially designed, especially for short peptide chains, to ensure the availability of a working site for protease. But the diversity of proteins has likewise facilitated the design of chemical probes or techniques to amplify the signal, and more diverse sensing techniques have been reported. Many methods that allow for convenient self-testing have also been reported (Figure 19) [220]. Although the target is not pancreatic-secreted trypsin, there is a commonality due to the use of its property of hydrolyzing peptide bonds.

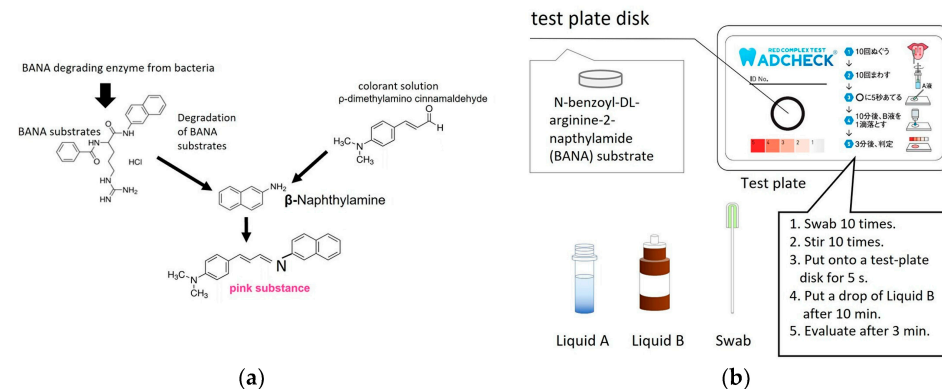


Figure 19. Convenient protease self-sensing method. (a) The mechanism of ADCHECK to detect TLP activity. (b) Components of the ADCHECK kit. Reproduced from [220] under the terms of the CC-BY Creative Commons Attribution License, copyright 2022 MDPI.

Chymotrypsin and elastase have a limited role in the detection of pancreatitis. However, they are still summarized due to their share in the digestive enzymes secreted by the pancreas and their disease association. Protease sensing alone is inaccurate as a diagnostic criterion for pancreatitis, but it is important in other physiological activities, so its detection techniques are abundant. In addition, related sensing studies can stimulate the idea of protease sensing.

Among the various types of sensing techniques studied for pancreatic enzymes, the sensing of proteases, especially trypsin, is a very rich category. Some of the techniques that enable POCT sensing, including those that can be measured directly by portable devices, cell phones, or the human eye, are summarized in Table 2.

Table 2. Trypsin and chymotrypsin sensing technology.

Type	Probes/Substrates	LOD	Sensing Range	POCT Progress	Ref.
TMB	Peptide-stabilized CuNPs	0.82 nM	3–1000 nM	Human-eye readable	[131]
	POD properties of trypsin-hydrolyzed Cyt c	4.5 ng/mL	5–20 ng/mL	Human-eye readable	[132]
	Immobilization of SAC in gel hydrogels	1 ng/mL	1–100 ng/mL	Human-eye readable	[133]
	Peptide-stabilized PtNPs	0.03 µg/mL	0.06–0.6 µg/mL	Human-eye readable	[133]
Hydrolysis (except TMB method)	CdTe	0.014 µM	0.15–4 µM	Using cell phone	[166]
	Fisetin, catechol B-TPE ratio change	\	\	Human-eye readable	[168]
	BSA inhibits the aggregation of AuNPs	1.2 µg/mL	0.3–4 µg/mL	Using cell phone	[174]
	Protein and enzyme conjugation with AuNPs	1.1 µM	\	Using cell phone	[175]
	Gel-protein-layer-covered electrodes	0.5 µg/mL	\	Portable device	[184]
	Changes in light transmission after alignment of LC molecules	34 ng/mL	1–1000 µg/mL	Portable device	[170]
	Release of redox fragments and reduction in electrochemical signals	\	\	Implantable potential	[188]
	Viscosity change after gelatin hydrolysis	1 ng/mL	\	Paper based	[204]
Fluorescent-containing gel fades after hydrolysis	\	0.5–5 mM	Human-eye readable	[167]	

4. Detection of Lipase

4.1. Lipase

Lipids are one of the most important nutrients needed by the body, supplying energy and essential fatty acids required by the organism. Fats, multivitamins, and phospholipids, which form the structure of cell membranes, are all lipids [1]. Correspondingly, the pancreas secretes a variety of lipases. Among them, triglyceride lipase (PTL) is the most widely studied one [221]. The activity of PLT is not controlled by trypsin.

An essential feature of a lipase is that it acts catalytically at the lipid–water interface, which may be related to the closure of the cap on its active site in an aqueous environment [222]. Catalysis at the lipid–water interface is an important feature of lipolytic enzymes [223,224].

There are fewer reports on lipase sensing than on trypsin and pancreatic amylase. This section divides the relevant studies into two main categories: optical and electrical methods. The portable methods are typical in the remaining digestive enzyme sensing and are summarized separately.

4.2. Optical Methods

Guo et al. investigated the measurement of optically silent fatty acids by a colorimetric method. The indicator (CHI) is a hydrophobic chromophore carrier that changes color from red to blue upon protonation. The triglycerides in the substrate are hydrolyzed by lipase to release the fatty acids and enter the small nanospheres to protonate the CHI. This process is also reversible, i.e., CHI can be deprotonated again to appear red, and the detection can be captured by the naked eye or a camera [225]. Wang et al. used Tween 20 as a stabilizer to avoid the clustering of AuNPs. Lipase hydrolyzed the ester bond of Tween 20, causing the clustering of AuNPs, and was measured colorimetrically. An LOD of 0.0528 U/mL and a detection range of 0.33–56.8 U/mL with an R² of 0.999 were achieved [226].

To achieve tryptic lipase detection in a similar way to amylase and protease, substrates that can be effectively broken down by them are required. Not all carboxyl ester compounds can be decomposed by lipase. Guan et al. conducted a study to find substrates that can react effectively with pancreatic lipase and release yellow fluorescence using AIE and ESIPT mechanisms [227]. In addition, the probe needs to be specially designed in order to fit the characteristics of lipases that undergo catalysis at the lipid–water interface. Shi et al. introduced hydrophilic amino and carboxyl groups based on functionalized tetraphenylethylene (TPE) as a fluorescent probe so that the probe can effectively contact the lipase at the lipid–water interface (Figure 20) [228]

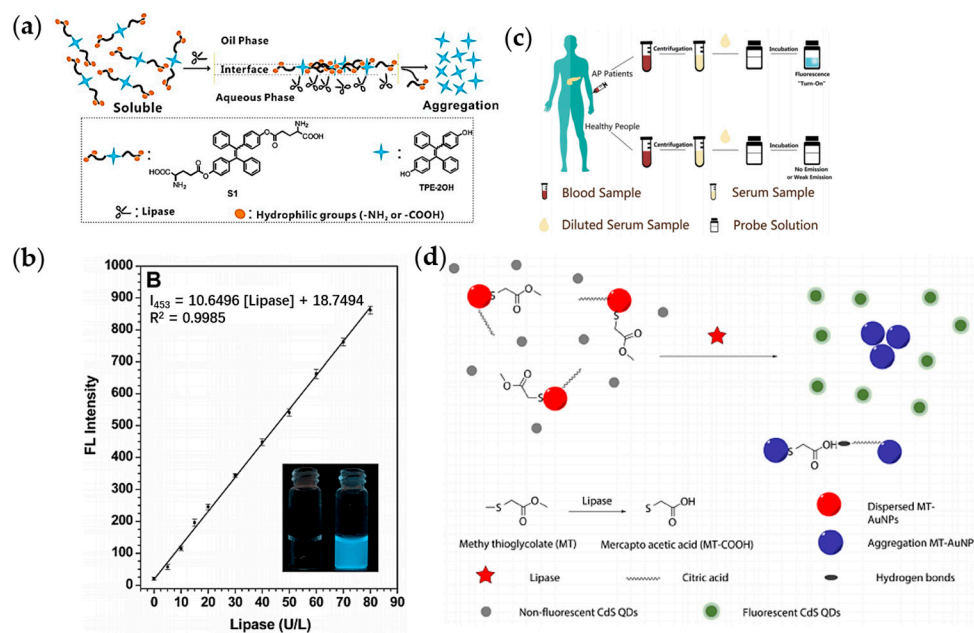


Figure 20. (a) TPE fluorescent probe sensing principle. (b) The relationship between trypsin concentration and fluorescence intensity. (c) Rapid trypsin detection method. Reproduced from [228] under the terms of the CC-BY Creative Commons Attribution License, copyright 2017 by the Royal Society of Chemistry. (d) Schematic illustration of the mechanism of sensing the activity of lipase based on fluorescence. Reproduced from [229] under the terms of the CC-BY Creative Commons Attribution License, copyright 2022 Sociedade Brasileira de Química.

The sensor designed by Zhang et al. was also based on the AIE + ESIPT mechanism. 2-(2-hydroxyphenyl)benzothiazole (HBT) is a Schiff base fluorescent moiety based on ESIPT, and a long dodecyl chain (LDC) was used as a fluorescence quencher to achieve the specific detection of lipase. The formation of hydrogen bonds in the HBT-LDC probe is responsible for the fluorescence change [230]. La Rocca et al. also investigated fluorescent labels that could be used for pancreatic lipase detection. They studied phenoxy-1,2-dioxetane luminophores carrying octane chains as lipase signature substrates. The luminescence reaction produces the chemiluminescence of the luminescent moiety [231]. Luo et al. then directly formed ester bonds between the energy donor group and the energy acceptor group that can be cleaved by lipase. Based on the FRET process, the rhodamine derivative (RA) quenches the fluorescence of the coumarin derivative (CA) and is reactivated by lipase catalysis [232].

Du et al. achieved a fluorescence detection of lipase. The fluorescence of CdS QDs was quenched by MT-AuNPs using the IFE effect. The surface of AuNPs was immobilized with methyl thioglycolate (MT), allowing its uniform diffusion in solution (Figure 20d). The lipase catalyzes the hydrolysis of carboxylate bonds, exposing partially protonated acid groups in a weakly acidic environment. In these bonds, there are sulfhydryl groups on the surface of AuNPs via hydrogen clusters. Clusters of AuNPs can be detected colorimetrically. Their clustering allows some of the CdS QDs to move away, activating fluorescence [229].

Tang et al. implemented the LC detection of lipase on the surface of an optical fiber. The D-shaped cross-sectional fiber was designed to provide a plane on which the sensing structure could be integrated, the LC layer was covered with a phospholipid as a substrate, and the LC molecules were rearranged after the phospholipid was broken down by amylase. This leads to a change in the refractive index, which in turn changes the transmitted optical power of the fiber. It is also possible to observe the transmitted light directly on the side of the fiber, which has the potential of a POC sensor [233].

4.3. Electrical Methods

Paper-based sensing using reduced graphene oxide (RGO) for electronic detection was reported by Middy et al. Olive oil was used as the substrate. The lipase hydrolyzes the substrate to release fatty acids, and the H^+ ions produced decrease the overall resistance. The LOD and limit of quantification (LOQ) were calculated to be 6.087 and 18.261 U/L, respectively [234]. Capacitive coupling can achieve a non-contact conductivity measurement in capillary electrophoresis. The breakdown of lipids by lipase produces small organic molecules, and the conductivity of the solution increases and can be detected by an external circuit capacitively coupled to the liquid in the capillary [234]. This method was also used by Banni et al. to detect lipase activity [235]. Lipase was measured using the impedance method by Zlatev et al. The specific detection of lipase was achieved by depositing a composite layer generated by mixing olive oil with SiO_2 particles on the electrode. The decomposition of the olive oil by lipase allowed the exposure and conduction of the electrode underneath, and the composite material could be redeposited for reuse after use. The relative error was 3.75% to 1.24% [236]. After that, they designed the capacitive sensor. The composites of olive oil mixed with $BaTiO_3$ nanoparticles have good insulating properties with high dielectric constants. The composite layer was used as an electrolyte layer between the electrode and the solution to form a capacitive structure. The decomposition effect of lipase on it led to the variation in thickness and changed the magnitude of capacitance [237].

Rogala et al. measured lipase activity electrochemically using a carbon paste electrode (CPE) containing MWCNTs. The CPE was prepared by mixing graphite powder with MWCNTs and further modified with cobalt(II)phthalocyanine (Co(II)PC), and both additions improved the charge transfer resistivity. The substrate was glycerol linoleate, and the enzymatic reaction of lipase formed linoleic acid (LA). The reductive LA is oxidized on the electrode surface, which in turn can be detected by cyclic voltammetry [238]. Sample preparation, the flow system, and electrochemical conditions were optimized by Sarakhman et al. [239].

Using an ion-sensitive field effect transistor (ISFET), Valek et al. measured the activity of lipase. Tween 20 was used as a substrate, which was hydrolyzed by lipase to form fatty acids, causing a decrease in solution pH. The pH measurement was achieved using the potentiometric method [240]. Wang et al. designed a photoelectrochemical sensor (PEC), which also enabled lipase detection by detecting the hydrolysis products. A three-dimensional graphene oxide (3DGO), poly(Nile blue) (PNb), and glycerol dehydrogenase (GDH) composite sensing structure was prepared on an indium tin oxide (ITO) electrode. The 3DGO provided many active sites and specific surface areas and the PNb was photoactive, and its high molecular weight could improve the stability of the 3DGO (Figure 21). The rice bran oil in the substrate was hydrolyzed by lipase to produce glycerol, which was further reacted by GDH on the electrode surface [241].

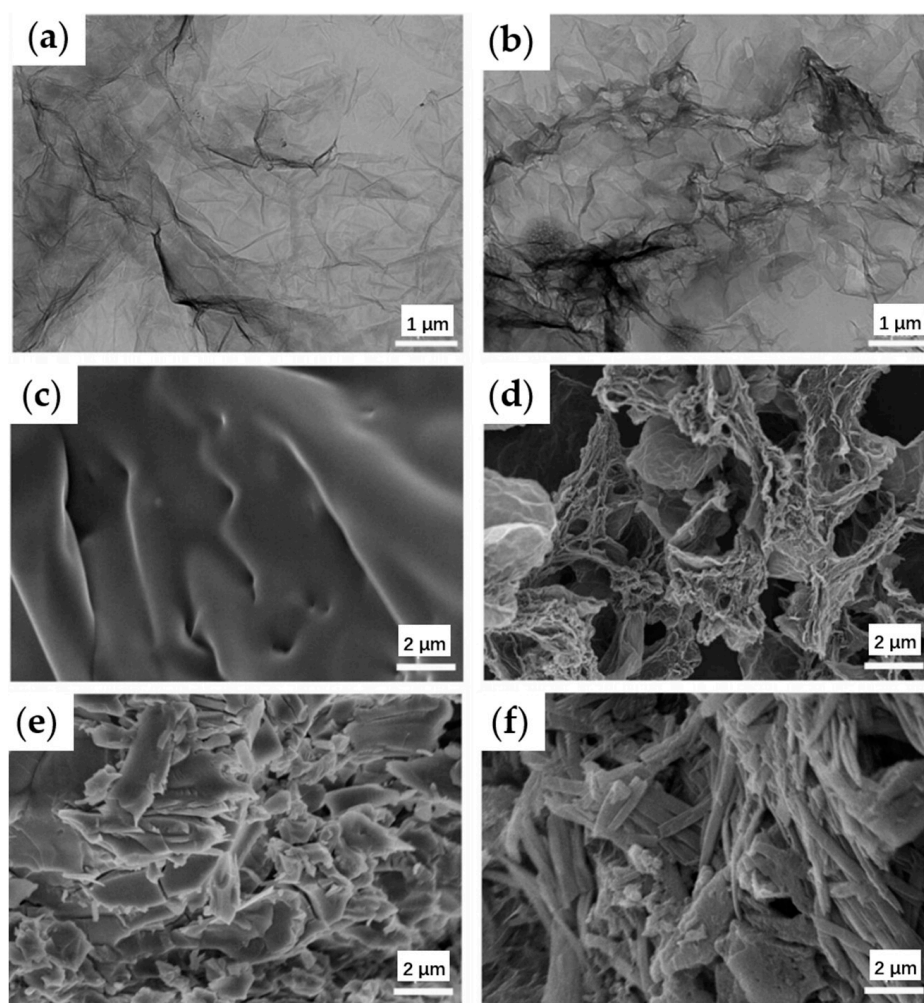


Figure 21. The process of functionalizing and immobilizing substrates on the GO surface in a photoelectrochemical (PEC) lipase sensor. TEM analysis of (a) GO and (b) 3DGO; SEM analysis of (c) GO-ITO, (d) 3DGO-ITO, (e) PNb-3DGO-ITO, and (f) GDH-PNb-3DGO-ITO. Reproduced from [241] under the terms of the CC-BY Creative Commons Attribution License, copyright 2022 Elsevier Ltd.

4.4. Other Methods

The previous sections introduced the implementation of portable sensors, such as paper-based sensing, a blood glucose meter, and a cell phone camera. Related techniques were also implemented in lipase sensing.

Xia et al. investigated the application of a pH-test-paper-based viscosity assay for lipase measurement. The addition of lipase causes phase separation of the substrate, which in turn flows over different lengths of the pH test paper due to viscosity changes. It catalyzes the formation of oleic acid and glycerol from the trioleic acid in the substrate. The oleic acid will form calcium oleate particles with Ca^{2+} ions, while the unreacted Ca^{2+} will form a hydrogel with alginate [242].

Zhang et al. implemented a lipase assay using a blood glucose meter (Figure 22). Lipase catalyzes the hydrolysis of 4-acetaminophen acetate to produce acetaminophen and triggers the reduction of $\text{K}_3[\text{Fe}(\text{CN})_6]$ to $\text{K}_4[\text{Fe}(\text{CN})_6]$ in glucose test strips. Since it is compatible with existing glucose test strips and blood glucose meters, it allows for convenient at-home self-testing [243].

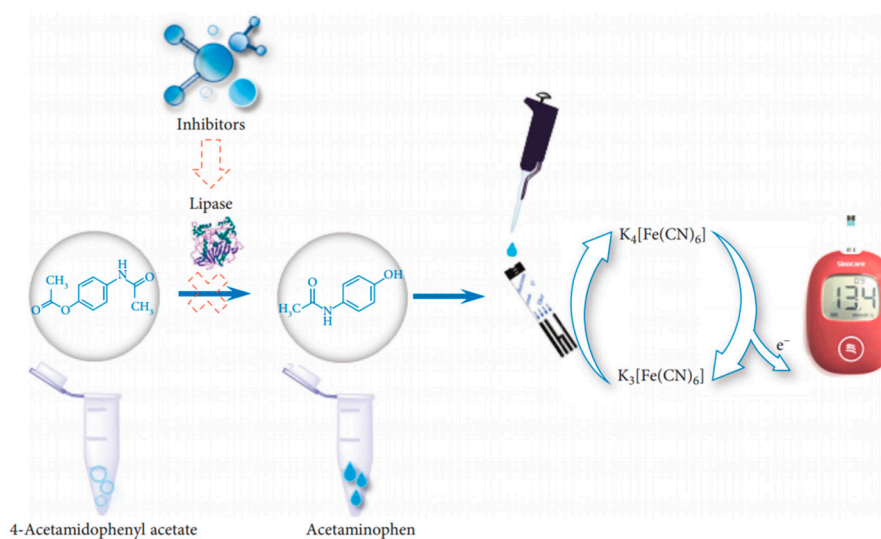


Figure 22. Portable lipase assay. Electrochemical sensing using a glucose meter. Reproduced [243] from under the terms of the CC-BY Creative Commons Attribution License, copyright 2022 Hindawi Ltd.

4.5. Summary

Because of its good specificity, lipase is an important basis for digestive enzyme sensing as a diagnosis of AP. Its combination with amylase is often used as a formal diagnostic criterion. Unlike several previous enzymes, lipids are not polymerized from a few monomers, and lipases need to be catalyzed at the lipid–water interface. Therefore, the sensing technique for lipases differs somewhat from previous studies regarding the chemical approach, especially in the design of probes and substrates. Some of the technologies that enable POCT sensing are summarized in Table 3.

Table 3. Lipase sensing technology.

Type	Probes/Substrates	LOD	Sensing Range	POCT Progress	Ref.
Hydrolysis	Fatty acids as ion exchangers	1.8 µg/mL	\	Human-eye readable	[225]
	Altered LC molecular arrangement of lipid molecules	1 nM	2–10 nM	Small fiber optic sensors	[233]
	Hydrolysis of polymer changes the conductive area of electrodes	8 mU/mL	0.0099–1.68 U/mL	Miniaturized equipment	[236]
	Hydrolysis of polymer changes the thickness of capacitors	\	0.0073–3.9 U/mL	Miniaturized equipment	[237]
	Viscosity change	0.052 U/mL	0.052–30 U/mL	Paper based	[242]
	Hydrolysis of 4-acetaminophen acetate	\	\	Blood glucose meter	[243]
	Hydrolysis releases H ⁺ ions to improve electrical conductivity	6.087 U/L	\	Paper based	[244]

5. Conclusions and Outlook

This paper systematically introduces the sensing methods for common digestive enzymes. Based on colorimetric, fluorescent, SPR, electrochemical, and liquid crystal methods, specific detection is achieved by the design of chemical structures such as special probes. Some methods have been studied extensively, such as the TMB-based fluorescence method. However, many methods have been studied less frequently.

The LOD of many studies has been far below the concentration of digestive enzymes in human body fluids. For example, blood trypsin concentrations range from about 40–180 U/L. The lowest limit of detection, however, can be as low as 0.5 U/L [184]. The

upper limit of the detection range in some studies is still below the diagnostic criterion of three times the standard value. New technologies such as MIP and ITC have excellent measurement performance, but overly specialized equipment limits their use. Therefore, more convenient detection is an important direction of development. Although there is a high diversity of enzymes, many sensing methods using their nature of hydrolyzing specific macromolecules have a high degree of commonality.

According to the authors, the way forward is to simultaneously measure multiple tryptases with a single, simple device based on the same principles and different substrates and probes. First, the paper-based approach, or technology that can be measured by the naked eye, a cell phone camera, or a home blood glucose meter, has a wide range of applications. This would allow people to self-measure and seek medical attention at the first sign of discomfort, avoiding delays in treatment. For the same level of detection, the ability to utilize non-invasive samples or as few body fluid samples as possible to achieve a warning of pancreatitis could be a future direction for research. However, such methods' linear range and accuracy are often small, and even quantitative measurements are not possible. In addition to this, it is also helpful to utilize miniaturized, low-cost devices to achieve sensing with relatively good performance. This could enable small hospitals in areas with fewer medical resources to diagnose and classify pancreatitis at a lower cost. Patients in larger hospitals can monitor their marker levels more frequently and receive personalized treatment promptly. The accurate diagnosis of pancreatitis and timely and personalized treatment are beneficial in any healthcare scenario.

It should also be noted when following research in this area that substances such as proteases and amylases are not only found in pancreatic fluid. The diversity of marker sources in samples such as saliva should be considered. And for sensing enzymes of non-pancreatic origin, slurries can likewise migrate more directly for pancreatic enzyme sensing if their hydrolyzed macromolecular nature is exploited.

The high mortality rate of pancreatitis should be of concern to the healthcare system and society as a whole. The ability to diagnose pancreatitis quickly, easily, and accurately can effectively reduce the rate of severe illness and mortality and reduce the cost of patient care. For patients recovering from AP, a quick diagnosis can provide more timely and accurate information about recovery and monitor the development of recurrence or chronic disease. The detection of pancreatic enzymes, especially convenient and rapid screening techniques, is an important direction. In addition, synergies with new imaging and artificial intelligence technologies should also be considered to comprehensively advance diagnostic and therapeutic techniques for pancreatitis.

Author Contributions: Conceived and designed the review, J.Y. and T.C.; writing—original draft preparation, J.Y.; writing—review and editing, T.C.; supervised the project, T.-L.R. and Y.Y.; J.Y. and T.C. contributed equally to this work. All authors have read and agreed to the published version of the manuscript.

Funding: This work was supported by the National Key R&D Program (2021YFC3002200 and 2022YFB3204100) and National Natural Science Foundation (U20A20168, 51861145202, 61874065, and 62022047) of China.

Institutional Review Board Statement: Not applicable.

Informed Consent Statement: Not applicable.

Data Availability Statement: Data are available in a publicly accessible repository.

Conflicts of Interest: The authors declare no conflict of interest.

References

1. Whitcomb, D.C.; Lowe, M.E. Human pancreatic digestive enzymes. *Dig. Dis. Sci.* **2007**, *52*, 1–17. [[CrossRef](#)] [[PubMed](#)]
2. Slack, J.M. Developmental Biology of The Pancreas. *Development* **1995**, *121*, 1569–1580. [[CrossRef](#)] [[PubMed](#)]
3. Rothman, S.S. Digestive Enzymes of Pancreas—Mixture of Inconstant Proportions. *Annu. Rev. Physiol.* **1977**, *39*, 373–389. [[CrossRef](#)]

4. Pallagi, P.; Hegyi, P.; Rakonczay, Z., Jr. The Physiology and Pathophysiology of Pancreatic Ductal Secretion The Background for Clinicians. *Pancreas* **2015**, *44*, 1211–1233. [[CrossRef](#)]
5. Ishiguro, H.; Yamamoto, A.; Nakakuki, M.; Yi, L.; Ishiguro, M.; Yamaguchi, M.; Kondo, S.; Mochimaru, Y. Physiology and Pathophysiology of Bicarbonate Secretion by Pancreatic Duct Epithelium. *Nagoya J. Med. Sci.* **2012**, *74*, 1–18. [[PubMed](#)]
6. Czaja, M.J. Functions of Autophagy in Hepatic and Pancreatic Physiology and Disease. *Gastroenterology* **2011**, *140*, 1895–1908. [[CrossRef](#)]
7. Logsdon, C.D.; Ji, B. The role of protein synthesis and digestive enzymes in acinar cell injury. *Nat. Rev. Gastroenterol. Hepatol.* **2013**, *10*, 362–370. [[CrossRef](#)]
8. Petrov, M.S.; Yadav, D. Global epidemiology and holistic prevention of pancreatitis. *Nat. Rev. Gastroenterol. Hepatol.* **2019**, *16*, 175–184. [[CrossRef](#)]
9. Beyer, G.; Habtezion, A.; Werner, J.; Lerch, M.M.; Mayerle, J. Chronic pancreatitis. *Lancet* **2020**, *396*, 499–512. [[CrossRef](#)]
10. Xiao, A.Y.; Tan, M.L.Y.; Wu, L.M.; Asrani, V.M.; Windsor, J.A.; Yadav, D.; Petrov, M.S. Global incidence and mortality of pancreatic diseases: A systematic review, meta-analysis, and meta-regression of population-based cohort studies. *Lancet Gastroenterol. Hepatol.* **2016**, *1*, 45–55. [[CrossRef](#)]
11. Machicado, J.D.; Dudekula, A.; Tang, G.; Xu, H.; Wu, B.U.; Forsmark, C.E.; Yadav, D. Period prevalence of chronic pancreatitis diagnosis from 2001–2013 in the commercially insured population of the United States. *Pancreatology* **2019**, *19*, 813–818. [[CrossRef](#)] [[PubMed](#)]
12. Boxhoorn, L.; Voermans, R.P.; Bouwense, S.A.; Bruno, M.J.; Verdonk, R.C.; Boermeester, M.A.; van Santvoort, H.C.; Besselink, M.G. Acute pancreatitis. *Lancet* **2020**, *396*, 726–734. [[CrossRef](#)] [[PubMed](#)]
13. Schepers, N.J.; Bakker, O.J.; Besselink, M.G.; Ali, U.A.; Bollen, T.L.; Gooszen, H.G.; van Santvoort, H.C.; Bruno, M.J. Impact of characteristics of organ failure and infected necrosis on mortality in necrotising pancreatitis. *Gut* **2019**, *68*, 1044–1051. [[CrossRef](#)] [[PubMed](#)]
14. van Santvoort, H.C.; Bakker, O.J.; Bollen, T.L.; Besselink, M.G.; Ali, U.A.; Schrijver, A.M.; Boermeester, M.A.; van Goor, H.; Dejong, C.H.; van Eijck, C.H.; et al. A Conservative and Minimally Invasive Approach to Necrotizing Pancreatitis Improves Outcome. *Gastroenterology* **2011**, *141*, 1254–1263. [[CrossRef](#)]
15. Gurusamy, K.S.; Belgaumkar, A.P.; Haswell, A.; Pereira, S.P.; Davidson, B.R. Interventions for necrotising pancreatitis. *Cochrane Database Syst. Rev.* **2016**, *4*. [[CrossRef](#)]
16. Young, B.J.; Melbern, W.C.; Pablo, A.J.; Shyam, V. Superiority of endoscopic interventions over minimally invasive surgery for infected necrotizing pancreatitis: Meta-analysis of randomized trials. *Dig. Endosc. Off. J. Jpn. Gastroenterol. Endosc. Soc.* **2020**, *32*, 298–308.
17. Lankisch, P.G.; Apte, M.; Banks, P.A. Acute pancreatitis. *Lancet* **2015**, *386*, 85–96. [[CrossRef](#)]
18. Tenner, S.; Baillie, J.; DeWitt, J.; Vege, S.S. American College of Gastroenterology Guideline: Management of Acute Pancreatitis. *Am. J. Gastroenterol.* **2013**, *108*, 1400–1415. [[CrossRef](#)]
19. Habtezion, A.; Gukovskaya, A.S.; Pandol, S.J. Acute Pancreatitis: A Multifaceted Set of Organelle and Cellular Interactions. *Gastroenterology* **2019**, *156*, 1941–1950. [[CrossRef](#)]
20. Yadav, D.; Lowenfels, A.B. The Epidemiology of Pancreatitis and Pancreatic Cancer. *Gastroenterology* **2013**, *144*, 1252–1261. [[CrossRef](#)]
21. Crockett, S.D.; Wani, S.; Gardner, T.B.; Falck-Ytter, Y.; Barkun, A.N.; American Gastroenterological Association Institute Clinical Guidelines Committee. American Gastroenterological Association Institute Guideline on Initial Management of Acute Pancreatitis. *Gastroenterology* **2018**, *154*, 1096–1101. [[CrossRef](#)] [[PubMed](#)]
22. Wang, F.; Wang, H.; Fan, J.; Zhang, Y.; Wang, H.; Zhao, Q. Pancreatic Injury Patterns in Patients With Coronavirus Disease 19 Pneumonia. *Gastroenterology* **2020**, *159*, 367–370. [[CrossRef](#)] [[PubMed](#)]
23. Hadi, A.; Werge, M.; Kristiansen, K.T.; Pedersen, U.G.; Karstensen, J.G.; Novovic, S.; Gluud, L.L. Coronavirus Disease-19 (COVID-19) associated with severe acute pancreatitis: Case report on three family members. *Pancreatology* **2020**, *20*, 665–667. [[CrossRef](#)] [[PubMed](#)]
24. de-Madaria, E.; Capurso, G. COVID-19 and acute pancreatitis: Examining the causality. *Nat. Rev. Gastroenterol. Hepatol.* **2021**, *18*, 3–4. [[CrossRef](#)] [[PubMed](#)]
25. Aloysius, M.M.; Thatti, A.; Gupta, A.; Sharma, N.; Bansal, P.; Goyal, H. COVID-19 presenting as acute pancreatitis. *Pancreatology* **2020**, *20*, 1026–1027. [[CrossRef](#)]
26. Kiyak, M.; Duzenli, T. Lipase elevation on admission predicts worse clinical outcomes in patients with COVID-19. *Pancreatology* **2022**, *22*, 665–670. [[CrossRef](#)]
27. Ali, U.A.; Issa, Y.; Hagenshaars, J.C.; Bakker, O.J.; van Goor, H.; Nieuwenhuijs, V.B.; Bollen, T.L.; van Ramshorst, B.; Witteman, B.J.; Brink, M.A.; et al. Risk of Recurrent Pancreatitis and Progression to Chronic Pancreatitis After a First Episode of Acute Pancreatitis. *Clin. Gastroenterol. Hepatol.* **2016**, *14*, 738–746.
28. Sankaran, S.J.; Xiao, A.Y.; Wu, L.M.; Windsor, J.A.; Forsmark, C.E.; Petrov, M.S. Frequency of Progression From Acute to Chronic Pancreatitis and Risk Factors: A Meta-analysis. *Gastroenterology* **2015**, *149*, 1490–1500.e1. [[CrossRef](#)]
29. Braganza, J.M.; Lee, S.H.; McCloy, R.F.; McMahan, M.J. Chronic pancreatitis. *Lancet* **2011**, *377*, 1184–1197. [[CrossRef](#)]
30. MBraganza, J.M.; Scott, P.; Bilton, D.; Schofield, D.; Chaloner, C.; Shiel, N.; Hunt, L.P.; Bottiglieri, T. Evidence for early oxidative stress in acute pancreatitis. *Int. J. Pancreatol.* **1995**, *17*, 69–81. [[CrossRef](#)]

31. Kamisawa, T.; Wood, L.D.; Itoi, T.; Takaori, K. Pancreatic cancer. *Lancet* **2016**, *388*, 73–85. [[CrossRef](#)] [[PubMed](#)]
32. Balthazar, E.J.; Robinson, D.L.; Megibow, A.J.; Ranson, J.H.C. Acute-Pancreatitis—Value of CT in Establishing Prognosis. *Radiology* **1990**, *174*, 331–336. [[CrossRef](#)] [[PubMed](#)]
33. Tonozuka, R.; Itoi, T.; Nagata, N.; Kojima, H.; Sofuni, A.; Tsuchiya, T.; Ishii, K.; Tanaka, R.; Nagakawa, Y.; Mukai, S. Deep learning analysis for the detection of pancreatic cancer on endosonographic images: A pilot study. *J. Hepato-Biliary-Pancreat. Sci.* **2021**, *28*, 95–104. [[CrossRef](#)] [[PubMed](#)]
34. Banks, P.A.; Bollen, T.L.; Dervenis, C.; Gooszen, H.G.; Johnson, C.D.; Sarr, M.G.; Tsiotos, G.G.; Vege, S.S.; Acute Pancreatitis, C. Classification of acute pancreatitis-2012: Revision of the Atlanta classification and definitions by international consensus. *Gut* **2013**, *62*, 102–111. [[CrossRef](#)] [[PubMed](#)]
35. Silva-Vaz, P.; Abrantes, A.M.; Castelo-Branco, M.; Gouveia, A.; Botelho, M.F.; Tralhao, J.G. Multifactorial Scores and Biomarkers of Prognosis of Acute Pancreatitis: Applications to Research and Practice. *Int. J. Mol. Sci.* **2020**, *21*, 338. [[CrossRef](#)] [[PubMed](#)]
36. Patel, H.R.R.; Almanzar, V.M.D.M.; LaComb, J.F.F.; Ju, J.; Bialkowska, A.B.B. The Role of MicroRNAs in Pancreatitis Development and Progression. *Int. J. Mol. Sci.* **2023**, *24*, 1057. [[CrossRef](#)]
37. Yan, X.; Li, J.; Wu, D. The Role of Short-Chain Fatty Acids in Acute Pancreatitis. *Molecules* **2023**, *28*, 4985. [[CrossRef](#)]
38. Waddell, H.; Stevenson, T.J.; Mole, D.J. The role of the circadian rhythms in critical illness with a focus on acute pancreatitis. *Heliyon* **2023**, *9*, e15335. [[CrossRef](#)]
39. Wang, H.; Kang, Z.L.; Peng, X.H.; Liu, L.M.; Liu, Y.X.; Feng, Y.J.; Tao, L.J. Misdiagnosed Analysis of Severe Acute Pancreatitis. *Clin. Misdiagn. Msther.* **2021**, *34*, 12–15.
40. Overbeek, K.A.; Levink, I.J.M.; Koopmann, B.D.M.; Harinck, F.; Konings, I.C.A.W.; Ausems, M.G.E.M.; Wagner, A.; Fockens, P.; van Eijck, C.H.; Koerkamp, B.G.; et al. Long-term yield of pancreatic cancer surveillance in high-risk individuals. *Gut* **2022**, *71*, 1152–1160. [[CrossRef](#)]
41. Corral, J.E.; Mareth, K.F.; Riegert-Johnson, D.L.; Das, A.; Wallace, M.B. Diagnostic Yield From Screening Asymptomatic Individuals at High Risk for Pancreatic Cancer: A Meta-analysis of Cohort Studies. *Clin. Gastroenterol. Hepatol.* **2018**, *17*, 41–53. [[CrossRef](#)] [[PubMed](#)]
42. Gardner, T.B. Fluid Resuscitation in Acute Pancreatitis—Going over the WATERFALL. *N. Engl. J. Med.* **2022**, *387*, 1038–1039. [[CrossRef](#)] [[PubMed](#)]
43. Drewes, A.M.; Olesen, A.E.; Farmer, A.D.; Szigethy, E.; Rebours, V.; Olesen, S.S. Gastrointestinal pain. *Nat. Rev. Dis. Prim.* **2020**, *6*, 1. [[CrossRef](#)] [[PubMed](#)]
44. Meyers, C.; Radler, D.R.; Zelig, R.S. Impact of solid food provision within 24 hours of hospital admission on clinical outcomes for adult patients with acute pancreatitis: A literature review. *Nutr. Clin. Pract.* **2023**, 1–11. [[CrossRef](#)] [[PubMed](#)]
45. Gubala, V.; Harris, L.F.; Ricco, A.J.; Tan, M.X.; Williams, D.E. Point of Care Diagnostics: Status and Future. *Anal. Chem.* **2012**, *84*, 487–515. [[CrossRef](#)]
46. Vashist, S.K.; Luppa, P.B.; Yeo, L.Y.; Ozcan, A.; Luong, J.H.T. Emerging Technologies for Next-Generation Point-of-Care Testing. *Trends Biotechnol.* **2015**, *33*, 692–705. [[CrossRef](#)]
47. Yager, P.; Domingo, G.J.; Gerdes, J. Point-of-care diagnostics for global health. *Annu. Rev. Biomed. Eng.* **2008**, *10*, 107–144. [[CrossRef](#)]
48. Pai, N.P.; Vadnais, C.; Denkinger, C.; Engel, N.; Pai, M. Point-of-Care Testing for Infectious Diseases: Diversity, Complexity, and Barriers in Low- And Middle-Income Countries. *PLoS Med.* **2012**, *9*, e1001306. [[CrossRef](#)]
49. Zerem, E.; Kurtcehajic, A.; Kunosic, S.; Malkocecic, D.Z.; Zerem, O. Current trends in acute pancreatitis: Diagnostic and therapeutic challenges. *World J. Gastroenterol.* **2023**, *29*, 2747–2763. [[CrossRef](#)]
50. Yamamiya, A.; Irisawa, A.; Abe, Y.; Arisaka, T.; Ohnishi, T.; Hoshi, K.; Suzuki, T.; Nagashima, K.; Kashima, K.; Kunogi, Y.; et al. Diagnosing chronic pancreatitis by endoscopic ultrasound assessing the association between ultrasound and pathological findings: A narrative review. *DEN Open* **2023**, *3*, e164. [[CrossRef](#)]
51. Berbis, M.A.; Paulano Godino, F.; Royuela del Val, J.; Alcalá Mata, L.; Luna, A. Clinical impact of artificial intelligence-based solutions on imaging of the pancreas and liver. *World J. Gastroenterol.* **2023**, *29*, 1427–1445. [[CrossRef](#)] [[PubMed](#)]
52. Corring, T. The Adaptation of Digestive Enzymes to The Diet—Its Physiological Significance. *Reprod. Nutr. Dev.* **1980**, *20*, 1217–1235. [[CrossRef](#)] [[PubMed](#)]
53. Isenman, L.; Liebow, C.; Rothman, S. The endocrine secretion of mammalian digestive enzymes by exocrine glands. *Am. J. Physiol. -Endocrinol. Metab.* **1999**, *276*, E223–E232. [[CrossRef](#)] [[PubMed](#)]
54. Rothman, S.; Liebow, C.; Isenman, L. Conservation of digestive enzymes. *Physiol. Rev.* **2002**, *82*, 1–18. [[CrossRef](#)] [[PubMed](#)]
55. Greaves, J.P.; Hollingsworth, D.F. Changes in the pattern of carbohydrates consumption in Britain. *Proc. Nutr. Soc.* **1964**, *23*, 136–143. [[CrossRef](#)]
56. Caspary, W.F. Physiology and pathophysiology of intestinal absorption. *Am. J. Clin. Nutr.* **1992**, *55*, 299S–308S. [[CrossRef](#)]
57. Salt, W.B.; Schenker, S. Amylase—Its Clinical Significance—Review of Literature. *Medicine* **1976**, *55*, 269–289. [[CrossRef](#)]
58. Ghelis, C.; Tempete-Gaillourdet, M.; Yon, J.M. The folding of pancreatic elastase: Independent domain refolding and inter-domain interaction. *Biochem. Biophys. Res. Commun.* **1978**, *84*, 31–36. [[CrossRef](#)]
59. Stiefel, D.J.; Keller, P.J. Preparation and some properties of human pancreatic amylase including a comparison with human parotid amylase. *Biochim. Biophys. Acta* **1973**, *302*, 345–361. [[CrossRef](#)]

60. Douglas, H.; Fraser, I.; Davidson, G.; Murphy, C.; Gorman, M.L.; Boyce, M.; Doole, S. Assessing the background levels of body fluids on hands. *Sci. Justice* **2023**, *63*, 493–499. [[CrossRef](#)]
61. Agatonovic-Kustrin, S.; Wong, S.; Dolzhenko, A.V.; Gegechkori, V.; Ku, H.; Tan, W.K.; Morton, D.W. Effect directed analysis of bioactive compounds in leaf extracts from two *Salvia* species by High-performance thin-layer chromatography. *J. Pharm. Biomed. Anal.* **2023**, *227*, 115308. [[CrossRef](#)] [[PubMed](#)]
62. Barber, E.; Houghton, M.J.; Visvanathan, R.; Williamson, G. Measuring key human carbohydrate digestive enzyme activities using high-performance anion-exchange chromatography with pulsed amperometric detection. *Nat. Protoc.* **2022**, *17*, 2882–2919. [[CrossRef](#)] [[PubMed](#)]
63. Mileski, K.S.; Ciric, A.D.; Gasic, U.M.; Zarkovic, L.D.; Krivosej, Z.D.; Dzamic, A.M. Comparative Analyses on Chemical Constituents and Biological Activities of *Laserpitium siler* L. from Serbia. *Rec. Nat. Prod.* **2022**. [[CrossRef](#)]
64. Weng, S.; Tang, L.; Wang, J.; Zhu, R.; Wang, C.; Sha, W.; Zheng, L.; Huang, L.; Liang, D.; Hu, Y.; et al. Detection of amylase activity and moisture content in rice by reflectance spectroscopy combined with spectral data transformation. *Spectrochim. Acta Part A Mol. Biomol. Spectrosc.* **2023**, *290*, 122311. [[CrossRef](#)] [[PubMed](#)]
65. Dutta, S.; Mandal, N.; Bandyopadhyay, D. Paper-based alpha-amylase detector for point-of-care diagnostics. *Biosens. Bioelectron.* **2016**, *78*, 447–453. [[CrossRef](#)] [[PubMed](#)]
66. Hyung, S.; Karima, G.; Shin, K.; Kim, K.S.; Hong, J.W. A Simple Paper-Based alpha-Amylase Separating System for Potential Application in Biological Sciences. *Biochip J.* **2021**, *15*, 252–259. [[CrossRef](#)]
67. Adhikary, R.R.; Banerjee, R. Development of smart core-shell nanoparticle-based sensors for the point-of-care detection of alpha amylase in diagnostics and forensics. *Biosens. Bioelectron.* **2021**, *184*, 113244. [[CrossRef](#)]
68. Fuentes, M.; Tecles, F.; Gutierrez, A.; Otal, J.; Martinez-Subiela, S.; Ceron, J.J. Validation of an automated method for salivary alpha-amylase measurements in pigs (*Sus scrofa domestica*) and its application as a stress biomarker. *J. Vet. Diagn. Investig.* **2011**, *23*, 282–287. [[CrossRef](#)]
69. Visvanathan, R.; Jayathilake, C.; Liyanage, R. A simple microplate-based method for the determination of alpha-amylase activity using the glucose assay kit (GOD method). *Food Chem.* **2016**, *211*, 853–859. [[CrossRef](#)]
70. Dehghani, Z.; Mohammadnejad, J.; Hosseini, M. A new colorimetric assay for amylase based on starch-supported Cu/Au nanocluster peroxidase-like activity. *Anal. Bioanal. Chem.* **2019**, *411*, 3621–3629. [[CrossRef](#)]
71. Chen, L.; Huang, W.; Hao, M.; Yang, F.; Shen, H.; Yu, S.; Wang, L. Rapid and ultrasensitive activity detection of & alpha;-amylase based on & gamma;-cyclodextrin crosslinked metal-organic framework nanozyme. *Int. J. Biol. Macromol.* **2023**, *242*, 124881. [[CrossRef](#)]
72. Hsiao, H.Y.; Chen, R.L.C.; Chou, C.C.; Cheng, T.J. Hand-held Colorimetry Sensor Platform for Determining Salivary -Amylase Activity and Its Applications for Stress Assessment. *Sensors* **2019**, *19*, 1571. [[CrossRef](#)] [[PubMed](#)]
73. Thongprajukaew, K.; Choodum, A.; Sa-E, B.; Hayee, U. Smart phone: A popular device supports amylase activity assay in fisheries research. *Food Chem.* **2014**, *163*, 87–91. [[CrossRef](#)] [[PubMed](#)]
74. Dangkulwanich, M.; Kongnithigarn, K.; Aurnoppakhun, N. Colorimetric Measurements of Amylase Activity: Improved Accuracy and Efficiency with a Smartphone. *J. Chem. Educ.* **2018**, *95*, 141–145. [[CrossRef](#)]
75. Ishikawa-Ankerhold, H.C.; Ankerhold, R.; Drummen, G.P.C. Advanced Fluorescence Microscopy Techniques-FRAP, FLIP, FLAP, FRET and FLIM. *Molecules* **2012**, *17*, 4047–4132. [[CrossRef](#)]
76. Wang, X.; Tang, Y.; Qin, Y.; Zhang, P.; Zhang, D.; Xue, K.; Cao, Y.; Qi, Z. Rational design of water-soluble supramolecular AIEgen with ultra-high quantum yield, and its application in α -amylase activity detection and wash-free lysosome imaging. *Chem. Eng. J.* **2022**, *448*, 137632. [[CrossRef](#)]
77. Shi, J.; Deng, Q.; Li, Y.; Zheng, M.; Chai, Z.; Wan, C.; Zheng, Z.; Li, L.; Huang, F.; Tang, B. A Rapid and Ultrasensitive Tetraphenylethylene-Based Probe with Aggregation-Induced Emission for Direct Detection of α -Amylase in Human Body Fluids. *Anal. Chem.* **2018**, *90*, 13775–13782. [[CrossRef](#)]
78. Li, Y.; Peng, Y.; Liu, W.; Fan, Y.; Wu, Y.; Li, X.; Fan, X. Hierarchical Self-Assembly of Amino Acid Derivatives into Enzyme-Responsive Luminescent Gel. *Chemosensors* **2017**, *5*, 6. [[CrossRef](#)]
79. Attia, M.S.; Zoulghena, H.; Abdel-Mottaleb, M.S.A. A new nano-optical sensor thin film cadmium sulfide doped in sol-gel matrix for assessment of alpha-amylase activity in human saliva. *Analyst* **2014**, *139*, 793–800. [[CrossRef](#)]
80. Attia, M.S.; Al-Radadi, N.S. Progress of pancreatitis disease biomarker alpha amylase enzyme by new nano optical sensor. *Biosens. Bioelectron.* **2016**, *86*, 413–419. [[CrossRef](#)]
81. Kim, S.; Lee, S.-M.; Yoon, J.P.; Lee, N.; Chung, J.; Chung, W.-J.; Shin, D.-S. Robust Magnetized Graphene Oxide Platform for In Situ Peptide Synthesis and FRET-Based Protease Detection. *Sensors* **2020**, *20*, 5275. [[CrossRef](#)] [[PubMed](#)]
82. Wells, P.K.; Smutok, O.; Guo, Z.; Alexandrov, K.; Katz, E. Fluorometric biosensing of alpha-amylase using an artificial allosteric biosensor immobilized on nanostructured interface. *Talanta* **2023**, *255*, 124215. [[CrossRef](#)] [[PubMed](#)]
83. Pham Thi Kim, H.; Jang, C.-H. Simple, sensitive technique for alpha-amylase detection facilitated by liquid crystal-based microcapillary sensors. *Microchem. J.* **2021**, *162*, 105864. [[CrossRef](#)]
84. Homola, J. Surface plasmon resonance sensors for detection of chemical and biological species. *Chem. Rev.* **2008**, *108*, 462–493. [[CrossRef](#)] [[PubMed](#)]
85. Homola, J.; Yee, S.S.; Gauglitz, G. Surface plasmon resonance sensors: Review. *Sens. Actuators B Chem.* **1999**, *54*, 3–15. [[CrossRef](#)]

86. Singh, A.K.; Anwar, M.; Pradhan, R.; Ashar, M.S.; Rai, N.; Dey, S. Surface plasmon resonance based-optical biosensor: Emerging diagnostic tool for early detection of diseases. *J. Biophotonics* **2023**, *16*, e202200380. [[CrossRef](#)]
87. Roh, S.; Chung, T.; Lee, B. Overview of the Characteristics of Micro- and Nano-Structured Surface Plasmon Resonance Sensors. *Sensors* **2011**, *11*, 1565–1588. [[CrossRef](#)]
88. Pasquardini, L.; Cennamo, N.; Malleo, G.; Vanzetti, L.; Zeni, L.; Bonamini, D.; Salvia, R.; Bassi, C.; Bossi, A.M. A Surface Plasmon Resonance Plastic Optical Fiber Biosensor for the Detection of Pancreatic Amylase in Surgically-Placed Drain Effluent. *Sensors* **2021**, *21*, 3443. [[CrossRef](#)]
89. Cennamo, N.; Massarotti, D.; Conte, L.; Zeni, L. Low Cost Sensors Based on SPR in a Plastic Optical Fiber for Biosensor Implementation. *Sensors* **2011**, *11*, 11752–11760. [[CrossRef](#)]
90. Teng, C.; Wang, Y.; Yuan, L. Polymer optical fibers based surface plasmon resonance sensors and their applications: A review. *Opt. Fiber Technol.* **2023**, *77*, 103256. [[CrossRef](#)]
91. Zhang, X.; Jia, Y.; Fei, Y.; Lu, Y.; Liu, X.; Shan, H.; Huan, Y. Cu/Au nanoclusters with peroxidase-like activity for chemiluminescence detection of alpha-amylase. *Anal. Methods* **2023**, *15*, 1553–1558. [[CrossRef](#)] [[PubMed](#)]
92. Diltemiz, S.E.; Kecili, R.; Ersoez, A.; Say, R. Molecular Imprinting Technology in Quartz Crystal Microbalance (QCM) Sensors. *Sensors* **2017**, *17*, 454. [[CrossRef](#)] [[PubMed](#)]
93. Ding, K.; Jia, Z.; Wang, Q.; Tian, N.; Tong, R.; Wang, X. The applications of electrochemical quartz crystal microbalance (EQCM) in recent years. *Chem. Res. Appl.* **2002**, *14*, 123–126.
94. He, J.; Fu, L.; Huang, M.; Lu, Y.; Lv, B.; Zhu, Z.; Fang, J. The development of quartz crystal microbalance. *Sci. Sin. Chim.* **2011**, *41*, 1679–1698.
95. Wei, X.; Wang, G.; Li, A.; Quan, Y.; Chen, J.; Wang, R. Application of Electrochemical Quartz Crystal Microbalance. *Prog. Chem.* **2018**, *30*, 1701–1721. [[CrossRef](#)]
96. Yuan, H.Y.; Ma, C.F.; Liu, G.M.; Zhang, G.Z. Applications of Quartz Crystal Microbalance in Polymer Studies. *Acta Polym. Sin.* **2021**, *52*, 806–821. [[CrossRef](#)]
97. Le Guillou-Buffello, D.; Helary, G.; Gindre, M.; Pavon-Djavid, G.; Laugier, P.; Migonney, V. Monitoring cell adhesion processes on bioactive polymers with the quartz crystal resonator technique. *Biomaterials* **2005**, *26*, 4197–4205. [[CrossRef](#)]
98. Poturnayova, A.; Karpisova, I.; Castillo, G.; Mezo, G.; Kocsis, L.; Csampai, A.; Keresztes, Z.; Hianik, T. Detection of plasmin based on specific peptide substrate using acoustic transducer. *Sens. Actuators B Chem.* **2016**, *223*, 591–598. [[CrossRef](#)]
99. Xiong, W.; Baker, M.D. Electrochemistry of zeolites on thickness shear mode oscillators. *J. Phys. Chem. B* **2005**, *109*, 13590–13596. [[CrossRef](#)]
100. Della Ventura, B.; Sakac, N.; Funari, R.; Velotta, R. Flexible immunosensor for the detection of salivary alpha-amylase in body fluids. *Talanta* **2017**, *174*, 52–58. [[CrossRef](#)]
101. Zhao, M.; Luo, L.; Guo, Y.; Zhao, B.; Chen, X.; Shi, X.; Khan, M.; Lin, J.-M.; Hu, Q. Viscosity-Based Flow Sensor on Paper for Quantitative and Label-Free Detection of alpha-Amylase and Its Inhibitor. *ACS Sens.* **2022**, *7*, 593–600. [[CrossRef](#)]
102. Bhattacharjee, M.; Middy, S.; Escobedo, P.; Chaudhuri, J.; Bandyopadhyay, D.; Dahiya, R. Microdroplet based disposable sensor patch for detection of alpha-amylase in human blood serum. *Biosens. Bioelectron.* **2020**, *165*, 112333. [[CrossRef](#)]
103. Mandal, N.; Bhattacharjee, M.; Chattopadhyay, A.; Bandyopadhyay, D. Point-of-care-testing of alpha-amylase activity in human blood serum. *Biosens. Bioelectron.* **2019**, *124*, 75–81. [[CrossRef](#)]
104. Cardoso, S.; Leitao, D.C.; Dias, T.M.; Valadeiro, J.; Silva, M.D.; Chicharo, A.; Silverio, V.; Gaspar, J.; Freitas, P.P. Challenges and trends in magnetic sensor integration with microfluidics for biomedical applications. *J. Phys. D-Appl. Phys.* **2017**, *50*, 213001. [[CrossRef](#)]
105. Murzin, D.; Mapps, D.J.; Levada, K.; Belyaev, V.; Omelyanchik, A.; Panina, L.; Rodionova, V. Ultrasensitive Magnetic Field Sensors for Biomedical Applications. *Sensors* **2020**, *20*, 1569. [[CrossRef](#)] [[PubMed](#)]
106. Jogschies, L.; Klaas, D.; Kruppe, R.; Rittinger, J.; Taptimthong, P.; Wienecke, A.; Rissing, L.; Wurz, M.C. Recent Developments of Magnetoresistive Sensors for Industrial Applications. *Sensors* **2015**, *15*, 28665–28689. [[CrossRef](#)]
107. Weddemann, A.; Ennen, I.; Regtmeier, A.; Albon, C.; Wolff, A.; Eckstaedt, K.; Mill, N.; Peter, M.K.H.; Mattay, J.; Plattner, C.; et al. Review and outlook: From single nanoparticles to self-assembled monolayers and granular GMR sensors. *Beilstein J. Nanotechnol.* **2010**, *1*, 75–93. [[CrossRef](#)] [[PubMed](#)]
108. Wu, K.; Tonini, D.; Liang, S.; Saha, R.; Chugh, V.K.; Wang, J.-P. Giant Magnetoresistance Biosensors in Biomedical Applications. *ACS Appl. Mater. Interfaces* **2022**, *14*, 9945–9969. [[CrossRef](#)]
109. Mabarroh, N.M.; Alfansuri, T.; Wibowo, N.A.; Istiqomah, N.I.; Tumbelaka, R.M.; Suharyadi, E. Detection of green-synthesized magnetite nanoparticles using spin-valve GMR-based sensor and their potential as magnetic labels. *J. Magn. Magn. Mater.* **2022**, *560*, 169645. [[CrossRef](#)]
110. Martins, B.R.; Sampaio, T.M.; de Farias, A.K.S.R.; Martins, R.d.P.; Teixeira, R.R.; Oliveira, R.T.S.; Oliveira, C.J.F.; da Silva, M.V.; Rodrigues, V.; Dantas, N.O.; et al. Immunosensor Based on Zinc Oxide Nanocrystals Decorated with Copper for the Electrochemical Detection of Human Salivary Alpha-Amylase. *Micromachines* **2021**, *12*, 657. [[CrossRef](#)]
111. Teixeira, S.R.; Lloyd, C.; Yao, S.; Gazze, A.S.; Whitaker, I.S.; Francis, L.; Conlan, R.S.; Azzopardi, E. Polyaniline-graphene based alpha-amylase biosensor with a linear dynamic range in excess of 6 orders of magnitude. *Biosens. Bioelectron.* **2016**, *85*, 395–402. [[CrossRef](#)] [[PubMed](#)]

112. Li, M.; Yin, X.; Shan, H.; Meng, C.; Chen, S.; Yan, Y. The Facile Preparation of PBA-GO-CuO-Modified Electrochemical Biosensor Used for the Measurement of alpha-Amylase Inhibitors' Activity. *Molecules* **2022**, *27*, 2395. [[CrossRef](#)] [[PubMed](#)]
113. Garcia, P.T.; Guimaraes, L.N.; Dias, A.A.; Ulhoa, C.J.; Coltro, W.K.T. Amperometric detection of salivary alpha-amylase on screen-printed carbon electrodes as a simple and inexpensive alternative for point-of-care testing. *Sens. Actuators B Chem.* **2018**, *258*, 342–348. [[CrossRef](#)]
114. Mahosenaho, M.; Caprio, F.; Micheli, L.; Sesay, A.M.; Palleschi, G.; Virtanen, V. A disposable biosensor for the determination of alpha-amylase in human saliva. *Microchim. Acta* **2010**, *170*, 243–249. [[CrossRef](#)]
115. Sun, M.; Ma, B.; Yuan, S.; Xin, L.F.; Zhao, C.; Liu, H. Mercury thermometer-inspired test strip for concentration cell-based potentiometric detection of salivary alpha-amylase. *Anal. Chim. Acta* **2022**, *1206*, 339770. [[CrossRef](#)] [[PubMed](#)]
116. Zhang, L.; Yang, W.; Yang, Y.; Liu, H.; Gu, Z. Smartphone-based point-of-care testing of salivary alpha-amylase for personal psychological measurement. *Analyst* **2015**, *140*, 7399–7406. [[CrossRef](#)] [[PubMed](#)]
117. Wang, Q.; Wang, H.; Yang, X.; Wang, K.; Liu, R.; Li, Q.; Ou, J. A sensitive one-step method for quantitative detection of alpha-amylase in serum and urine using a personal glucose meter. *Analyst* **2015**, *140*, 1161–1165. [[CrossRef](#)]
118. Casey, D.G.; Price, J. The sensitivity and specificity of the RSID (TM)-saliva kit for the detection of human salivary amylase in the Forensic Science Laboratory, Dublin, Ireland. *Forensic Sci. Int.* **2010**, *194*, 67–71. [[CrossRef](#)]
119. Grant, B.D.; Anderson, C.E.; Williford, J.R.; Alonzo, L.F.; Glukhova, V.A.; Boyle, D.S.; Weigl, B.H.; Nichols, K.P. SARS-CoV-2 Coronavirus Nucleocapsid Antigen-Detecting Half-Strip Lateral Flow Assay Toward the Development of Point of Care Tests Using Commercially Available Reagents. *Anal. Chem.* **2020**, *92*, 11305–11309. [[CrossRef](#)]
120. Haupt, K.; Mosbach, K. Molecularly imprinted polymers and their use in biomimetic sensors. *Chem. Rev.* **2000**, *100*, 2495–2504. [[CrossRef](#)]
121. Freire, E.; Mayorga, O.L.; Straume, M. Isothermal Titration Calorimetry. *Anal. Chem.* **1990**, *62*, A950–A959. [[CrossRef](#)]
122. Siddiqui, K.S.; Poljak, A.; Ertan, H.; Bridge, W. The use of isothermal titration calorimetry for the assay of enzyme activity: Application in higher education practical classes. *Biochem. Mol. Biol. Educ.* **2022**, *50*, 519–526. [[CrossRef](#)] [[PubMed](#)]
123. Zhang, N.; Yang, G. alpha-amylase detection methods and applications. *Sheng Wu Gong Cheng Xue Bao = Chin. J. Biotechnol.* **2023**, *39*, 898–911. [[CrossRef](#)]
124. Lehoczki, G.; Kandra, L.; Gyemant, G. The use of starch azure for measurement of alpha-amylase activity. *Carbohydr. Polym.* **2018**, *183*, 263–266. [[CrossRef](#)]
125. Lehoczki, G.; Szabo, K.; Takacs, I.; Kandra, L.; Gyemant, G. Simple ITC method for activity and inhibition studies on human salivary alpha-amylase. *J. Enzym. Inhib. Med. Chem.* **2016**, *31*, 1648–1653. [[CrossRef](#)]
126. Pilvenyte, G.; Ratautaite, V.; Boguzaitė, R.; Samukaite-Bubniene, U.; Plausinaitis, D.; Ramanaviciene, A.; Bechelany, M.; Ramanavicius, A. Molecularly imprinted polymers for the recognition of biomarkers of certain neurodegenerative diseases. *J. Pharm. Biomed. Anal.* **2023**, *228*, 115343. [[CrossRef](#)]
127. Rebelo, T.S.C.R.; Miranda, I.M.; Brandão, A.T.S.C.; Sousa, L.I.G.; Ribeiro, J.A.; Silva, A.F.; Pereira, C.M. A Disposable Saliva Electrochemical MIP-Based Biosensor for Detection of the Stress Biomarker α -Amylase in Point-of-Care Applications. *Electrochem* **2021**, *2*, 427–438. [[CrossRef](#)]
128. Yan, R.-Y.; Lin, W.-H.; Lu, T.-L.; Chen, J.-L. Conjugated hypercrosslinked polymers imprinted with 3,5-dinitrosalicylic acid for the fluorescent determination of alpha-amylase activity. *Spectrochim. Acta Part A Mol. Biomol. Spectrosc.* **2023**, *291*, 122383. [[CrossRef](#)]
129. Arakawa, M.; Yoshida, A.; Okamura, S.; Ebina, H.; Morita, E. A highly sensitive NanoLuc-based protease biosensor for detecting apoptosis and SARS-CoV-2 infection. *Sci. Rep.* **2023**, *13*, 1753. [[CrossRef](#)]
130. Kaur, J.; Malegaonkar, J.N.; Bhosale, S.V.; Singh, P.K. An anionic tetraphenyl ethylene based simple and rapid fluorescent probe for detection of trypsin and paraoxon methyl. *J. Mol. Liq.* **2021**, *333*, 115980. [[CrossRef](#)]
131. Cai, Y.; Dong, T.; Zhang, X.; Liu, A. Morphology and Enzyme-Mimicking Activity of Copper Nanoassemblies Regulated by Peptide: Mechanism, Ultrasensitive Assaying of Trypsin, and Screening of Trypsin Inhibitors. *Anal. Chem.* **2022**, *94*, 18099–18106. [[CrossRef](#)] [[PubMed](#)]
132. Zhang, L.; Du, J. A sensitive and label-free trypsin colorimetric sensor with cytochrome c as a substrate. *Biosens. Bioelectron.* **2016**, *79*, 347–352. [[CrossRef](#)] [[PubMed](#)]
133. Wu, W.; Xia, S.; Liu, Y.; Ma, C.; Lyu, Z.; Zhao, M.; Ding, S.; Hu, Q. Single-atom catalysts with peroxidase-like activity boost gel-sol transition-based biosensing. *Biosens. Bioelectron.* **2023**, *225*, 115112. [[CrossRef](#)]
134. Wang, G.-L.; Jin, L.-Y.; Dong, Y.-M.; Wu, X.-M.; Li, Z.-J. Intrinsic enzyme mimicking activity of gold nanoclusters upon visible light triggering and its application for colorimetric trypsin detection. *Biosens. Bioelectron.* **2015**, *64*, 523–529. [[CrossRef](#)] [[PubMed](#)]
135. Luo, Q.; Tian, M.; Luo, F.; Zhao, M.; Lin, C.; Qiu, B.; Wang, J.; Lin, Z. Multicolor Biosensor for Trypsin Detection Based on the Regulation of the Peroxidase Activity of Bovine Serum Albumin-Coated Gold Nanoclusters and Etching of Gold Nanobipyramids. *Anal. Chem.* **2023**, *95*, 2390–2397. [[CrossRef](#)] [[PubMed](#)]
136. Lin, X.; Zhu, Z.; Zhao, C.; Li, S.; Liu, Q.; Liu, A.; Lin, L.; Lin, X. Robust oxidase mimicking activity of protamine-stabilized platinum nanoparticles units and applied for colorimetric sensor of trypsin and inhibitor. *Sens. Actuators B Chem.* **2019**, *284*, 346–353. [[CrossRef](#)]
137. Lin, X.; Zhu, Z.; Lin, D.; Bao, Q.; Gao, Y.; Liu, Q.; Liu, A.; Lin, L.; Lin, X. Boosting the oxidase-like activity of platinum nanozyme in MBTH-TOOS chromogenic system for detection of trypsin and its inhibitor. *Talanta* **2021**, *234*, 122647. [[CrossRef](#)]

138. Chen, X.; Liang, Y. Colorimetric sensing strategy for multiplexed detection of proteins based on three DNA-gold nanoparticle conjugates sensors. *Sens. Actuators B Chem.* **2021**, *329*, 129202. [[CrossRef](#)]
139. Liu, L.; Zhang, L.; Liang, Y. A Simple Visual Strategy for Protein Detection Based on Oxidase-Like Activity of Silver Nanoparticles. *Food Anal. Methods* **2021**, *14*, 1852–1859. [[CrossRef](#)]
140. Arora, A.; Sharma, K.; Tripathi, S.K. Impact of luminescent MoSe₂ quantum dots on activity of trypsin under different pH environment. *Spectrochim. Acta Part A Mol. Biomol. Spectrosc.* **2023**, *302*, 122958. [[CrossRef](#)]
141. Liu, W.; Li, H.; Wei, Y.; Dong, C. A label-free phosphorescence sensing platform for trypsin based on Mn-ZnS QDs. *RSC Adv.* **2017**, *7*, 26930–26934. [[CrossRef](#)]
142. Zhuo, C.-X.; Wang, L.-H.; Feng, J.-J.; Zhang, Y.-D. Label-Free Fluorescent Detection of Trypsin Activity Based on DNA-Stabilized Silver Nanocluster-Peptide Conjugates. *Sensors* **2016**, *16*, 1477. [[CrossRef](#)] [[PubMed](#)]
143. Jingjing, W.; Manning, W.; Jie, G.; Meixian, G.; Ya, Y. Preparation of AgInS₂ quantum dots and their application for trypsin detection. *J. Mater. Sci. Mater. Electron.* **2021**, *32*, 26490–26502.
144. Milicevic, D.; Hlavac, J. Triple-FRET multi-purpose fluorescent probe for three-protease detection. *RSC Adv.* **2022**, *12*, 28780–28787. [[CrossRef](#)]
145. Hu, L.; Han, S.; Parveen, S.; Yuan, Y.; Zhang, L.; Xu, G. Highly sensitive fluorescent detection of trypsin based on BSA-stabilized gold nanoclusters. *Biosens. Bioelectron.* **2012**, *32*, 297–299. [[CrossRef](#)]
146. Qu, F.; Wang, Z.; Li, C.; Jiang, D.; Zhao, X.-E. Peptide cleavage-mediated aggregation-enhanced emission from metal nanoclusters for detecting trypsin and screen its inhibitors from foods. *Sens. Actuators B Chem.* **2022**, *359*, 131610. [[CrossRef](#)]
147. Xue, F.; Qu, F.; Han, W.; Xia, L.; You, J. Aggregation-induced emission enhancement of gold nanoclusters triggered by silicon nanoparticles for ratiometric detection of protamine and trypsin. *Anal. Chim. Acta* **2019**, *1046*, 170–178. [[CrossRef](#)]
148. Zhao, D.; Chen, C.; Zhao, J.; Sun, J.; Yang, X. Label-free fluorescence turn-on strategy for trypsin activity based on thiolate-protected gold nanoclusters with bovine serum albumin as the substrate. *Sens. Actuators B Chem.* **2017**, *247*, 392–399. [[CrossRef](#)]
149. Zheng, X.; Chen, S.; Fu, B.; Cao, Y.; Li, H.; Wang, F.; Pan, Q. Improved sensitivity of gold nanoclusters toward trypsin under synergistic adsorption of CdTe quantum dots. *Microchem. J.* **2023**, *187*, 108457. [[CrossRef](#)]
150. Zhou, J.; Zhang, F.; Zhao, R.; Liu, S.; Li, W.; He, F.; Gai, S.; Yang, P. A novel “off-on-off” fluorescent sensor based on inner filter effect for ultrasensitive detection of protamine/trypsin and subcellular colocalization. *Sens. Actuators B Chem.* **2021**, *340*, 129930. [[CrossRef](#)]
151. Hou, S.; Feng, T.; Zhao, N.; Zhang, J.; Wang, H.; Liang, N.; Zhao, L. A carbon nanoparticle-peptide fluorescent sensor custom-made for simple and sensitive detection of trypsin. *J. Pharm. Anal.* **2020**, *10*, 482–489. [[CrossRef](#)] [[PubMed](#)]
152. Poon, C.-Y.; Li, Q.; Zhang, J.; Li, Z.; Dong, C.; Lee, A.W.-M.; Chan, W.-H.; Li, H.-W. FRET-based modified graphene quantum dots for direct trypsin quantification in urine. *Anal. Chim. Acta* **2016**, *917*, 64–70. [[CrossRef](#)] [[PubMed](#)]
153. Wu, M.; Wang, X.; Wang, K.; Guo, Z. An ultrasensitive fluorescent nanosensor for trypsin based on upconversion nanoparticles. *Talanta* **2017**, *174*, 797–802. [[CrossRef](#)] [[PubMed](#)]
154. Xu, S.; Zhang, F.; Xu, L.; Liu, X.; Ma, P.; Sun, Y.; Wang, X.; Song, D. A fluorescence resonance energy transfer biosensor based on carbon dots and gold nanoparticles for the detection of trypsin. *Sens. Actuators B Chem.* **2018**, *273*, 1015–1021. [[CrossRef](#)]
155. Chen, Y.; Lin, Z.; Miao, C.; Cai, Q.; Li, F.; Zheng, Z.; Lin, X.; Zheng, Y.; Weng, S. A simple fluorescence assay for trypsin through a protamine-induced carbon quantum dot-quenching aggregation platform. *RSC Adv.* **2020**, *10*, 26765–26770. [[CrossRef](#)]
156. Huang, S.; Yao, J.D.; Ning, G.; Li, B.; Mu, P.P.; Xiao, Q. Ultrasensitive ratiometric fluorescent probes for Hg(II) and trypsin activity based on carbon dots and metalloporphyrin via a target recycling amplification strategy. *Analyst* **2022**, *147*, 1457–1466. [[CrossRef](#)]
157. Chen, S.; Fu, J.; Zhou, S.; Wu, X.; Tang, S.; Zhao, P.; Zhang, Z. An eco-friendly near infrared fluorescence molecularly imprinted sensor based on zeolite imidazolate framework-8 for rapid determination of trace trypsin. *Microchem. J.* **2021**, *168*, 106449. [[CrossRef](#)]
158. Giel, M.C.; Zhang, S.X.; Hu, Q.; Ding, D.; Tang, Y.H.; Hong, Y.N. Synthesis of a beta-Arylethenesulfonyl Fluoride-Functionalized AIEgen for Activity-Based Urinary Trypsin Detection. *ACS Appl. Bio Mater.* **2022**, *5*, 4321–4326. [[CrossRef](#)]
159. Sun, W.; Zhang, F.; Wang, M.; Wang, N.; Wang, G.; Su, X. A ratiometric fluorescence strategy based on polyethyleneimine surface-modified carbon dots and Eosin Y for the ultrasensitive determination of protamine and trypsin. *Analyst* **2022**, *147*, 677–684. [[CrossRef](#)]
160. Park, T.; Han, M.; Schanze, K.S.S.; Lee, S.H. Ultrasensitive Determination of Trypsin in Human Urine Based on Amplified Fluorescence Response. *ACS Sens.* **2023**, *8*, 2591–2597. [[CrossRef](#)]
161. Li, F.; Chen, Y.; Lin, R.; Miao, C.; Ye, J.; Cai, Q.; Huang, Z.; Zheng, Y.; Lin, X.; Zheng, Z.; et al. Integration of fluorescent polydopamine nanoparticles on protamine for simple and sensitive trypsin assay. *Anal. Chim. Acta* **2021**, *1148*, 338201. [[CrossRef](#)] [[PubMed](#)]
162. Gu, P.; Lu, Y.; Li, S.; Ma, C. A Label-Free Fluorescence Aptasensor Based on G-Quadruplex/Thioflavin T Complex for the Detection of Trypsin. *Molecules* **2022**, *27*, 6093. [[CrossRef](#)]
163. Duan, X.; Li, N.; Wang, G.; Su, X. High sensitive ratiometric fluorescence analysis of trypsin and dithiothreitol based on WS₂ QDs. *Talanta* **2020**, *219*, 121171. [[CrossRef](#)]
164. Ou, L.-J.; Li, X.-Y.; Li, L.-J.; Liu, H.-W.; Sun, A.-M.; Liu, K.-J. A sensitive assay for trypsin using poly(thymine)-templated copper nanoparticles as fluorescent probes. *Analyst* **2015**, *140*, 1871–1875. [[CrossRef](#)] [[PubMed](#)]

165. Yin, C.; Chen, L.; Niu, N. Nitrogen-doped carbon quantum dots fabricated from cellulolytic enzyme lignin and its application to the determination of cytochrome c and trypsin. *Anal. Bioanal. Chem.* **2021**, *413*, 5239–5249. [[CrossRef](#)] [[PubMed](#)]
166. Hu, W.; Feng, S.; Pei, F.; Du, B.; Liu, B.; Mu, X.; Tong, Z. A novel smartphone-integrated binary-emission molecularly imprinted fluorescence sensor embedded with MIL-101(Cr) for sensitive and real-time detection of protein. *Talanta* **2023**, *260*, 124563. [[CrossRef](#)]
167. Manmana, Y.; Kubo, T.; Otsuka, K. Protein Determination by Distance and Color Changing via PEG-Based Hydrogels. *Chromatography* **2023**, *44*, 27–32. [[CrossRef](#)]
168. Zhao, L.; Wang, T.; Wu, Q.; Liu, Y.; Chen, Z.; Li, X. Fluorescent Strips of Electrospun Fibers for Ratiometric Sensing of Serum Heparin and Urine Trypsin. *ACS Appl. Mater. Interfaces* **2017**, *9*, 3400–3410. [[CrossRef](#)]
169. Hu, Q.-Z.; Jang, C.-H. Imaging Trypsin Activity through Changes in the Orientation of Liquid Crystals Coupled to the Interactions between a Polyelectrolyte and a Phospholipid Layer. *ACS Appl. Mater. Interfaces* **2012**, *4*, 1791–1795. [[CrossRef](#)]
170. Ping, J.; Qi, L.; Wang, Q.; Liu, S.; Jiang, Y.; Yu, L.; Lin, J.-M.; Hu, Q. An integrated liquid crystal sensing device assisted by the surfactant-embedded smart hydrogel. *Biosens. Bioelectron.* **2021**, *187*, 113313. [[CrossRef](#)]
171. Mayer, K.M.; Hafner, J.H. Localized Surface Plasmon Resonance Sensors. *Chem. Rev.* **2011**, *111*, 3828–3857. [[CrossRef](#)] [[PubMed](#)]
172. Willets, K.A.; Van Duyne, R.P. Localized surface plasmon resonance spectroscopy and sensing. *Annu. Rev. Phys. Chem.* **2007**, *58*, 267–297. [[CrossRef](#)] [[PubMed](#)]
173. Miao, P.; Liu, T.; Li, X.; Ning, L.; Yin, J.; Han, K. Highly sensitive, label-free colorimetric assay of trypsin using silver nanoparticles. *Biosens. Bioelectron.* **2013**, *49*, 20–24. [[CrossRef](#)]
174. Guo, Q.; Zhou, J.; Hu, K.; He, Y.; Huang, K.; Chen, P. Enzymatic reaction modulated gold nanoparticle aggregation-induced photothermal and smartphone readable colorimetry dual-mode biosensing platform for trypsin detection in clinical samples. *Sens. Actuators B Chem.* **2023**, *374*, 132841. [[CrossRef](#)]
175. Dutta, S.; Saikia, K.; Nath, P. Smartphone based LSPR sensing platform for bio-conjugation detection and quantification. *RSC Adv.* **2016**, *6*, 21871–21880. [[CrossRef](#)]
176. Liu, H.; Yin, H.; Dong, Y.; Ding, H.; Chu, X. Electrochemiluminescence resonance energy transfer between luminol and black phosphorus nanosheets for the detection of trypsin via the “off-on-off” switch mode. *Analyst* **2020**, *145*, 2204–2211. [[CrossRef](#)]
177. Dong, Z.-M.; Cheng, L.; Zhang, P.; Zhao, G.-C. Label-free analytical performances of a peptide-based QCM biosensor for trypsin. *Analyst* **2020**, *145*, 3329–3338. [[CrossRef](#)]
178. Dizon, M.; Tatarko, M.; Hianik, T. Advances in Analysis of Milk Proteases Activity at Surfaces and in a Volume by Acoustic Methods. *Sensors* **2020**, *20*, 5594. [[CrossRef](#)]
179. Piovarci, I.; Melikishvili, S.; Tatarko, M.; Hianik, T.; Thompson, M. Detection of Sub-Nanomolar Concentration of Trypsin by Thickness-Shear Mode Acoustic Biosensor and Spectrophotometry. *Biosensors* **2021**, *11*, 117. [[CrossRef](#)]
180. Lee, A.-W.; Cheng, C.-C.; Chang, C.-J.; Lu, C.-H.; Chen, J.-K. Optical assay of trypsin using a one-dimensional plasmonic grating of gelatin-modified poly(methacrylic acid). *Microchim. Acta* **2020**, *187*, 1–8. [[CrossRef](#)]
181. Erturk, G.; Hedstrom, M.; Mattiasson, B. A sensitive and real-time assay of trypsin by using molecular imprinting-based capacitive biosensor. *Biosens. Bioelectron.* **2016**, *86*, 557–565. [[CrossRef](#)]
182. Palomar, Q.; Svard, A.; Zeng, S.; Hu, Q.; Liu, F.; Aili, D.; Zhang, Z. Detection of gingipain activity using solid state nanopore sensors. *Sens. Actuators B Chem.* **2022**, *368*, 132209. [[CrossRef](#)]
183. Zaccheo, B.A.; Crooks, R.M. Self-Powered Sensor for Naked-Eye Detection of Serum Trypsin. *Anal. Chem.* **2011**, *83*, 1185–1188. [[CrossRef](#)] [[PubMed](#)]
184. Zhou, S.; Wang, L.; Chen, X.; Guan, X. Label-Free Nanopore Single-Molecule Measurement of Trypsin Activity. *ACS Sens.* **2016**, *1*, 607–613. [[CrossRef](#)] [[PubMed](#)]
185. Yi, Q.; Liu, Q.; Gao, F.; Chen, Q.; Wang, G. Application of an Electrochemical Immunosensor with a MWCNT/PDAA Modified Electrode for Detection of Serum Trypsin. *Sensors* **2014**, *14*, 10203–10212. [[CrossRef](#)]
186. Rahmati, Z.; Roushani, M.; Hosseini, H. Amorphous Ni(OH)₂ nano-boxes as a high performance substrate for aptasensor application. *Measurement* **2022**, *189*, 110649. [[CrossRef](#)]
187. Hu, J.; Li, Q.; Chen, J.; Chen, S.; Cai, Y.; Zhao, C. A label-free Electrochemical Immunosensor Based on Polythionine-nanogold Nanocomposite for Detection of Trypsin Using screen-printed Electrode. *Int. J. Electrochem. Sci.* **2022**, *17*, 220617. [[CrossRef](#)]
188. Ucar, A.; Gonzalez-Fernandez, E.; Stadenni, M.; Avlonstis, N.; Murray, A.F.; Bradley, M.; Mount, A.R. Miniaturisation of a peptide-based electrochemical protease activity sensor using platinum microelectrodes. *Analyst* **2020**, *145*, 975–982. [[CrossRef](#)] [[PubMed](#)]
189. Adjemian, J.; Anne, A.; Cauet, G.; Demaille, C. Cleavage-Sensing Redox Peptide Monolayers for the Rapid Measurement of the Proteolytic Activity of Trypsin and alpha-Thrombin Enzymes. *Langmuir* **2010**, *26*, 10347–10356. [[CrossRef](#)]
190. Barsan, M.M.; Serban, A.; Onea, M.; Wysocka, M.; Lesner, A.; Diculescu, V.C. Synthetic peptide array on gold for the electrochemical assessment of the 20S proteasome activity and effect of inhibitory compounds. *Appl. Surf. Sci.* **2023**, *610*, 155620. [[CrossRef](#)]
191. Hu, Q.; Bao, Y.; Gan, S.; Zhang, Y.; Han, D.; Niu, L. Electrochemically controlled grafting of polymers for ultrasensitive electrochemical assay of trypsin activity. *Biosens. Bioelectron.* **2020**, *165*, 112358. [[CrossRef](#)]
192. Poma, N.; Vivaldi, F.; Bonini, A.; Biagini, D.; Bottai, D.; Tavanti, A.; Di Francesco, F. Voltammetric sensing of trypsin activity using gelatin as a substrate. *Microchem. J.* **2023**, *190*, 108631. [[CrossRef](#)]

193. Shin, J.; Park, K.; Park, S.; Yang, H. Trypsin Detection Using Electrochemical Reduction-based Redox Cycling. *Bull. Korean Chem. Soc.* **2021**, *42*, 37–42. [[CrossRef](#)]
194. Choi, D.Y.; Yang, J.C.; Park, J. Optimization and characterization of electrochemical protein Imprinting on hemispherical porous gold patterns for the detection of trypsin. *Sens. Actuators B Chem.* **2022**, *350*, 130855. [[CrossRef](#)]
195. Zhao, W.; Li, B.; Xu, S.; Zhu, Y.; Liu, X. A fabrication strategy for protein sensors based on an electroactive molecularly imprinted polymer: Cases of bovine serum albumin and trypsin sensing. *Anal. Chim. Acta* **2020**, *1117*, 25–34. [[CrossRef](#)]
196. Carrere, J.; Figarella, C.; Guy, O.; Thouvenot, J.P. Human pancreatic chymotrypsinogen A: A non-competitive enzyme immunoassay, and molecular forms in serum and amniotic fluid. *Biochim. Biophys. Acta (BBA)-Gen. Subj.* **1986**, *883*, 46–53. [[CrossRef](#)]
197. Keim, V.; Teich, N.; Moessner, J. Clinical value of a new fecal elastase test for detection of chronic pancreatitis. *Clin. Lab.* **2003**, *49*, 209–215.
198. Liu, L.; Liu, C.; Zhang, B.; Gao, L. Detection of chymotrypsin using a peptide sensor based on graphene oxide modified with sulfhydryl groups and gold nanoparticles. *New J. Chem.* **2022**, *46*, 16303–16308. [[CrossRef](#)]
199. Gao, L.; Shi, H.; Liu, C.; Xia, N.; Cheng, J.; Liu, L. The detection of chymotrypsin using peptides covalent bound to the surface of graphene oxide and gold nanoparticles. *New J. Chem.* **2021**, *45*, 7946–7950. [[CrossRef](#)]
200. Liu, L.; Liu, C.; Gao, L. Highly Sensitive Detection of Chymotrypsin Based on Metal Organic Frameworks with Peptides Sensors. *Biosensors* **2023**, *13*, 263. [[CrossRef](#)] [[PubMed](#)]
201. Qu, Y.; Xu, Z.; Wang, J.; Liu, W.; Iqbal, A.; Iqbal, K.; Su, Y.; Cao, Y.; Yang, J.; Qin, W.; et al. Strong red fluorescent probe for detecting chymotrypsin activity in vivo and in vitro. *Sens. Actuators B Chem.* **2023**, *382*, 133552. [[CrossRef](#)]
202. Lan, T.; Tian, Q.-Q.; Li, M.-H.; He, W. Activatable endoplasmic reticulum-targeted NIR fluorescent probe with a large Stokes shift for detecting and imaging chymotrypsin. *Analyst* **2022**, *147*, 4098–4104. [[CrossRef](#)] [[PubMed](#)]
203. Piovarci, I.; Hianik, T.; Ivanov, I.N. Detection of Chymotrypsin by Optical and Acoustic Methods. *Biosensors* **2021**, *11*, 63. [[CrossRef](#)] [[PubMed](#)]
204. Ping, J.; Wu, W.; Qi, L.; Liu, J.; Liu, J.; Zhao, B.; Wang, Q.; Yu, L.; Lin, J.-M.; Hu, Q. Hydrogel-assisted paper-based lateral flow sensor for the detection of trypsin in human serum. *Biosens. Bioelectron.* **2021**, *192*, 113548. [[CrossRef](#)]
205. Kakizaki, E.; Seo, Y.; Takahama, K. A sandwich enzyme immunoassay for human pancreatic elastase III. *Forensic Sci. Int.* **2000**, *113*, 189–192. [[CrossRef](#)] [[PubMed](#)]
206. Ogawa, M. Pancreatic elastase 1. *Rinsho Byori. Jpn. J. Clin. Pathol.* **2001**, *Suppl 116*, 131–134.
207. Huta, Y.; Ashorov, O.; Hamouda, D.; Boltin, D.; Dickman, R.; Perets, T.T. A Novel Fecal Elastase Assay for the Detection of Pancreatic Exocrine Insufficiency. *Clin. Lab.* **2022**, *68*, 1476–1480. [[CrossRef](#)]
208. Benini, L.; Amodio, A.; Campagnola, P.; Agugiaro, F.; Cristofori, C.; Micciolo, R.; Magro, A.; Gabbrielli, A.; Cabrini, G.; Moser, L.; et al. Fecal elastase-1 is useful in the detection of steatorrhea in patients with pancreatic diseases but not after pancreatic resection. *Pancreatology* **2013**, *13*, 38–42. [[CrossRef](#)]
209. Leeds, J.S.; Oppong, K.; Sanders, D.S. The role of fecal elastase-1 in detecting exocrine pancreatic disease. *Nat. Rev. Gastroenterol. Hepatol.* **2011**, *8*, 405–415. [[CrossRef](#)]
210. Edwards, J.V.; Prevost, N.; Sethumadhavan, K.; Ullah, A.; Condon, B. Peptide conjugated cellulose nanocrystals with sensitive human neutrophil elastase sensor activity. *Cellulose* **2013**, *20*, 1223–1235. [[CrossRef](#)]
211. Edwards, J.V.; Prevost, N.T.; French, A.D.; Concha, M.; Condon, B.D. Kinetic and structural analysis of fluorescent peptides on cotton cellulose nanocrystals as elastase sensors. *Carbohydr. Polym.* **2015**, *116*, 278–285. [[CrossRef](#)]
212. Hasmann, A.; Gewessler, U.; Hulla, E.; Schneider, K.P.; Binder, B.; Francesko, A.; Tzanov, T.; Schintler, M.; Van der Palen, J.; Guebitz, G.M.; et al. Sensor materials for the detection of human neutrophil elastase and cathepsin G activity in wound fluid. *Exp. Dermatol.* **2011**, *20*, 508–513. [[CrossRef](#)] [[PubMed](#)]
213. He, J.-L.; Wu, Z.-S.; Zhang, S.-B.; Shen, G.-L.; Yu, R.-Q. Fluorescence aptasensor based on competitive-binding for human neutrophil elastase detection. *Talanta* **2010**, *80*, 1264–1268. [[CrossRef](#)] [[PubMed](#)]
214. Ling, Z.; Xu, F.; Edwards, J.V.; Prevost, N.T.; Nam, S.; Condon, B.D.; French, A.D. Nanocellulose as a colorimetric biosensor for effective and facile detection of human neutrophil elastase. *Carbohydr. Polym.* **2019**, *216*, 360–368. [[CrossRef](#)] [[PubMed](#)]
215. Sun, Q.; Li, J.; Liu, W.-N.; Dong, Q.-J.; Yang, W.-C.; Yang, G.-F. Non-Peptide-Based Fluorogenic Small-Molecule Probe for Elastase. *Anal. Chem.* **2013**, *85*, 11304–11311. [[CrossRef](#)]
216. Li, W.K.; Yang, Y.J. Mixed self-assembled monolayers modified electrode for the detection of human neutrophil elastase. *Adv. Mater. Res.* **2014**, *898*, 308–311. [[CrossRef](#)]
217. Yang, T.; Pan, S.-C.; Cheng, C.-M. Paper-based human neutrophil elastase detection device for clinical wound monitoring. *Lab A Chip* **2020**, *20*, 2709–2716. [[CrossRef](#)]
218. Huang, L.; Su, W.; Zhu, L.; Li, J.; Quan, W.; Yoon, J.; Lin, W. A Biocompatible Probe for the Detection of Neutrophil Elastase Free from the Interference of Structural Changes and Its Application to Ratiometric Photoacoustic Imaging In Vivo. *Angew. Chem. -Int. Ed.* **2023**, *62*, e202217508. [[CrossRef](#)]
219. Li, X.; Zhao, Y.; Qiu, Y.; Luo, X.; Liu, G.; Sun, Q. Phenoxazine-based red-emitting fluorescence probe for specific detection and imaging of endogenous neutrophil elastase in vitro and in vivo. *Dye. Pigment.* **2023**, *210*, 110966. [[CrossRef](#)]
220. Usui, M.; Iwasaki, M.; Ariyoshi, W.; Kobayashi, K.; Kasai, S.; Yamanaka, R.; Nakashima, K.; Nishihara, T. The Ability of a Novel Trypsin-like Peptidase Activity Assay Kit to Detect Red-Complex Species. *Diagnostics* **2022**, *12*, 2172. [[CrossRef](#)]

221. Lowe, M.E. The triglyceride lipases of the pancreas. *J. Lipid Res.* **2002**, *43*, 2007–2016. [[CrossRef](#)] [[PubMed](#)]
222. Verger, R.; Cambillau, C.; Tilbeurgh, H.V.; Eglloff, M.P.; Martinez, C.; Rugani, N. Interfacial activation of the lipase-procolipase complex by mixed micelles revealed by X-ray crystallography. *Nature* **1993**, *362*, 814–820.
223. Verger, R. ‘Interfacial activation’ of lipases: Facts and artifacts. *Trends Biotechnol.* **1997**, *15*, 32–38. [[CrossRef](#)]
224. Winkler, F.K.; Darcy, A.; Hunziker, W. Structure of Human Pancreatic Lipase. *Nature* **1990**, *343*, 771–774. [[CrossRef](#)]
225. Guo, C.; Zhai, J.; Chen, Q.; Du, X.; Xie, X. Phase transfer of fatty acids into ultrasmall nanospheres for colorimetric detection of lipase and albumin. *Chem. Commun.* **2022**, *58*, 5037–5040. [[CrossRef](#)]
226. Wang, L.; Song, Y.; Yao, J.; Wang, R.; Zhang, N.; Zou, D.; Yu, D.; Elfalleh, W. Detection of lipase activity in rice bran with AuNPs colorimetric sensor. *J. Food Meas. Charact.* **2021**, *15*, 3461–3470. [[CrossRef](#)]
227. Guan, P.; Liu, Y.; Yang, B.; Wu, Y.; Chai, J.; Wen, G.; Liu, B. Fluorometric probe for the lipase level: Design, mechanism and biological imaging application. *Talanta* **2021**, *225*, 121948. [[CrossRef](#)]
228. Shi, J.; Deng, Q.; Wan, C.; Zheng, M.; Huang, F.; Tang, B. Fluorometric probing of the lipase level as acute pancreatitis biomarkers based on interfacially controlled aggregation-induced emission (AIE). *Chem. Sci.* **2017**, *8*, 6188–6195. [[CrossRef](#)]
229. Du, T.; Zhang, F.; Jiang, L.; Tian, D. A Colorimetric and Fluorescent Dual-Signal Sensor for Detecting Lipase Activity Based on Inner Filter Effect. *J. Braz. Chem. Soc.* **2022**, *33*, 1255–1262. [[CrossRef](#)]
230. Zhang, F.; Du, T.; Jiang, L.; Zhu, L.; Tian, D. A combined “AIE+ESIPT” fluorescent probe for detection of lipase activity. *Bioorg. Chem.* **2022**, *128*, 106026. [[CrossRef](#)]
231. La Rocca, P.; Mingione, A.; Casati, S.; Ottria, R.; Allevi, P.; Ciuffreda, P.; Rota, P. Small-Molecules as Chemiluminescent Probes to Detect Lipase Activity. *Int. J. Mol. Sci.* **2022**, *23*, 9039. [[CrossRef](#)] [[PubMed](#)]
232. Luo, J.; Zhang, H.; Guan, J.; An, B.; Peng, J.; Zhu, W.; Wei, N.; Zhang, Y. Detection of lipase activity in human serum based on a ratiometric fluorescent probe. *New J. Chem.* **2021**, *45*, 9561–9568. [[CrossRef](#)]
233. Tang, J.Y.; Li, Z.B.; Xie, M.Y.; Zhang, Y.; Long, W.J.; Long, S.; Wen, T.J.; Fang, Z.X.; Zhu, W.G.; Zheng, H.D.; et al. Optical fiber bio-sensor for phospholipase using liquid crystal. *Biosens. Bioelectron.* **2020**, *170*, 112547. [[CrossRef](#)]
234. Schuchert-Shi, A.; Hauser, P.C. Following the Lipase Catalyzed Enantioselective Hydrolysis of Amino Acid Esters with Capillary Electrophoresis Using Contactless Conductivity Detection. *Chirality* **2010**, *22*, 331–335. [[CrossRef](#)]
235. Banni, G.A.H.D.; Nasreddine, R.; Fayad, S.; Phu, C.-N.; Rossi, J.-C.; Leclercq, L.; Cottet, H.; Marchal, A.; Nehme, R. Screening for pancreatic lipase natural modulators by capillary electrophoresis hyphenated to spectrophotometric and conductometric dual detection. *Analyst* **2021**, *146*, 1386–1401. [[CrossRef](#)]
236. Zlatev, R.; Stoytcheva, M.; Valdez, B.; Montero, G.; Toscano, L. Simple impedimetric sensor for rapid lipase activity quantification. *Talanta* **2019**, *203*, 161–167. [[CrossRef](#)]
237. Zlatev, R.; Stoytcheva, M.; Gochev, V.; Velkova, Z.; Valdez, B.; Montero, G. Rapid disposable lipase activity sensor for automatic industrial application. *Biotechnol. Biotechnol. Equip.* **2021**, *35*, 366–375. [[CrossRef](#)]
238. Rogala, A.; Rechberger, J.; Vasold, V.; Samphao, A.; Kalcher, K.; Ortner, A. Voltammetric lipase activity assay based on dilinolein and a modified carbon paste electrode. *Anal. Bioanal. Chem.* **2022**, *414*, 5033–5041. [[CrossRef](#)]
239. Sarakhman, O.; Wenninger, N.; Rogala, A.; Svorc, L.; Kurt, K.; Ortner, A. Electrochemical flow injection approach for routine screening of lipase activity in pancreatic preparations. *Talanta* **2023**, *260*, 124588. [[CrossRef](#)]
240. Valek, T.; Pohanka, M. The Determination of Lipase Activity by Measuring pH Using ion-Sensitive Field-effect Transistor. *Int. J. Electrochem. Sci.* **2021**, *16*, 210760. [[CrossRef](#)]
241. Wang, L.; Zhang, H.; Li, Z.; Qu, J.; Xing, K.; Wang, M.; Han, C.; Qiu, Z.; Yu, D. Development of a three-dimensional graphene-based photoelectrochemical biosensor and its use for monitoring lipase activity. *LWT-Food Sci. Technol.* **2022**, *170*, 114076. [[CrossRef](#)]
242. Xia, S.; Yin, F.; Xu, L.; Zhao, B.; Wu, W.; Ma, Y.; Lin, J.-M.; Liu, Y.; Zhao, M.; Hu, Q. Paper-Based Distance Sensor for the Detection of Lipase via a Phase Separation-Induced Viscosity Change. *Anal. Chem.* **2022**, *94*, 17055–17062. [[CrossRef](#)] [[PubMed](#)]
243. Zhang, H.; Yang, F.-Q.; Gao, J.-L. A Simple and Portable Personal Glucose Meter Method Combined with Molecular Docking for Screening of Lipase Inhibitors. *Evid.-Based Complement. Altern. Med.* **2022**, *2022*, 4430050. [[CrossRef](#)]
244. Middya, S.; Bhattacharjee, M.; Mandal, N.; Bandyopadhyay, D. RGO-Paper Sensor for Point-of-Care Detection of Lipase in Blood Serum. *IEEE Sens. Lett.* **2018**, *2*, 1–4. [[CrossRef](#)]

Disclaimer/Publisher’s Note: The statements, opinions and data contained in all publications are solely those of the individual author(s) and contributor(s) and not of MDPI and/or the editor(s). MDPI and/or the editor(s) disclaim responsibility for any injury to people or property resulting from any ideas, methods, instructions or products referred to in the content.